DOI:10.14753/SE.2022.2639

SEMMELWEIS EGYETEM

DOKTORI ISKOLA

Ph.D. értekezések

2639.

MORITZ ZÜRN

A gyógyszerészeti tudományok korszerű kutatási irányai

című program

Programvezető: Dr. Antal István, egyetemi tanár

Témavezető: Dr. Boldizsár Imre, egyetemi docens

DOI:10.14753/SE.2022.2639

Phenylethanoid glycosides in selected species of *Fraxinus, Plantago,* and *Forsythia* plants

Ph.D. thesis

Moritz Zürn

Doctoral School of Pharmaceutical Sciences

Semmelweis University

Supervisor: Imre Boldizsár, Ph.D.

Official reviewers: Sándor Gonda, Ph.D.,
Krisztina Ludányi, Ph.D.

Head of the Complex Exam Committee:
István Antal, D.Sc.

Members of the Complex Exam Committee:
Anna Sólyomváry, Ph.D.,
Anikó Zsigrainé Vasanits, Ph.D.

Budapest
2021

DOI:10.14753/SE.2022.2639

TABLE OF CONTENTS

DOI:10.14753/SE.2022.2639

DOI:10.14753/SE.2022.2639

DOI:10.14753/SE.2022.2639

1 LIST OF ABBREVIATIONS

(q)NMR	(Quantitative) Nuclear magnetic resonance
(Δ)*CA%*	(Change of) Carbonylicity percentage
(Δ)*G*	(Change of) Gibbs free energy
(Δ)*H*	(Change of) Enthalpy
(Δ)*S*	(Change of) Entropy
% v/v	Percent by volume
5-CQA	5-caffeoylquinic acid
ABTS	2-2'-azino-bis(3-ethylbenzothiazoline-6-sulfonic acid)
ACE	Angiotensin-converting enzyme
ACN	Acetonitrile
AO	Acteoside
ATCC	American Type Culture Collection
Bald.	Antonio Baldacci (1867 – 1950)
BBM	Bayesian Binary Method
Ca^{2+}	Calcium cation
CD_3OD	Methanol-d_4
CID	Collision-induced dissociation
D	Deuterium
DAD	Diode array detector
DeAO	Desrhamnosylacteoside
Degen	Árpád von Degen (1866 – 1934)
DeIsAO	Desrhamnosylisoacteoside
DMSO-d_6	Dimethyl sulfoxide-d_6
(nr)DNA	Nuclear ribosomal desoxyribonucleic acid
DPPH	2,2-diphenyl-1-picrylhydrazyl
DSS-d_6	3-(trimethylsilyl)-1-propanesulfonic acid-d_6 sodium salt
DW	Distilled water
E.	*Escherichia*
e.g.	*lat.* exempli gratia (for example)
EC_{50}	Half maximal effective concentration
EICs	Extracted ion chromatograms

ESI	Electrospray ionization
eV	Unit symbol for electronvolt
FA	Forsythoside A
FF	Forsythiae fructus
FH	Forsythoside H
FI	Forsythoside I
Fo.	*Forsythia*
Fr.	*Fraxinus*
GS(s)	Gall sample(s)
h	Unit symbol for hour
HIV	Human immunodeficiency virus
HR-MS	High-resolution mass spectra
HT	Hydroxytyrosol
i.e.	*lat.* id est (that is)
i.v.	Intravenous
IC_{50}	Half maximal inhibitory concentration
IDPFG	Indirect-detection with z-pulsed-field-gradient
IEFPCM	Integral equation formalism polarizable continuum model
IsAO	Isoacteoside
IsoPM	Isoplantamajoside
ITS	Internal transcribed spacer
IUPAC	International Union of Pure and Applied Chemistry
K	Kelvin
L.	Carl Linnaeus (1707 – 1778)
LPS	Lipopolysaccharide
GalN	D-galactosamine
M	Molar (moles per litre)
m/z	Mass-to-charge-ratio
MeDCG	Methoxy-dihydroxycoumarin-glucoside
MRPs	Multidrug resistance proteins
MTT	(4,5-dimethylthiazol-2-yl)-2,5-diphenyltetrazolium bromide
N_2	Nitrogen gas

NE	Norepinephrine
NF-κB	Nuclear factor ‘kappa-light-chain-enhancer’ of activated B-cells
NOAEL	No observed adverse effect level
Nrf2/ARE	Nuclear factor erythroid 2-related factor 2/antioxidant response element
Nrf2/HO-1	Nuclear factor erythroid 2-related factor 2/heme oxygenase-1
P.	*Plantago*
PAL	Phenylalanine ammonia lyase
Ph. Eur.	European Pharmacopoeia
PhEG(s)	Phenylethanoid glycoside(s)
PM	Plantamajoside
r^2	Coefficient of determination
RSD%	Relative standard deviation percentage
RSV	Respiratory syncytial virus
S.	*Staphylococcus*
SARS-CoV-2	Severe acute respiratory syndrome coronavirus type 2
Sect.	Section
SEM	Standard error of the mean
SFIs	Selected fragment ions
SM(s)	Secondary metabolite(s)
StA	Unripe green, closed fruits of *Forsythia* species
StB	Ripe, yellow-brown, closed fruits of *Forsythia* species
StC	Ripe, yellow-brown, opened fruits of *Forsythia* species
Subg.	Subgenus
TCM	Traditional Chinese Medicine
TFA	Trifluoroacetic acid
Thunb.	Carl Peter Thunberg (1743 – 1828)
TS	Transition state
(U)HPLC(-MS)	(Ultra) High performance liquid chromatography (-mass spectrometry)
USA	United States of America
UV	Ultraviolet

Vahl.	Martin Vahl (1749 – 1804)
WCSP	World Checklist of Selected Plant Families
Zabel	Hermann Zabel (1832 – 1912)
λ	Wavelength
μg/mL	Microgram per millilitre
μM	Micromolar (micromoles per litre)

DOI:10.14753/SE.2022.2639

2 INTRODUCTION

Phenylethanoid glycosides (PhEGs) represent a specific group of pharmacologically active secondary metabolites (SMs), which are also isolated from representatives of the genera *Forsythia*, *Fraxinus,* and *Plantago* (1). PhEGs can be characterized as dimeric or oligomeric SMs consisting of aromatic and saccharide structural units. Depending on the connecting positions of the structural units, PhEGs consisting of identical aromatic and saccharide moieties might be present in plants in form of multiple regioisomers. Regarding the accumulation of regioisomeric PhEGs in plant tissues, one isomer can be determined as the main PhEG while other regioisomers are present only in small amounts. However, interconversions between regioisomers can occur during heat treatment, and thus, the minor regioisomers can be isolated after optimized heat treatment of the intact plant tissue, resulting in their formation from the main PhEG isomer.

The majority of the plant species investigated in this thesis are officially mentioned as natural medicines in the European Pharmacopoeia (Ph. Eur.) or used as agents in Eastern traditional medicine, such as Traditional Chinese Medicine (TCM). However, phytochemical studies are limited to those organs used as phytotherapeutic agents and, therefore, the phytochemical composition of other parts remains unknown.

Based on the phytochemical composition of the various organs of *Forsythia*, *Fraxinus,* and *Plantago* plants analyzed so far, we hypothesized that tissues of these plants, which have not yet been studied, may also accumulate valuable PhEG-type metabolites. In addition, plant tissues containing a high amount of a certain PhEG may also be used to isolate its regioisomer(s), following an optimized heat treatment resulting in isomerization(s).

Plants – like all organisms – depend on the transformation and interconversion of a myriad of organic compounds enabling them to live, grow, and reproduce. As autotrophic organisms, plants are very efficient in synthesizing the required molecules via photosynthesis from inorganic materials present in the environment.

2.1 Cinnamic acid derivatives and PhEGs

The SM cinnamic acid and its 4-hydroxy derivatives (i.e., *p*-coumaric, caffeic, ferulic, 5-hydroxyferulic, and sinapic acids) belong to a group of phenolic acids, usually

found in form of esters or glucosides throughout the plant kingdom (2, 3). They are characterized by C6-C3 entities, i.e., by a chain of three carbon units (C3), which is attached to a phenolic ring (C6) (4). In the case of the 4-hydroxyderivatives, the phenolic ring is complemented by one *p*-hydroxyl function for *p*-coumaric acid. Subsequent addition of hydroxyl and methoxyl groups leads to caffeic, ferulic, 5-hydroxyferulic, and sinapic acids (**Figure 6**). (4, 5) The higher stability of the (*E*)-/*trans*-configuration might explain that the compounds are usually found in form of their (*E*)-/*trans*-isomers, although the (*Z*)-/*cis*-forms occur naturally as well (2, 6, 7).

The cinnamic acid derivative caffeic acid can be esterified with one or more quinic acid moieties, forming a group of SMs known as caffeoylquinic acids (syn. chlorogenic acids). Traditionally, 3-*O*-caffeoylquinic acid is referred to as chlorogenic acid, however, based on the numbering system of the quinic acid moiety, chlorogenic acid can also be referred to as 5-*O*-caffeoylquinic acid (5-CQA), following the nomenclature of the International Union of Pure and Applied Chemistry (IUPAC) (**Figure 1**). (3, 8, 9)

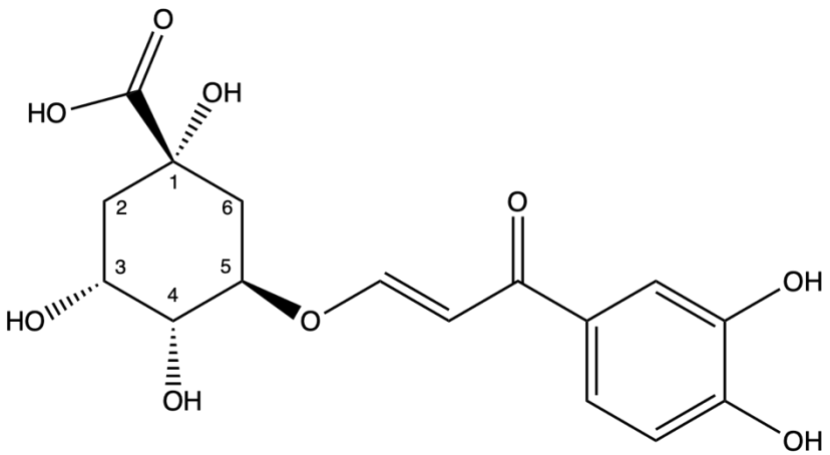

Figure 1: Structure of 5-CQA (syn. chlorogenic acid), according to IUPAC.

Structurally and biosynthetically, cinnamic acid and related compounds derive from the aromatic acids L-phenylalanine and L-tyrosine, supplied by the endogenous shikimate pathway (**chapter 2.2**). As C6-C3 compounds, they provide building blocks for more complex SMs, such as PhEGs, lignans, coumarins, and flavonoids (10, 11).

PhEGs are widely distributed water-soluble natural products (1). As the name suggests, their core structure is a phenylethyl alcohol moiety connected to a central β-D-glucopyranose via a glycosidic bond (12). Usually, this molecular skeleton is complemented by further substituents, such as aromatic acids (e.g., cinnamic acid

derivatives, syringic acid, sinapic acid, gallic acid) and various sugars (e.g., rhamnose, xylose, apiose, glucose, lyxose, allose, arabinose), via ester and glycosidic bonds to the central glucose residue, respectively (12, 13). The general structure of PhEGs and the substituents of the PhEGs investigated in this thesis are shown in **Figure 2**.

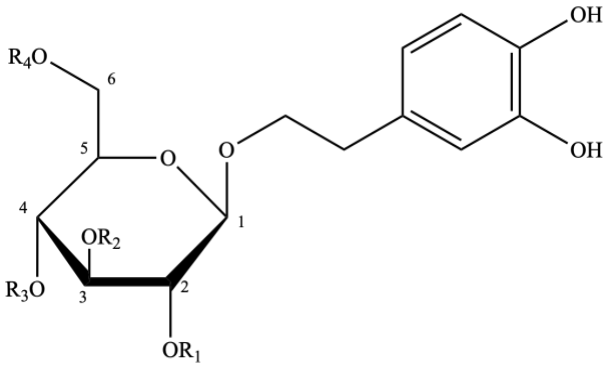

R_1	R_2	R_3	R_4	
-H	Rhamnosyl	*(E)*-caffeoyl	-H	Acteoside
-H	Rhamnosyl	-H	*(E)*-caffeoyl	Isoacteoside
-H	-H	*(E)*-caffeoyl	-H	Desrhamnosylacteoside
-H	-H	-H	*(E)*-caffeoyl	Desrhamnosylisoacteoside
-H	Glucosyl	*(E)*-caffeoyl	-H	Plantamajoside
-H	Glucosyl	-H	*(E)*-caffeoyl	Isoplantamajoside
-H	-H	*(E)*-caffeoyl	Rhamnosyl	Forsythoside A
-H	*(E)*-caffeoyl	-H	Rhamnosyl	Forsythoside I
(E)-caffeoyl	-H	-H	Rhamnosyl	Forsythoside H

Figure 2: General structure of PhEGs investigated in this thesis.

Due to the presence of one phenylpropyl moiety (i.e., caffeoyl moiety), the compounds investigated in this thesis are also known as phenylpropanoid glycosides (13) or caffeoyl PhEGs (14).

PhEGs are categorized based on the number, type, and position of the sugar moieties or the variation of the core structure. Currently, there are seven groups of PhEGs, listed in the following **chapters 2.1.1 – 2.1.7** (12, 13).

2.1.1 PhEGs with α-L-rhamnose at C-3 of the glucose

The most abundant substituent at C-3 of the glucose is α-L-rhamnose. In general, PhEGs possess less than 4 sugar moieties. The most frequently occurring ester-forming aromatic acids are caffeic, ferulic, *p*-coumaric, and gallic acids. Furthermore, vanillic, *cis*-caffeic, *cis*-ferulic, *cis*-*p*-coumaric, isoferulic, syringic, and sinapic acids may be present. The stem bark of *Newbouldia laevis* has been shown to contain newbouldioside

B in salt form (15). Other common examples include acteoside (AO) and isoacteoside (IsAO) (16).

2.1.2 PhEGs without substitution at C-3 of the glucose or other sugars than α-L-rhamnose at C-3 of the glucose

The glucose of desrhamnosylacteoside (DeAO) and desrhamnosylisoacteoside (DeIsAO) is not substituted at C-3 with another sugar moiety (16). The only lyxose-containing PhEGs are the teucriosides identified in the aerial parts of *Teucrium chamaedrys* (17). PhEGs in this group are often esterified with caffeic, ferulic, or cinnamic acid at the C-4 of the central glucose moiety. Xylose, apiose, arabinose, and rhamnose often bind to the central glucose residue via its C-2 or C-6 positions. Mostly, representatives of this group are disaccharides, such as plantamajoside (PM), isoplantamajoside (IsoPM), and forsythosides A (FA), H (FH), and I (FI), or trisaccharides (18).

2.1.3 PhEGs with substituents at the phenylethyl moiety

Substituents at C-2, C-3, C-4, C-5, and C-7 of the phenylethyl moiety include hydroxyl and various alkoxyl (methoxyl, ethoxyl, butoxyl) groups (12, 13) (**Figure 3**). Examples include suspensaside B from the fruits of *Forsythia suspensa* (19) and 1'-(4-hydroxyphenyl)ethane-1',2'-diol 2'-*O*-β-D-apiofuranosyl-(1→6)-β-D-glucopyranoside from the fruits of *Coriandrum sativum* (20).

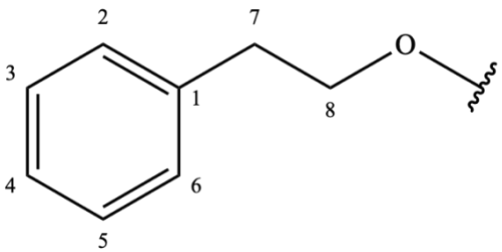

Figure 3: Phenylethyl moiety showing the numbering of carbon atoms.

2.1.4 PhEGs with 1,4-dioxane

These rarely occurring compounds are formed via condensation between C-7,8 of the phenylpropyl and C-1',2' of the glucose moiety (13), e.g., cuneatasides A and B from the stem of *Sargentodoxa cuneata* (**Figure 4**) (21).

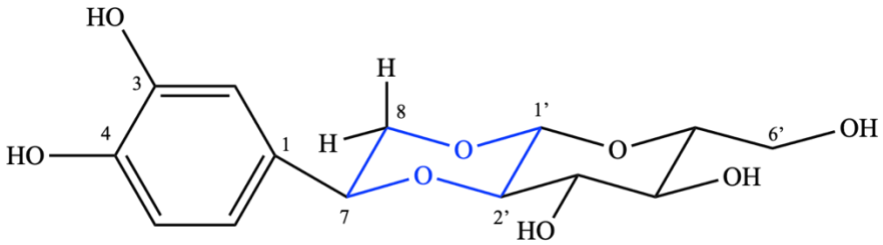

Figure 4: Structure of cuneataside A showing the rarely occurring 1,4-dioxane moiety (marked in blue).

2.1.5 PhEGs fused to other kinds of compound units

PhEGs can be fused to other kinds of compound units (12, 13). Secoiridoid moieties are mostly attached to the glucose, with the exceptions of safghanoside E from the leaves of *Syringa afghanica*, where the secoiridoid is directly fused to the phenylpropyl moiety (22) and strobilanthosides A and B from the aerial parts of *Strobilanthes cusia*, where the phenylethyl alcohol of the PhEG is attached to an indole alkaloid moiety (23).

2.1.6 PhEGs with glucose at the 4-hydroxyl of the phenylethyl moiety

PhEGs in this group are characterized by the presence of a glucose molecule attached to the phenolic 4-hydroxyl function of the phenylethyl moiety, e.g., the PhEG in the bark of *Tabebuia impetiginosa* (24). 6’’-*O*-β-D-glucopyranosyloleuropin (25) and neopolyanoside (26) from the flowers of *Jasminum polyanthum* contain an additional secoiridoid moiety attached to C-8 of the phenylethyl moiety via an ester linkage.

2.1.7 PhEGs with uncommon structural features

Uncommon structural features in PhEGs include 1) the rarely occurring dopaol 2,3-diketo and 2-keto glycosides from *Chelone obliqua* (27), 2) the compounds with a 7,2’-epoxy moiety (e.g., lianqiaoxinoside B from the fruits of *Forsythia suspensa*) (28), and 3) the compounds with a C-6 hydroxyl group at the phenylethyl alcohol moiety (e.g., ternstroside F from the leaves of *Ternstroemia japonica*) (29). Furthermore, substitution of the central glucose moiety by allopyranose (PhEGs from the stem bark of *Magnolia officinalis*) (30) or galactopyranose (PhEG from *Brandisia hancei*) (13) is also described.

DOI:10.14753/SE.2022.2639

PhEGs are not specific for any plant organ, i.e., they have been isolated from plant roots, barks, leaves, whole aerial parts, as well as callus and suspension cultures (13). The majority of PhEGs have been found in families of the order Lamiales, namely Scrophulariaceae, Oleaceae, Lamiaceae, and Orobanchaceae. In fact, several PhEGs have been suggested as chemotaxonomic markers, such as acteoside for the order Lamiales (31) and plantamajoside for the genus *Plantago* (32).

The wide variety of possible substituents to the core structure has led to some confusion in the literature about the identity of the given PhEG. **Table 1** summarizes the various synonyms of the PhEGs investigated in this thesis.

DOI:10.14753/SE.2022.2639

Table 1: Synonyms and semisystematic names of PhEGs investigated in this thesis.

Compound	Synonym(s)	Semisystematic name
Acteoside	Verbascoside, kusaginin	2-(3,4-dihydroxyphenyl)ethyl-1-*O*-α-L-rhamnopyranosyl(1→3)-(4-*O*-*E*-caffeoyl)-β-D-glucopyranoside
Isoacteoside	Isoverbascoside	2-(3,4-dihydroxyphenyl)ethyl-1-*O*-α-L-rhamnopyranosyl(1→3)-(6-*O*-*E*-caffeoyl)-β-D-glucopyranoside
Desrhamnosyl-acteoside	Calceolarioside A	2-(3,4-dihydroxyphenyl)ethyl-(4-*O*-*E*-caffeoyl)-β-D-glucopyranoside
Desrhamnosyl-isoacteoside	Calceolarioside B	2-(3,4-dihydroxyphenyl)ethyl-(6-*O*-*E*-caffeoyl)-β-D-glucopyranoside
Plantamajoside	Purpureaside A, plantamoside	2-(3,4-dihydroxyphenyl)ethyl-1-*O*-β-D-glucopyranosyl(1→3)-(4-*O*-*E*-caffeoyl)-β-D-glucopyranoside
Isoplantamajoside	Plantainoside D	2-(3,4-dihydroxyphenyl)ethyl-1-*O*-β-D-glucopyranosyl(1→3)-(6-*O*-*E*-caffeoyl)-β-D-glucopyranoside
Forsythoside A	Forsythiaside, forsythiaside A	2-(3,4-dihydroxyphenyl)ethyl-1-*O*-α-L-rhamnopyranosyl(1→6)-(4-*O*-*E*-caffeoyl)-β-D-glucopyranoside
Forsythoside H	-	2-(3,4-dihydroxyphenyl)ethyl-1-*O*-α-L-rhamnopyranosyl(1→6)-(2-*O*-*E*-caffeoyl)-β-D-glucopyranoside
Forsythoside I	Isoforsythiaside, isoforsythoside, isoforsythoside A, lianqiaoxinoside A	2-(3,4-dihydroxyphenyl)ethyl-1-*O*-α-L-rhamnopyranosyl(1→6)-(3-*O*-*E*-caffeoyl)-β-D-glucopyranoside

2.2 Biosynthesis of PhEGs

As detailed before, the three key features of PhEGs are 1) a phenylethyl alcohol moiety, 2) an aromatic acid unit, and 3) one or more saccharides (**chapter 2.1**). Simple PhEGs (e.g., salidroside) however only contain one aromatic unit. The biosynthesis of the three building blocks is known in detail. The phenylethyl alcohol and aromatic acid moieties are produced via the shikimate pathway (11), which is responsible for the production of aromatic amino acids L-phenylalanine and L-tyrosine from glucose. (33)

Typical representatives of the phenylethyl alcohol moiety include tyrosol and hydroxytyrosol. Tyrosol has been reported to derive from L-tyrosine via two putative pathways in plants (34) (**Figure 5**).

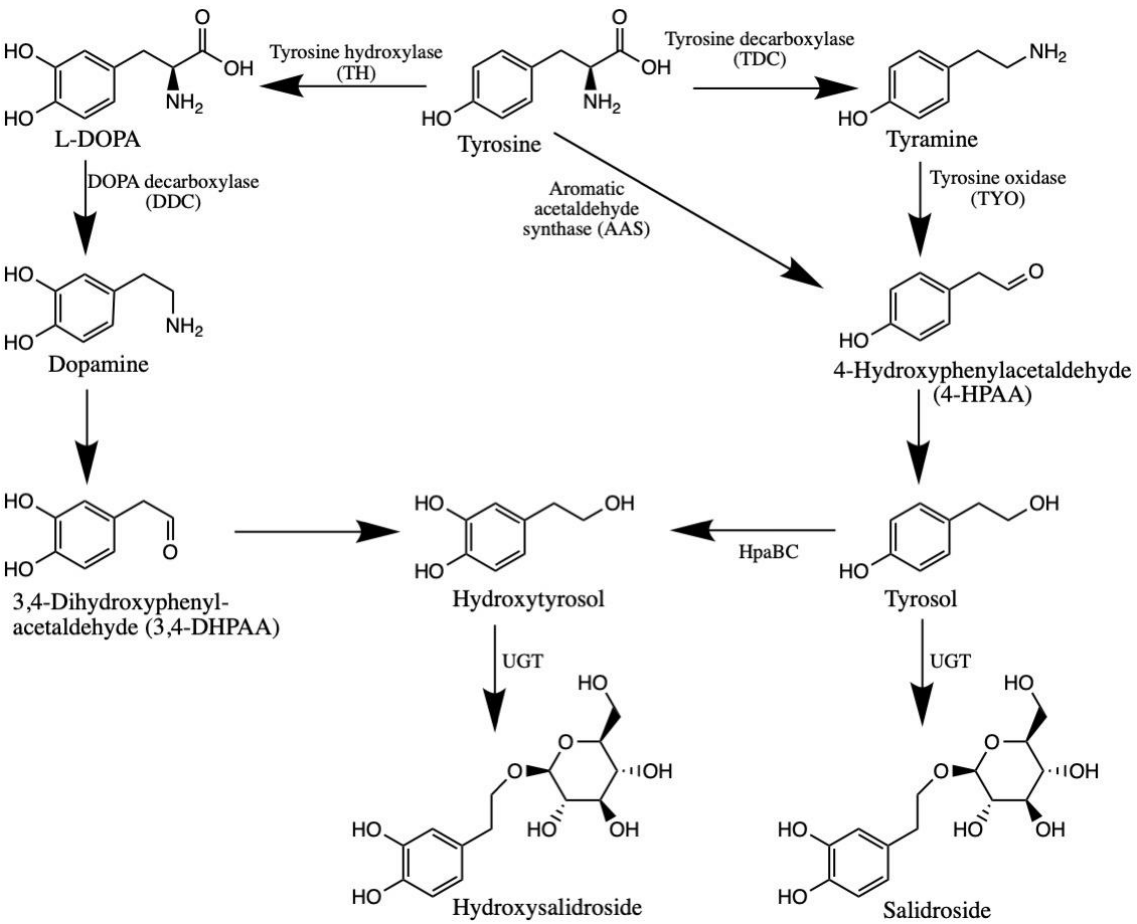

Figure 5: Synthesis of tyrosol, hydroxytyrosol, salidroside, and hydroxysalidroside from tyrosine (34).

The aromatic acid moiety is synthesized via the general phenylpropanoid pathway, starting with the deamination of L-phenylalanine via the phenylalanine ammonia-lyase (PAL), yielding cinnamic acid. Subsequent hydroxylation and methylation steps lead to the cinnamic acid derivatives *p*-coumaric, caffeic, ferulic, 5-hydroxyferulic, and sinapic acids, mediated by specific enzymes (**Figure 6**). L-tyrosine could directly be transformed into *p*-coumaric acid; however, this ability is mainly limited to members of the grass family (Poaceae). (35)

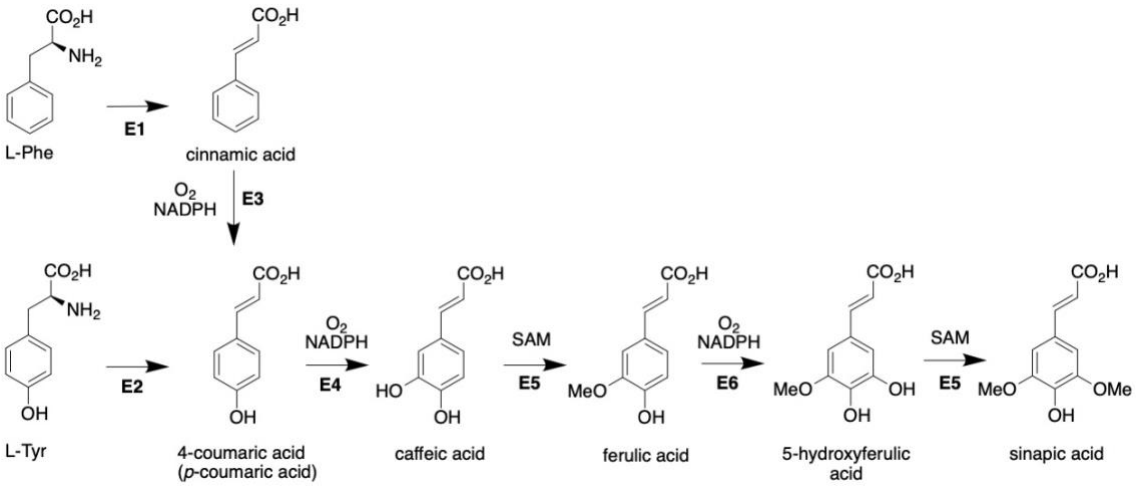

Figure 6: Synthesis of hydroxylated and methoxylated cinnamic acid derivatives; E1: phenylalanine ammonia-lyase (PAL); E2: tyrosine ammonia-lyase (TAL); E3: cinnamate-4-hydroxylase; E4: *p*-coumarate 3-hydroxylase; E5: caffeic acid *O*-methyltransferase; E6: ferulate 5-hydroxylase (35).

It has been shown that plants can increase the biosynthesis of phenylpropanoids under certain circumstances, such as defense against herbivores, protection against microorganisms, or invasion by other species (36, 37). Additionally, external factors, which increase the levels of free radicals (e.g., stress, incidence of more UV light, low temperatures, pathogen infections, nutrient deficiency, drought, ozone exposition) are also able to increase the production of PhEGs in plants (38, 39).

Among the investigated PhEGs, the biosynthesis of AO is known, based on feeding experiments with stable isotope labeled precursors (**Figure 7**). It has been suggested that the aromatic acid moiety in AO (i.e., *trans*-caffeic acid) is incorporated into the structure in form of caffeoyl-CoA (40). However, the assembly of the building blocks into the SM remains to be elucidated, since several downstream intermediates, key enzymes, and their corresponding genes are yet to de discovered (11).

DOI:10.14753/SE.2022.2639

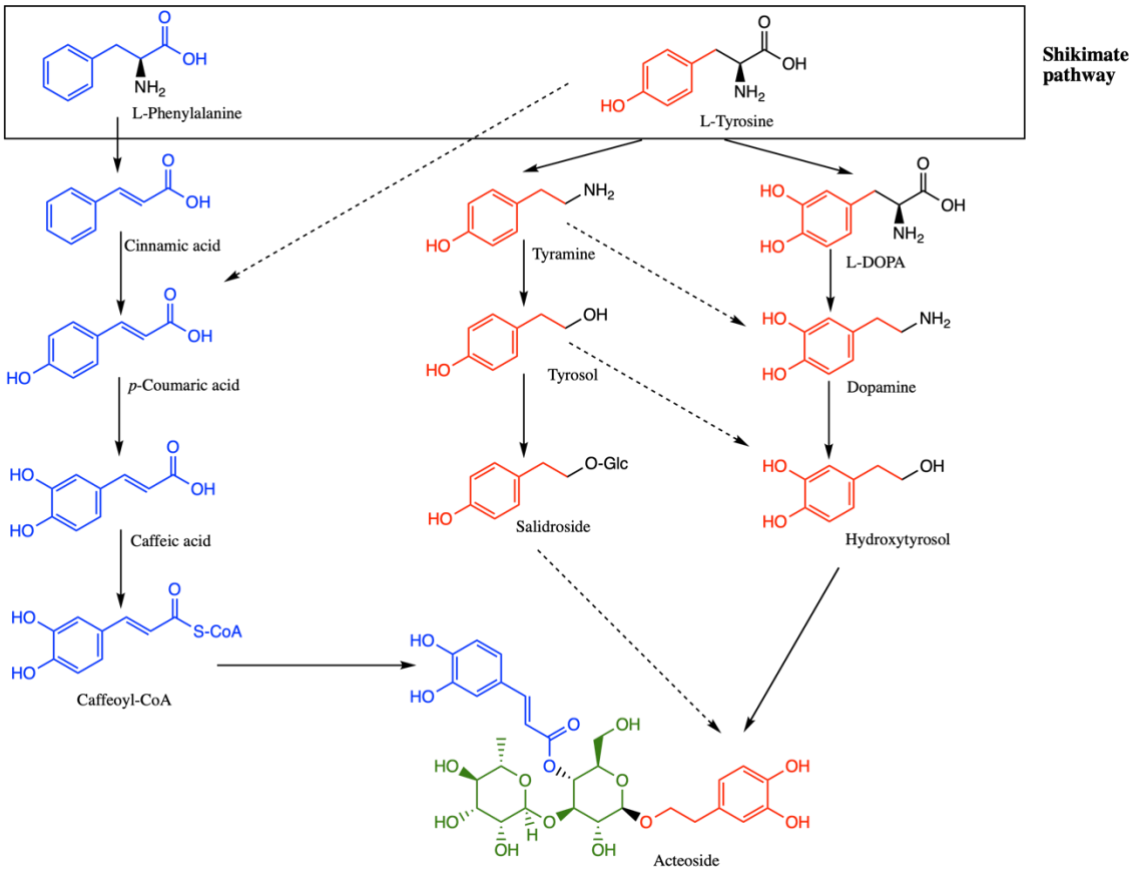

Figure 7: Modified, tentative pathway of AO biosynthesis (11, 40).

2.3 Acteoside and related compounds

AO is constructed from a centrally positioned β-D-glucose that is connected via glycosidic bonds to hydroxytyrosol and α-L-rhamnose units, as well as via an ester bond to a caffeic acid molecule at the C1-OH, C3-OH, and C4-OH positions, respectively (**Figure 8**).

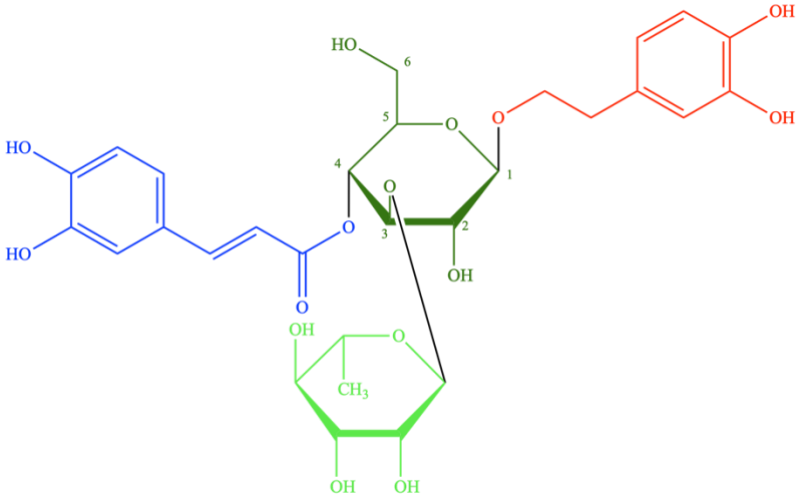

Figure 8: Structure of the PhEG acteoside, showing the phenylethyl moiety (hydroxytyrosol, red), the aromatic acid moiety (caffeoyl, blue), and sugar units (glucose, dark green; rhamnose, light green) as well as the numbering of the central β-D-glucose.

AO was already identified in different organs of European *Fraxinus* species, with the highest amount in the leaf of *Fr. excelsior* (41 mg/g, on dried material basis) (41). In addition to *Fraxinus* trees, more than 200 plant species were described to contain AO (11). It was a minor compound in many species (e.g., *Sideritis trojana* dried root, 0.02 mg/g), but its abundant sources were also determined, such as the dried leaves of *Sesamum indicum* (129 mg/g), *Ligustrum purpurascens* (13 – 73 mg/g), *Euphrasia rostkoviana* (25.6 mg/g), *Syringa vulgaris* (24.8 mg/g), and *Olea europaea* (17.2 mg/g) (11, 42-46). Despite these high-level accumulations of AO, the highest isolated yield of AO was only 2.5% (which corresponds to 28 g AO isolated from 1.1 kg dried leaves of *Stachys sieboldii*) (47).

A regioisomer of AO, namely IsAO, which is esterified with caffeic acid at the C6-OH position (**Figure 8**), and the corresponding desrhamnosyl derivatives of AO and IsAO, desrhamnosyl-AO (DeAO), and desrhamnosyl-IsAO (DeIsAO), were also present in some AO-containing plants as minor compounds. A review of the content of these three

PhEGs among plants found that 37.3 mg/g of IsAO (48), 0.8 mg/g of DeAO (49), and 2.5 mg/g of DeIsAO (50) were the highest amounts, in *Castilleja tenuiflora* (dried root culture treated with indole 3-acetic acid), *Isoplexis sceptrum* (fresh leaf) and *Nematanthus wettsteinii* (fresh plant), respectively.

The isomerization of AO into IsAO (51) and the desrhamnosylation of AO and IsAO (52) during heat treatments performed in water and acidic media, respectively, and the mass fragmentation patterns of AO, IsAO, DeAO, and DeIsAO, were also described (44, 53, 54). However, the regioisomeric pairs AO-IsAO and DeAO-DeIsAO were not distinguished from each other by their specific fragment ions. Furthermore, conversion procedures (isomerization and hydrolysis) were not optimized regarding yields (avoiding unwanted decomposition) and time consumption.

2.4 Plantamajoside and related compounds

PM is derived from the same core structure as AO, containing a central β-D-glucose moiety connected to hydroxytyrosol and caffeic acid via glycosidic and ester bonds at C1-OH and C4-OH, respectively. However, instead of the α-L-rhamnose of AO, PM contains a β-D-glucose molecule at C3-OH of the central β-D-glucose moiety (**Figure 9**).

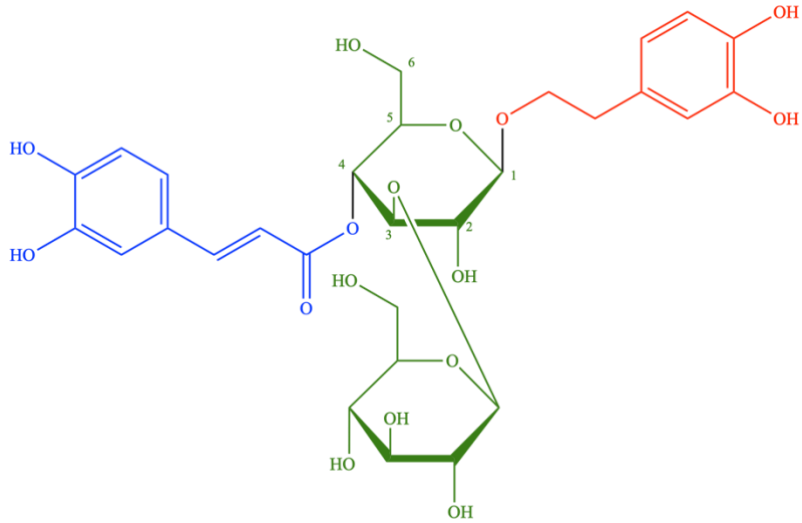

Figure 9: Structure of the PhEG plantamajoside, showing the phenylethyl moiety (hydroxytyrosol, red), the aromatic acid moiety (caffeoyl, blue), and sugar units (two glucose molecules, dark green) as well as the numbering of the central β-D-glucose.

PM is described as a key metabolite in the family Plantaginaceae and mainly present in aerial parts of the genus *Plantago* (45.2 mg/g, leaves of *P. major* grown outdoors) (55). However, much higher concentrations have been determined in with *Agrobacterium rhizogenes* biotransformed roots of *P. lanceolata* (30 – 80 mg/g) (37). Additionally, representatives of the families Gesneriaceae (0.94 mg/g, whole plant of *Aeschynanthus speciosus*) (50) and Orobanchaceae (0.04 mg/g, whole plant of *Boschniakia himalaica*) (56) have also been described to contain small amounts of PM.

IsoPM, the regioisomer of PM, which is esterified with caffeic acid at C6-OH (**Figure 9**), was mainly present in small amounts in some PM-containing plants (57). However, the aerial parts of *Digitalis purpurea* were an exception, since they contained IsoPM (3.2 mg/g), while PM was absent (58).

The tissue- and age-specific accumulation of PM was also described. One study found that the accumulation of PM in cultured roots is age-dependent and higher than in

leaves of *P. lanceolata*, which was not influenced by age (59, 60). However, it was shown that the concentration of PM in leaves of *P. major* decreases with age (61).

The tandem mass spectra of PM and IsoPM were analyzed, confirming identical fragment ion profiles of these PhEGs (62). However, there is no data to differentiate between PM and IsoPM based on the intensity of specific fragment ions. Furthermore, the isomerization of PM has not yet been described.

2.5 Forsythoside A and related compounds

FA derives from the same skeletal structure as AO and PM, consisting of a centrally positioned β-D-glucose, which is connected via ester bonds at C1-OH and C4-OH to hydroxytyrosol and caffeic acid, respectively. In contrast to AO, the second sugar moiety, i.e., the α-L-rhamnose unit, is glycosidically bound to C6-OH of the glucose (**Figure 10**). In the structure of AO, the α-L-rhamnose unit can be found at C3-OH of the central glucose moiety.

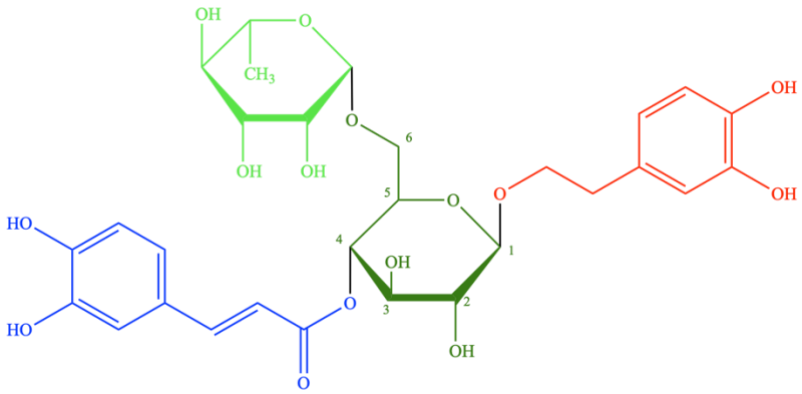

Figure 10: Structure of the PhEG forsythoside A, showing the phenylethyl moiety (hydroxytyrosol, red), the aromatic acid moiety (caffeoyl, blue), and sugar units (glucose, dark green; rhamnose, light green) as well as the numbering of the central β-D-glucose.

FA is described as a major constituent in fruits, leaves, and bark of the genus *Forsythia* (63). In fact, its highest amount was detected in the leaves of *Fo. suspensa* (77.9 mg/g) (64). Furthermore, the fruits of *Fo. suspensa* have been shown to contain FA as a main metabolite (2.57 – 47.17 mg/g, depending on the developmental stage and organ) (65) and it has been detected in much smaller amounts in representatives of the families Plantaginaceae (4 mg/g, whole fresh plant of *Isoplexis chalcantha*) (49), Orobanchaceae (0.33 mg/g, callus of *Rehmannia glutinosa*) (66), Calceolariaceae (>0.5 mg/g, fresh aerial parts of *Calceolaria biflora*) (67) and Verbenaceae (2.06 mg/g, leaves of *Aloysia polystachya*) (68). The tissue- and age-dependent accumulation of FA has been investigated in the fruits of *Fo. suspensa*, describing its accumulation in the green, young fruit and especially in the seed (known as qingqiao and qiaoxin in TCM, respectively). It was also found that the FA content decreases with the age of the fruit (65, 69) Furthermore, the leaves of *Fo. europaea*, collected in Japan were shown to contain FA as the main PhEG (12.58 mg/g) (70).

Both isomers of FA, namely FH and FI, which are esterified with caffeic acid at C2-OH and C3-OH, respectively (**Figure 10**), are known to occur in very low amounts in the fruits of *Fo. suspensa*, ranging from 0.0025 – 0.221 mg/g for FI and 0.0024 – 0.012 mg/g for FH (71-74).

The isomerization of FA via FI to FH and the tandem mass spectra of the three regioisomers have also been described recently (75, 76). The isomerization process is part of FA's degradation with FI and FH being intermediary compounds, which can further decompose by either loss of the caffeoyl moiety or oxidation (76). The isomerization of FA into FI and FH is achieved easily in heated aqueous solution and its complete putative degradation process resulting in the formation of caffeic acid is described, without the exact identification of FI and FH. Namely, the isomerization products were identified only by LC-MS, thus their structures remain to be confirmed. (75) FA, FI, and FH were described to produce the same fragment ions during their MS/MS analysis (75), and so far, there is no possibility to differentiate the three isomers from each other based on fragment ion profiles.

2.6 Biological effects and structure-activity relationships of selected PhEGs

2.6.1 Antioxidant and free-radical scavenging activities

All four AO-related compounds, i.e., AO, IsAO, DeAO, and DeIsAO, showed *in vitro* antioxidant and free-radical scavenging activity with IC_{50} values being comparable to the respective reference compound in several assays, such as the 2,2-diphenyl-1-picrylhydrazyl (DPPH), nitric oxide, and superoxide dismutase assay (77-80).

The DPPH radical scavenging activity of IsoPM was comparable to ascorbic acid (80) and the compound showed potent scavenging effects on hydroxyl radicals produced by H_2O_2/Fe^{2+} and superoxide anion radicals produced by the xanthin/xanthinoxidase system (81).

The H_2O_2-induced cell death of rat pheochromocytoma cell line PC12 as well as the cell death and reactive oxygen species production of lipopolysaccharide (LPS)-treated cells, was prevented by pretreatment with FA (82). Furthermore, FA and one of its isomers, FI, exerted remarkable DPPH scavenging activity (83, 84). However, FI was shown to be more potent antioxidant in this model (74). Moreover, FH exhibited significant ABTS radical scavenging activity, comparable to ascorbic acid (28).

The antioxidant activity of PhEGs is described to be related to the number of aromatic methoxy and hydroxy groups and the structure of the acyl moiety, while the modification of the sugar chain or the replacement of hydroxy by methoxy groups was shown to be of minor importance (28, 78, 85, 86).

2.6.2 Antiviral activities

AO and IsAO exhibited potent *in vitro* activity against the human respiratory syncytial virus (RSV), which can cause severe respiratory tract infections in infants and young children. Both compounds displayed lower EC_{50} values than ribavirin, an approved drug for RSV treatment. (87) Furthermore, AO showed good *in vitro* activity against the human dengue virus serotype 2 (88). The antiviral activity of AO and IsAO can be attributed to their *ortho*-dihydroxy systems (87, 88). DeAO and DeIsAO prevented the fusion of human immunodeficiency virus (HIV) with a host cell by binding a transmembrane glycoprotein (gp41) on the surface of the virus *in vitro*. In contrast, AO showed no inhibitory activity, which might be due to the presence of the rhamnosyl moiety. (89)

FA inhibited the infectivity of the avian infectious bronchitis virus in cell culture in a dose-dependent manner (90) and exerted *in vitro* and *in vivo* antiviral activity against various strains of human influenza A virus subtype H1N1 (91, 92).

The antiviral effects of PM and IsoPM were not tested so far.

2.6.3 Antimicrobial activity

AO exerted antileishmanial activity *in vitro* by inhibiting promastigote growth and arginase activity (which is responsible for the synthesis of essential polyamines) of *Leishmania amazonensis* (93).

PM showed significant *in vitro* activity against several bacteria, including plant pathogenic bacteria *Escherichia coli* ML30 and *Staphylococcus aureus* 502A (94). Moreover, considerable *in vitro* activity of PM against *Corynebacterium* spp. was also reported (95).

As principal antibacterial compounds in *Fo. suspensa*, FA, and FI exhibited dose-dependent inhibitory activities *in vitro* against several bacteria, including commonly occurring *S. aureus, E. coli,* and *Pseudomonas aeruginosa*. The minimal inhibitory concentrations (MICs) of FA were comparable to the antibiotic tetracycline. (73, 96) FH displayed strong *in vitro* antibacterial activities against *Bacillus vulgare, Aeruginosus bacillus,* and *Micrococcus pneumoniae* (28).

2.6.4 Cytotoxic and antiproliferative effect

The AO derivatives were shown to exert cytotoxic activities against various cell lines (52, 77, 97) and suppressed the lung metastasis of B16 melanoma cells (98). The cytotoxic effects of AO and its derivatives were described to depend on the presence of the 3,4-dihydroxyphenylethyl group and, to a lesser extent, the caffeoyl moiety (52), while rhamnose substitution did not affect the bioactivities (77).

The dose-dependent antiproliferative activity of PM in esophageal squamous cell carcinoma cells was reported (99). Furthermore, PM showed promising activity against gastric cancer cell line MGC-803 (100) and inhibited the growth of breast cancer cells without side effects on normal cells *in vitro* (101).

2.6.5 Anti-inflammatory, analgesic, and antiallergic activities

AO and IsAO showed moderate anti-inflammatory activity in mouse ear edema. Additionally, their anti-ulcerogenic activity was tested in absolute ethanol-induced acute gastric ulcer and the efficacy of both compounds was comparable to famotidine. (102) The two isomers also inhibited certain macrophage functions *in vitro*, which are involved in the inflammatory process while cytotoxic effects were not observed, even in a concentration of 100 μM (103). The analgetic activity of intravenously (i.v.) administered AO was comparable to aminopyrine on acetic acid-induced writhing and tail pressure pain tests in mice. Deletion of the rhamnose moiety decreased the activity, while substitution of the rhamnose by a glucose moiety did not influence it. (104)

FA inhibited LPS-induced inflammatory responses in BV2 and primary microglia cells as well as in the bursa of Fabricius of chicken, the site of hematopoiesis, via inhibition of NF-κB activation and activation of the Nrf2/HO-1 signaling pathway (105, 106). Moreover, FA protected against cigarette-induced lung injury and ovalbumin induced asthma in mice through the same mechanisms (107, 108).

The anti-inflammatory effect of PM was tested in LPS-induced airway inflammation and lung injury. In both cases, PM decreased the expression of inflammatory cytokines IL-6 and IL-1β and suppressed the NF-κB signaling pathway. (109, 110) Furthermore, PM inhibited the LPS-induced expression of inducible nitric oxide synthase in macrophages via suppression of activator protein-1 (111).

2.6.6 Effects on the central nervous system

AO and IsAO pretreatment of PC12 cells, commonly used as a model for neuronal differentiation, suppressed H_2O_2-induced cytotoxicity and reversed H_2O_2-downregulation of several antioxidant enzymes (79, 112). AO alone was described to exert possible neuroprotective effects against hypoxic-ischemic brain damage in rats (113). Since it penetrated the blood-brain-barrier, activated Nrf2/ARE signaling pathway and attenuated oxidative stress, it might be of potential therapeutic value for Parkinson's disease (114).

The beneficial effects of FA in scopolamine-induced memory impairment and its neuroprotective effect in learning and memory deficits in senescence-accelerated mice indicated a therapeutic value for FA in amnesia treatments (115, 116). FA was described

to have therapeutic potential in the treatment of Alzheimer's disease since it suppressed β-amyloid-induced overexpression of cyclooxygenase-2 and monoacylglycerol lipase and inhibited the activity of acetylcholinesterase (117, 118).

2.6.7 Effects on the cardiovascular system

AO and IsAO were shown to inhibit the angiotensin-converting enzyme (ACE), a key enzyme in the development of hypertension (*in vitro*) (119). Furthermore, AO was shown to inhibit the low-density lipoprotein-induced secretory increase of endothelin 1, a potent vasoconstrictor relating hypercholesterolemia to atherosclerosis in bovine aortic endothelial cells (120). Another study suggested that AO prevents atherosclerosis via its antiproliferative effect on cultured A7r5 rat aortic smooth muscle cells (121).

The influences of PM and IsoPM on the cardiovascular system were described *in vitro*. The anti-hypertensive effect of PM was attributed to its ACE-inhibiting activity (122). Furthermore, IsoPM prevented the adriamycin (doxorubicin)-induced apoptosis of cardiac muscle cells (123).

FA was shown to exert relaxation activity on norepinephrine (NE)-induced contractions of isolated rat aorta by decreasing the NE-mediated Ca^{2+}-influx from the extracellular space (124).

2.6.8 Hepato- and nephroprotective activities

AO and IsAO exerted hepatoprotective activities via numerous mechanisms in mice and rats (125, 126).

PM's protective effects against cadmium-induced kidney injury were reported in rats (127).

The hepatoprotective effect of FA was tested and confirmed in LPS/ D-galactosamine (GalN)-induced liver injury in mice (128).

2.6.9 Miscellaneous effects

Additional effects of the PhEGs included the ergogenic (rats) (129), immunoenhancing (*in vitro*) (130), calcineurin-inhibiting (*in vitro*) (131), photoprotective (*in vitro*) (132), and wound-healing (rats) (133) activities of AO, anti-alopecia (mice)

(134) and enzyme-inducing (*in vitro* and *in vivo* in rats) (135) effects of FA, and the antispasmodic effect of PM (*ex vivo* in guinea-pig ileum and trachea) (136).

2.6.10 Toxicity

Recently, AO was tested for its cytotoxicity against Vero E6 cells, and its non-toxicity in the concentration range applied (0 – 200 µg/mL) was confirmed (88). Furthermore, AO showed no acute oral toxicity up to a dosage of 2000 mg/kg in rats (137) and there has been no sign of gastric damage in rats and mice (133).

The no observed adverse effect level (NOAEL) of PM in rats was reported to be higher than 2000 mg/kg (138), however, the safety of PM as a phytotherapeutic agent still needs to be confirmed, since it caused significant structural aberrations in mammalian chromosomes (139).

FA's non-toxicity has been shown for lung and liver in mice (140), however, there are local Chinese reports suggesting the toxicity of FA (69).

2.7 Genus *Fraxinus*

2.7.1 Botanical characterization and traditional uses of the genus *Fraxinus*

The cosmopolitan genus *Fraxinus* L. (ash trees) comprises 43 accepted species, distributed in temperate and subtropical regions of the Northern Hemisphere, including North America (20 species), Eastern Asia (20 species) as well as Western Asia and Europe (3 species) (141). *Fraxinus angustifolia* Vahl (narrow-leafed ash; syn. *Fr. oxycarpa*), *Fr. excelsior* L. (European ash), and *Fr. ornus* L. (flowering ash) are the three European representatives of the genus (16). Traditionally, the genus has been placed as the sole member of the tribe Fraxinae of the subfamily Oleoideae of the Oleaceae family. Based on morphological traits, the genus was divided into two sections or subgenera. The section or subgenus *Fraxinus* included all taxa with lateral inflorescences, while the section or subgenus *Ornus* included taxa, which bore flowers in terminal panicles together with the leaves. Based on the presence or absence of calyx, the number of petals, and winged or unwinged petals, the section *Fraxinus* was further subdivided into five subsections. Section *Ornus* was subdivided into subsections *Ornus* with petals and *Ornaster* without petals. The most recent classification of the genus *Fraxinus* abandoned the subfamily level dividing the Oleaceae family into five tribes, namely Fontanesieae, Forsythieae, Jasmineae, Myxopyreae, and Oleeae. The genus *Fraxinus* was placed in the subtribe Fraxininae of the tribe Oleeae and divided into six sections based on morphological traits: *Dipetalae, Fraxinus*, *Melioides*, *Ornus*, *Pauciflorae*, and *Sciadanthus* (**Figure 11**). A key to the sections of *Fraxinus* is described. (141)

DOI:10.14753/SE.2022.2639

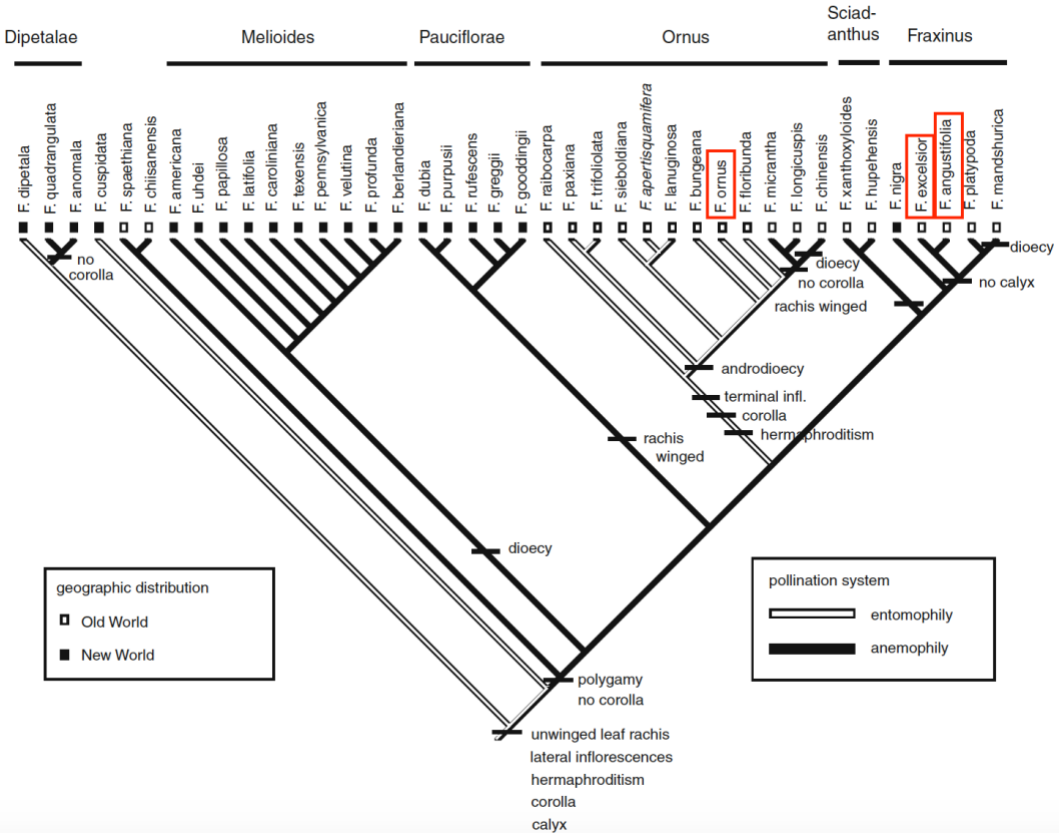

Figure 11: Summary of *Fraxinus* phylogeny and their geographical distribution (141). *Fr. malacophylla*, *Fr. baroniana*, and *Fr. griffithii*, belonging to the section *Ornus* are not included in the figure.

The deciduous or rarely evergreen trees or rarely shrubs of the genus usually contain odd-pinnate leaves (rarely whorled at branch apices). Their petiole and petiolule is often basally thickened. Terminal or axillary inflorescences are equipped with small, unisexual, bisexual, or polygamous flowers with a white to yellowish, 4-lobed corolla. The samara fruit bears an elongated wing, usually containing one ovate-oblong seed with a fleshy endosperm (142, 143) (**Figure 12**).

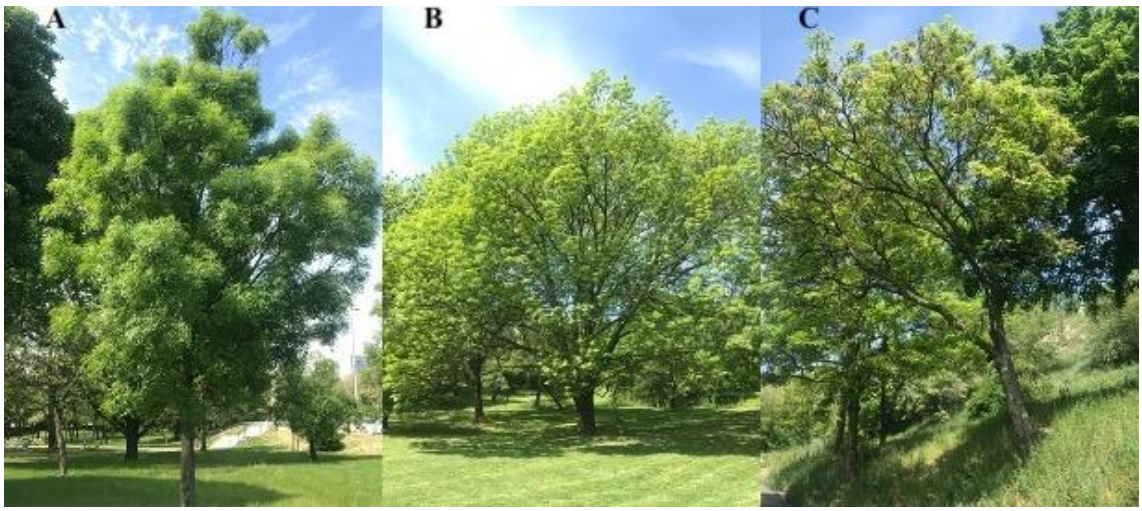

Figure 12: European *Fraxinus* species growing in Hungary. The species were identified in the field based on macromorphological characteristics, i.e., unbranched inflorescences and dark-brown terminal buds for *Fr. angustifolia* (A), branched inflorescences and black terminal buds for *Fr. excelsior* (B), and unbranched inflorescences containing small white flowers, smooth, dark grey bark, and hairy, silver-grey terminal buds for *Fr. ornus* (C) (own picture).

The inflorescences of *Fraxinus* trees were described to frequently contain abnormal outgrowths of plant tissues, known as galls (**Figure 14**). These galls can be caused by the phytophagous mite *Aceria fraxinivora*, which attacks the inflorescences, resulting in sizable, irregular deformities formed mainly from the flower stalks (144). The mite is reported to stress the host by flushing salivary chemicals, such as high-molecular-weight proteins, bruchins, and mitogenic lipids, on the wounded plant site, which is entailed by altered gene expression in adjacent cells. This caused an isolated cell to deviate from its normal course of differentiation, resulting in a metaplasied cell, which reacted to the external stimuli by growth and differentiation, leading to the development of the gall. (145) High-yield harvesting of galls from infected *Fraxinus* trees is feasible, without damaging the plants (**Figure 13**).

DOI:10.14753/SE.2022.2639

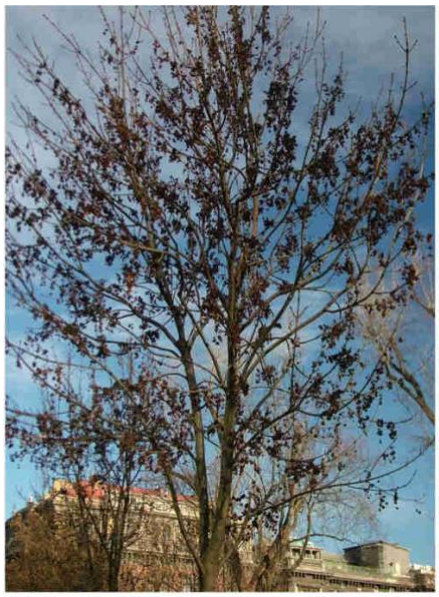

Figure 13: Galls on a *Fr. excelsior* tree in late autumn (own picture).

Figure 14: Galls in the inflorescences of *Fr. excelsior* (own picture).

The genus *Fraxinus* is widely applied in the wood-working industry and many of the included species are commonly used in folk medicine as well as contemporary medicine due to their considerable medicinal properties. In different parts of the world various parts of several *Fraxinus* spp. attract attention for their diuretic and mild laxative effects and are used for the treatment of constipation, edema, rheumatic pain, cystitis, and itching scalp (146). Leaves and bark of *Fr. excelsior*, which is native to Europe and Asia, have been known as a diuretic and rheumatic remedy since Hippocrates (147). The use of *Fr. excelsior* and *Fr. ornus* bark and leaves is described in the Bulgarian and Polish folk medicine to treat various diseases, such as diarrhea and dysentery (148). Furthermore, the European Pharmacopoeia (Ph. Eur. 9.2.) includes a monograph on the dried leaves of *Fr. angustifolia* and *Fr. excelsior* (148, 149).

2.7.2 Phytochemical characterization of the genus *Fraxinus*

The presence of coumarins, PhEGs and secoiridoids is described as the characteristic feature of the *Fraxinus* species. Other common SMs included flavonoids, lignans and simple phenolic compounds; however, they seemed to appear in a much more limited distribution. (148)

2.7.2.1 Coumarins

Free or glycosidically bound coumarins appeared in all investigated *Fraxinus* species, therefore distinguishing the genus from other genera in the familiy Oleaceae. Esculin and fraxin occured in all investigated species with varying ratios for different plant sources. (148)

2.7.2.2 Phenylethanoid glycosides

All in all, 9 PhEGs have been isolated from *Fraxinus* species. Among them, AO was the most abundant being isolated from 10 *Fraxinus* species, including *Fr. angustifolia* (150), *Fr. excelsior* (151), and *Fr. ornus* (152). Additionally, IsAO and DeIsAO were isolated from the bark of *Fr. ornus* (152). The vast majority of PhEGs in *Fraxinus* were shown to be present as caffeoyl esters, with salidroside being the only exception (148).

2.7.2.3 Secoiridoids

Oleoside-type secoiridoids usually occurred as glycosides in *Fraxinus* trees. In general, they formed esters with the hydroxyphenylethyl alcohols tyrosol and dopaol. (148)

Leaves of *Fr. angustifolia* yielded acylated derivatives of 10-hydroxyoleuropin, namely fraxicarbosides A, B, and C (150). The presence of methylated secoiridoid glycosides was reported in leaves of *Fr. angustifolia* (153). *Fr. angustifolia* was also shown to contain non-glucosidic secoiridoids oleobutyl and ligstrobutyl (153) as well as ligstral, the only secoiridoid having a rearranged secoiridoid nucleus in *Fraxinus* (146).

It has been suggested that macrocyclic secoiridoids may be considered as chemotaxonomic markers of *Fraxinus* species (154).

2.7.2.4 Compounds belonging to multiple structural classes

Esculeside from *Fr. ornus* bark was described to consist of a coumarin glucoside and a secoiridoid glucoside, which are ester-linked through the glucose of the coumarin and the carboxyl group of the secoiridoid moiety (149, 155, 156).

2.7.2.5 Flavonoids

The leaves of *Fr. angustifolia*, *Fr. excelsior*, and *Fr. ornus* mainly contained flavones and flavonols. The most frequently occurring compounds were kaempferol and quercetin, both in form of their aglycones and glycosides. (148, 150, 157)

2.7.2.6 Lignans

Fraxinus' lignans were found free or in form of their glucosides. Mainly, they belonged to the tetrahydrofurofuran type. (158, 159)

2.7.2.7 Simple phenolic compounds

4-hydroxybenzene, protocatechuic, vanillic, syringic, 2,4-dihydroxybenzoic, and gallic acids, as well as hydroxyderivatives of cinnamic acid (*p*-coumaric, caffeic, ferulic, sinapic acids), were found *Fr. excelsior* and *Fr. ornus* (148, 160). Furthermore, the free form of tyrosol and trace amounts of ornosol were present in *Fr. angustifolia* (148, 150).

2.7.2.8 Sterols and triterpenes

The leaves of *Fr. excelsior* contained the triterpenes ursolic acid, betulinic acid, and betulin. Sitosterol is known to be present in the leaves of *Fr. excelsior* and *Fr. ornus.* (148)

2.7.2.9 Other compounds

The water-soluble part of the bark extracts of *Fr. excelsior* and *Fr. ornus* contained the polyalcohol mannitol (148, 161, 162). Tannins of pyrocatechol type were found in the bark of *Fr. ornus*. Carotene was detected in leaves of *Fr. ornus*. Amino acids have been reported from the pollen of *Fr. excelsior*. (148) The seeds of *Fr. excelsior* have been shown to contain abscisic acid, indole-3-acetic acid, jasmonic acid, methyl jasmonate, and gibberellins. (148, 163)

2.8 Genus *Plantago*

2.8.1 Botanical characterization and traditional uses of the genus *Plantago*

The globally distributed *Plantago* species (Plantaginaceae) form a large genus comprising more than 200 annual and perennial species (164, 165). Among them, *Plantago lanceolata* L. (ribwort plantain), *P. major* L. (broadleaf plantain), and *P. media* L. (hoary plantain) are commonly found in Hungary as well (166, 167). The phylogeny of *Plantago* species is described as relying mainly upon morphological and embryological attributes (168). The most recent review classified the genus by molecular data and analyzed the internal transcribed spacer (ITS) matrix of 56 taxa, resulting in the division of the genus into five subgenera: *Plantago, Coronopus, Psyllium, Littorella*, and *Bougueria*, which in turn were subdivided into one or more sections (**Figure 15**) (169). The chemotaxonomical classification of the genus confirmed iridoid glucosides as chemotaxonomical markers. They were found to be helpful at the subgenus and section levels, but could not differentiate on the species level, partly due to the restricted number of compounds. (32)

DOI:10.14753/SE.2022.2639

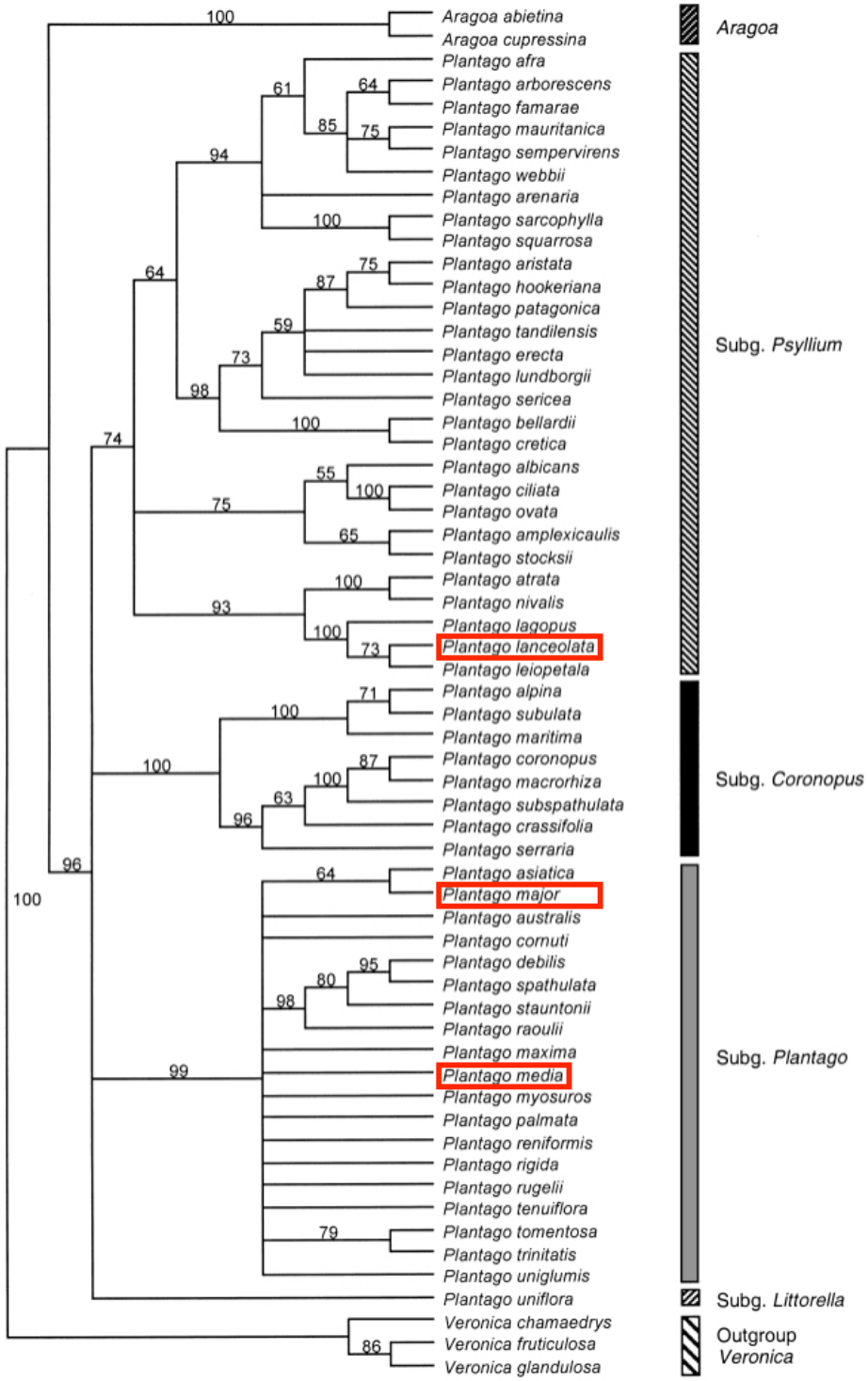

Figure 15: One of 72 most parsimonious trees obtained from the combined analysis of ITS nrDNA and *trnL-F* plastid DNA sequences. The figure indicates that *Plantago* subgenus *Albicans* is paraphyletic to subgenus *Psyllium sensu stricto* and therefore should be included in a broader subgenus *Psyllium sensu lato* (169).

DOI:10.14753/SE.2022.2639

The *Plantago* species are small herbs or rarely shrubs. Herbaceous species develop a taproot, or only numerous fibrous roots bearing rhizome systems as the underground organs. The simple petiolate leaves are ovate, elliptic, oblong, lanceolate, linear or subulate with entire, repand, erose or toothed, rarely pinnately or palmately cleft margin. The pyxis or rarely indehiscent capsule or nutlet contains one to numerous seeds. The spike arises from the rosette or leaf axil of the stem and contains tiny flowers (rarely 1-flowered) (**Figure 16, Figure 17**). (170)

Figure 16: Representatives of wild-grown *Plantago* in Hungary. The species were identified in the field based on macromorphological attributes, i.e., lanceolate leaves and short inflorescence for *P. lanceolata* (A), elliptic leaves, and short inflorescences for *P. media* (B), and ovate leaves and long inflorescences for *P. major* (C) (own work).

Figure 17: Underground parts of several years old *P. major*, consisting of a rhizome (A) and numerous fibrous roots (B) (own work).

Representatives of the genus are listed in the pharmacopoeias of several countries as safe medicinal plants (164). The aerial parts of *P. lanceolata* and *P. major* are used for the treatment of infections of the skin, digestive system, and respiratory tract due to the variety of active compounds (164, 171). The fresh leaves of *P. major* can also be used in the preparation of salads (172). There is no published data on the biological effects of *P. media*.

Industrially, the seeds of *Plantago* species are of special importance, because the psyllium could be used as a disintegrant in the formulation of fast-dissolving tablets (173), while the mucilage of *P. major* seeds is described as an easily obtainable and cheap coagulant for the treatment of dye-containing industrial wastewater (174).

2.8.2 Phytochemical characterization of the genus *Plantago*

Mostly, the aerial parts of *Plantago* species have been investigated, mainly regarding PhEGs and iridoid glycosides (164). The main bioactive compounds in the genus are PhEGs, iridoids, triterpenes, flavonoids, phenolic acids, and polysaccharides (164, 171).

2.8.2.1 Phenylethanoid glycosides

PhEGs are reported as key metabolites in *Plantago* species. Prevalent examples in the genus included PM and AO (175), while the presence of their isomers, IsoPM and IsAO, respectively, was much more limited (51, 80). Furthermore, the herb of *P. lanceolata* has been shown to contain cistanoside F and lavandulifolioside (176).

2.8.2.2 Iridoids and iridoid glycosides

Iridoids and iridoid glycosides were described as valuable intrageneric taxonomic markers for subgenera and sections, respectively (32, 175). Most *Plantago* species produced aucubin, bartsioside, catalpol, and 5-substituted iridoids, which were each specific for certain subgenera (32).

2.8.2.3 Flavonoids

Flavonoids were reported from several *Plantago* species, also including *P. lanceolata* and *P. major* (164, 177, 178). The main flavonoids present belonged to the

flavone subgroup, including luteolin and apigenin, which were present in form of their respective aglycones and glycosides (178).

2.8.2.4 Terpenoids

The terpenoids loliolid, ursolic acid, oleanolic acid, sitosterol, and 18β-glycyrrhetinic acid were present in the leaf of *P. major* (179, 180). Furthermore, triterpene acids were reported from aerial and underground parts of *P. major* (181, 182).

2.8.2.5 Alkaloids

The alkaloids indicain and plantagonin could be isolated from *P. major* (183).

2.8.2.6 Fatty acids

The seeds of *P. major* contained various fatty acids, including lignoceric (179), palmitic, oleic, linoleic, linolenic acids (184), and 9-hydroxy-*cis*-11-octadecenoic acid (185). Furthermore, unusual fatty acids were present, which may be useful in the oleochemical industry (186). *P. major* leaves contained arachidic and behenic acids (187).

2.8.2.7 Polysaccharides

Several polysaccharides were present in the seeds of *P. major* (188, 189) and the leaves of *P. media* (190). Furthermore, a highly esterified pectin polysaccharide was present in the leaves of *P. major* (191).

2.8.2.8 Vitamins

P. major was described as a good source of vitamin C and carotenoids (192).

2.9 Genus *Forsythia*

2.9.1 Botanical characterization and traditional uses of the genus *Forsythia*

Forsythia is a genus of 10 – 15 flowering plants in the tribe Forsythieae of the family Oleaceae, mainly found in East Asia (**Figure 18**). The exact number of species varies with the authors. (193). Currently, the World Checklist of Selected Plant Families (WCSP) recognizes 12 distinct species, which include 6 species in China (among them *Fo. suspensa* (Thunb.) Vahl.), 3 in Korea, 2 in Japan, and one in Europe (*Fo. europaea* Degen & Bald.). In addition to these species, a hybrid *Forsythia* (*Fo.* × *intermedia* Zabel) is also known. It is usually described as the natural hybrid of *Fo. suspensa* and *Fo. viridissima*, however, its origin is still disputed. (194-196)

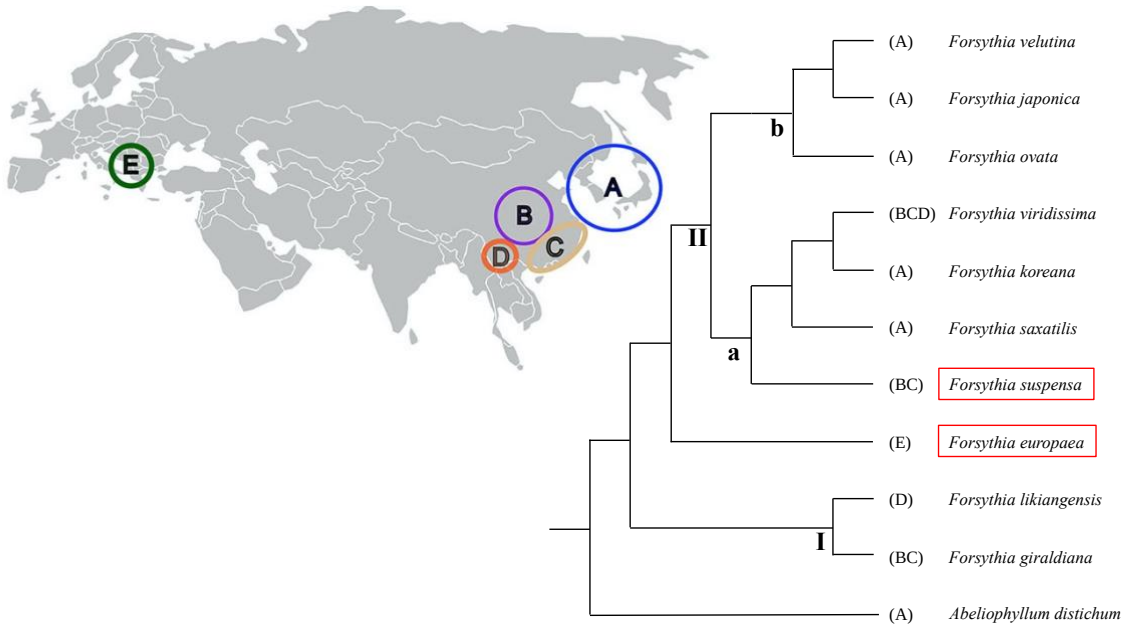

Figure 18: Phylogenetic tree resulting from Bayesian inference analysis and summary of Bayesian Binary Method (BBM) model of ancestral area reconstruction in Forsythieae. Clades and subclades are indicated by I, II, and a, b, respectively. Biogeographic regions used in BBM: A, Korea, and Japan; B, Central China; C, East China; D, Sikang-Yuennan; E, West Europe. *Fo. mira*, *Fo. nakaii* and *Fo. mandschurica* are not included; *Fo. togashii* is listed under its synonym *Fo. velutina* (194).

The deciduous shrubs produce yellow flowers in the early spring before the development of opposite simple leaves, hence the common name golden bells. The hollow branches of *Fo. suspensa* provide an important characteristic for its macromorphological differentiation from other *Forsythia* species, whose branches are

filled with a lamellate pith. The loculicidal capsules contain several winged seeds in each locule (196, 197) (**Figure 19, Figure 20**)

Figure 19: Unidentified *Fo.* × *intermedia* cultivar in Hungary (own work).

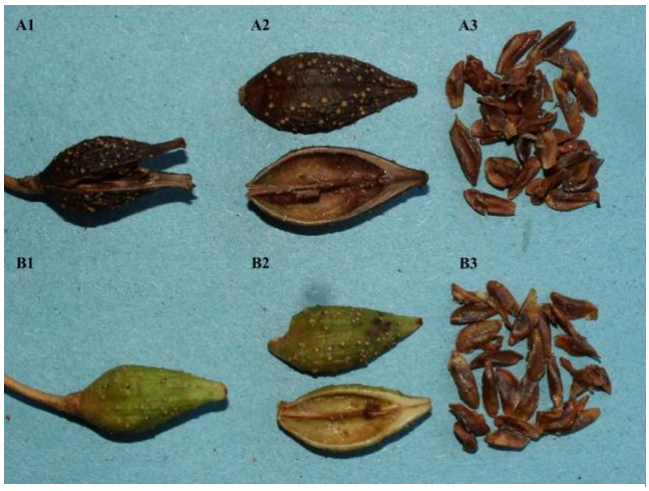

Figure 20: Mature (A) and immature (B) *Fo. suspensa* fruits, showing the whole fruits (A1, B1) as well as manually separated fruit walls (A2, B2) and seeds (A3, B3) (own work).

Extensive selection and breeding efforts following the introduction of oriental *Forsythia* species into western countries resulted in numerous cultivars, which are characterized by improved winter hardiness and abundant flowering in spring. Most of them derive from *Fo.* × *intermedia* and are of horticultural importance. (193)

The fruits and leaves of *Fo. suspensa* and *Fo. viridissima* are used in Chinese, Japanese, and Korean medicine to treat a variety of symptoms (198). TCM employs the fruits of *Fo. suspensa* ("Forsythiae Fructus", FF) for the treatment of pyrexia, inflammation, gonorrhea, carbuncle, and erysipelas. There is a variety of maturation stages available commercially, ranging from the greenish fruits, which are starting to ripe ("qingqiao") to yellow, fully ripened fruits ("laoqiao") (**Figure 20**). Both types serve as sources for FF. (69) Furthermore, the immature leaves are used as a health tea (199). The Korean Pharmacopoeia lists the fruits of *Fo. suspensa* and *Fo. viridissima* as the origin of FF, which is widely used for its antipyretic, antidotal, and anti-inflammatory effect. Additionally, the preparation was reported to suppress vomiting, resist hepatic injury, inhibit elastase activity, and exhibit diuretic, analgesic, antioxidant, antiendotoxin, and antiviral effects (200).

2.9.2 Phytochemical characterization of the genus *Forsythia*

The most current review of *Fo. suspensa* listed more than 230 constituents, 211 of which were isolated from FF (69). An earlier review on the whole genus *Forsythia* only listed 141 compounds (198). Nevertheless, both reviews agreed that PhEGs and lignans may be considered as the main active compounds in representatives of the genus.

2.9.2.1 PhEGs

PhEGs are described as the most important group of SMs present in *Forsythia* species, mainly occurring as caffeoyl esters (198). Until 2018, 31 PhEGs were isolated and identified from the fruits of *Fo. suspensa* (69). Their analysis started in 1982 with the isolation of FA and forsythoside D from fruits of *Fo. suspensa* (201). The regioisomers of FA, i.e., FI and FH, were also isolated; however, they only occurred in very small amounts (71). Due to its important role in the bioactivity of *Fo. suspensa*, FA is listed as a marker compound in the quality control standard of FF in the Chinese Pharmacopoeia (198).

2.9.2.2 Lignans

Lignans are reported as the second major group of SMs in *Forsythia* species. They occurred as free aglycones or glycosides. *Forsythia* lignans were classified into six groups: dibenzylbutanes, dibenzylbutyrolactones, arylnaphthalens, tetrahydrofurans, furofurans, and neolignans. According to the Chinese Pharmacopoeia, the most prevalent example phyllirin (syn. forsythin) is considered as the primary quality control standard in the crude drug analysis of *Fo. suspensa*. (198) Other common lignans included arctiin, arctigenin, matairesinol, pinoresinol, pinoresinol-β-D-glucoside, and phillygenin (70, 202-204).

2.9.2.3 Flavonoids

Rutin was the first flavonoid isolated from FF (205). Furthermore, wogonin-7-*O*-glucoside, hesperidin, hyperin, quercetin, kaempferol, and isorhamnetin were also reported (199, 206, 207).

2.9.2.4 Terpenoids

Up to 2017, 80 terpenoids have been isolated from representatives of the genus, mainly from the fruits of *Fo. suspensa*. The majority of them were triterpenoids, which were further categorized in penta- and tetracyclic triterpenoids (69). 2α,23-hydroxy ursolic acid and 2α-hydroxy betulinic acid were isolated from the genus (198). The first diterpenoids were isolated from FF in 2014 (206). *Forsythia'*s monoterpenes were categorized into monoterpene hydrocarbons and oxygenated monoterpenes. All of them were reported to be present in the essential oil of FF. (208, 209)

2.9.2.5 Iridoids

Iridoids are considered as a taxonomic marker in the family Oleaceae (210). Nevertheless, only a small number of iridoid glycosides have been isolated from the genus *Forsythia* (211-213).

2.9.2.6 C6-C2 natural alcohols

The three unique C6-C2 natural alcohols rengyol, rengyoxide, and rengyolone were firstly isolated from the fruits of *Fo. suspensa.* In the following years, more related compounds could be isolated from the fruits of *Fo. suspensa* (198, 214, 215).

2.9.2.7 Alkaloids

So far, nine alkaloids were isolated from *Forsythia* species, among them nortropine, tropine, suspensine A, (-)-egenine, and (-)-bicuculline (198, 203, 216).

2.9.2.8 Others

Other compounds isolated from the genus *Forsythia* included steroidals, organic acids, cinnamic acid derivatives, coumarins, and sugars (199, 203, 217-219).

Data on the metabolic profile of the various cultivars is scarce and so far, only two cultivars of *Fo.* × *intermedia* ('Golden Nugget' and an unknown cultivar) and *Fo. ovata* ('Robusta' and 'Tetragold') are described to contain lignans, carboxylic acids, and sugars (220).

DOI:10.14753/SE.2022.2639

2.10 Concluding remarks on the literary survey

Considering the biological effects of PhEGs summarized in **chapter 2.6**, their antiviral properties seem to be the most promising, since some PhEGs exhibit more potent antiviral effect than the approved antiviral drug. Prior to performing further efficacy studies (e.g., antiviral tests) with these natural products, their *in vitro* cytotoxic side effects on mammalian cells, such as Vero E6 cells should also be investigated. Vero E6 cells are often used in microbiology as a host cell model for growing viruses. In this model, promising drug candidates should have no cytotoxic effect against the Vero E6 cells (221). In addition, the safe use of PhEGs as natural medicines can also be presumed if they do not express toxicity against these cells.

DOI:10.14753/SE.2022.2639

3 OBJECTIVES

The main objective of this thesis was the determination of the main SMs, especially the PhEG-type compounds in *Fraxinus, Plantago,* and *Forsythia* tissues, which have not (or not extensively) been analyzed before. Namely, the analysis of 1) the galls of three European *Fraxinus* species, 2) the underground parts of wild-grown *Plantago* species, commonly found in Hungary, and 3) the leaves and separated fruit parts of *Forsythia* species, was planned. Based on this, our aims were to:

1) Determine the main SMs in the galls of *Fr. angustifolia, Fr. excelsior,* and *Fr. ornus*,
2) Determine the PhEG composition in the roots and rhizomes of wild-grown *P. lanceolata, P. major* and *P. media*,
3) Compare the PhEG profiles of *Forsythia* leaves (represented by *Fo.* × *intermedia, Fo. europaea,* and *Fo. suspensa*), and track changes in the phytochemical composition of *Fo. europaea* and *Fo. suspensa* fruit parts (i.e., fruit wall and seed) during their ripening process,
4) Develop an ultra high performance liquid chromatography-mass spectrometry (UHPLC-MS) method to achieve baseline separation of related PhEG-type compounds being present next to each other,
5) Increase the yield of minor PhEGs (IsAO, DeAO, DeIsAO, IsoPM, FI, FH) by optimizing heat treatments of AO, PM, and FA, allowing the isolation of minor PhEGs by one-step preparative HPLC,
6) Study conversion processes of AO, PM, and FA during their heat treatments resulting in the formation of corresponding minor PhEGs and interpret the isomerization processes of PhEGs induced by heat treatments at the atomic level, using a computational method,
7) Analyze MS fragment profiles of PhEGs to determine diagnostic ions suitable for the distinction of regioisomeric pairs AO-IsAO, DeAO-DeIsAO, FA-FI-FH, and PM-IsoPM,
8) Confirm the real potential of selected *Fraxinus, Plantago,* and *Forsythia* tissues for the high-yield isolation of PhEGs,

9) Determine the *in vitro* toxicity of isolated compounds against normal cells (Vero E6), aiming to confirm their safe use as natural medicines and allowing to test their antiviral potency.

4 MATERIALS AND METHODS

4.1 Plant material and reagents

Galls of *Fr. angustifolia* Vahl, *Fr. excelsior* L., and *Fr. ornus* L. (caused by the phytophagous mite *Aceria fraxinivora*) (144) and underground parts of *P. major* L., *P. media* L., and *P. lanceolata* L. were collected from different Hungarian locations between May and November 2015 (*Fraxinus* species) and in June 2018 (*Plantago* species). The leaf and fruit samples of *Fo. europaea* Degen & Bald., *Fo. suspensa* (Thunb.) Vahl, and *Fo.* × *intermedia* Zabel cultivars were collected from the Botanical Garden of Szent István University, Villányi street 29 – 43, Budapest between July and October 2018.

The voucher specimens were deposited in the Department of Plant Anatomy, Eötvös Loránd University, Budapest, Hungary. The materials and reagents applied in the isolation and analysis of plant metabolites, such as acetonitrile (ACN), distilled water (DW), formic acid, methanol (Reanal, Hungary), methanol-d_4 (CD_3OD, 99.80% D), deuterium oxide (D_2O, 99.96% D) (VWR chemicals, Belgium), dimethyl sulfoxide-d_6 (DMSO-d_6), maleic acid, 3-(trimethylsilyl)-1-propane sulfonic acid-d_6 sodium salt (DSS-d_6), aesculin, 5-CQA (Sigma-Aldrich, USA) and trifluoroacetic acid (TFA; Serva, Germany) were all of analytical reagent grade of the highest purity available.

4.2 Preparation of extracts from *Plantago* and *Forsythia* plants for analyses and isolations

4.2.1 Performing heat treatments

Lyophilized and pulverized plant tissues (100.0 mg) were suspended in 2.0 mL DW in 5 mL screw-capped vials. These suspensions were heated at 100 °C for 30, 60, 120, 180, 300, and 420 min. After heating, the samples were lyophilized.

4.2.2 Preparation of plant extracts

Lyophilized and pulverized intact plant tissues (100.0 mg), as well as heat-treated and lyophilized tissues were extracted three times consecutively with 5 mL of 80 % v/v methanol at 60 °C for 30 min via a reflux condenser to prepare 15.0 mL stock solutions: the samples were centrifugated between each step and the insoluble material was reextracted and, finally, supernatants were combined. Aliquots of the stock solutions were used for UHPLC-UV-HR-MS analyses after their dilution with 80 % v/v methanol

(**chapter 4.4.1**). Dried stock solutions, prepared from the intact and from the 300 min heat-treated *P. major* rhizome samples (marked with collection number 2) and those from the 300 min heat-treated *Fo. suspensa* unripe fruit wall sample (marked with collection number 1) were dissolved in 2.0 mL of methanol for the isolation of PM, IsoPM, and forsythoside isomers (FA, FH, FI) by preparative HPLC (**chapter 4.4.2**), respectively.

4.3 Preparation of extracts and heat treatments of *Fraxinus* gall samples

4.3.1 Preparation of extracts

Lyophilized and pulverized gall samples (100.0 mg) were extracted three times consecutively with 5 mL of methanol as described above in **chapter 4.2.2** to prepare 15 mL stock solutions. These stock solutions were used after dilution with methanol for UHPLC-UV-HR-MS analyses (**chapter 4.4.1**). Dried aliquots (5.0 mL) of the stock solution prepared from *Fr. angustifolia* gall sample 1 and *Fr. ornus* gall sample 3 were dissolved in 1.0 mL of methanol (for the isolation of AO and cichoriin by preparative HPLC, **chapter 4.4.2**), DW (for performing heat treatments, **chapter 4.3.2.2**), and methanol-d_4 (for performing NMR analyses, **chapter 4.4.3**).

4.3.2 Performing heat treatments in distilled water and trifluoroacetic acid

4.3.2.1 Treatment optimization of isolated AO

0.624 mg amounts of isolated AO were dissolved in 1.0 mL DW, 0.2 M TFA, 0.6 M TFA and 2 M TFA (in 4 mL screw-capped vials). These solutions were heated for 7, 15, 30, 60, 120, 300, and 600 min at either 50 °C or 100 °C. The samples were dried using a vacuum evaporator (at 30 – 40 °C). The dried samples were analyzed after their dissolution in 80 % v/v methanol by UHPLC-UV-HR-MS (**chapter 4.4.1**).

4.3.2.2 Optimized treatments of gall extracts for isolation purposes

Dried aliquots (5.0 mL) of the stock solution, prepared from *Fr. angustifolia* gall sample 1, were dissolved in 1.0 mL DW to isolate IsAO, DeAO, and DeIsAO. This solution was heated at 100 °C for 300 min (as optimum condition) to prepare IsAO. A two-step heating procedure was applied to prepare DeAO and DeIsAO. The first step was the same as that for IsAO preparation, and then TFA (0.181 mL) was added to the DW solution to prepare 2 M TFA medium. In the second step of the treatment, this acidified

solution was heated at 100 °C for 15 min (as optimum condition). After heat treatment, the samples were dried using a vacuum evaporator (at 30 – 40 °C). The dried samples were dissolved in methanol before isolations were performed using preparative HPLC (**chapter 4.4.2**).

4.4 Instruments

4.4.1 Analytical UHPLC hyphenated with UV and high-resolution Orbitrap mass spectrometric detections

A Dionex Ultimate 3000 UHPLC system (3000RS diode array detector (DAD), TCC-3000RS column thermostat, HPG-3400RS pump, SRD-3400 solvent rack degasser, WPS-3000TRS autosampler), hyphenated with an Orbitrap Q Exactive Focus Mass Spectrometer equipped with electrospray ionization (ESI) (Thermo Fischer Scientific, Waltham, Massachusetts, USA) was used for chromatographic separation and high-resolution mass spectral (HR-MS) analysis. The column temperature was set to 25 °C, flow rate to 0.3 mL/min. DAD spectra were recorded between 250 and 600 nm. The other UHPLC parameters are summarized in **Table 2**.

The ESI source was operated in negative ionization mode and operation parameters were optimized automatically using the built-in software. The working parameters were as follows: spray voltage, 2500 V (-); capillary temperature, 320 °C; sheath-, auxiliary- and spare-gases (N_2): 47.52, 11.25, and 2.25 arbitrary units, respectively. The resolution of the full scan was 70.000 in the scanning range of *m/z* 100 – 1000. MS/MS scans were acquired at a resolution of 35.000 in the scanning range of *m/z* 80 – 1000, using collision energies of 10, 20, 30, and 45 eV for *Fraxinus* gall samples and 20, 25, 30, 35, and 45 eV for *Plantago* and *Forsythia* samples.

Table 2: Parameters for analytical UHPLC of *Fraxinus*, *Plantago*, and *Forsythia* samples.

Parameter	*Fraxinus* gall samples (separation method 1)	*Plantago* and *Forsythia* samples (separation method 2)
Column	Kinetex C18 (75 × 3.0 mm; 3.5 µm) (Phenomenex, USA)	Kinetex XB-C18 (50 × 3.0 mm; 1.7 µm) (Phenomenex, USA)
Mobile phase	Solution A: 0.1 % v/v formic acid Solution B: ACN	Solution A: 0.1 % v/v formic acid Solution B: 8:2 ACN:0.1 % v/v formic acid

Gradient	Linear 0.0 min, 20% B; 12.0 min, 60% B	0.0 min, 10% B; 4.0 min, 20% B (linear); 8.0 min, 20% B (isocratic); 13.0 min, 70% B (linear)
Injected volume	1.0 µL	1.0 – 5.0 µL

4.4.2 Preparative HPLC

A Pharmacia LKB HPLC (Uppsala, Sweden) system (2248 pumps, VWM 2141 UV detector) was connected to a preparative HPLC column: Nucleosil100, C18 (10 µm), 15 x 1 cm (Teknokrama, Sant Cugat del Vallès, Barcelona, Spain). The mobile phases were the same as described for the analytical UHPLC. DAD spectra were recorded between 250 and 600 nm. The other parameters are summarized in **Table 3**.

Table 3: Parameters for preparative HPLC of *Fraxinus*, *Plantago*, and *Forsythia* samples.

Parameter	*Fraxinus* gall samples	*Plantago* and *Forsythia* samples
Gradient	See **Table 2**	Isocratic 10% B
Flow rate	3.0 mL/min	3.0 mL/min
Injected volume	200 µL per injection	300 µL per injection

4.4.3 Nuclear magnetic resonance (NMR) spectroscopy

NMR spectra of the isolated compounds were recorded in CD_3OD (PM, IsoPM, AO, IsAO, DeAO, DeIsAO, cichoriin) or DMSO-d_6 (FA, FI, FH) at 25 °C on a Varian DDR spectrometer (599.9 MHz for ^{1}H and 150.9 MHz for ^{13}C) equipped with a dual 5 mm inverse detection gradient (IDPFG) probe-head. NMR and quantitative NMR (qNMR) analyses were conducted and evaluated at the Department of Pharmaceutical Chemistry, Semmelweis University, Budapest, Hungary.

4.5 Compound quantification by UHPLC-MS

To quantify compounds by UHPLC-MS, extracted ion chromatograms (EICs) of their molecular ions were recovered from the total ion current chromatograms, and an external standard method was applied using EICs. Linear regression analyses of the isolated PhEGs AO, IsAO, DeAO, DeIsAO, PM, IsoPM, FA, FH, and FI, as well as that

of the standards aesculin, 5-CQA and rutin, were performed in the range of 0.057 – 10.00 ng of their injected amounts, resulting in appropriate r^2 values (higher than 0.9997 for each compound). Amounts of cichoriin and methoxy-dihydroxycoumarin-glucoside were calculated using the calibration curve for standard aesculin.

4.6 Computational modeling of the isomerization

Computations were carried out with the Gaussian09 (isomerization of AO) or Gaussian16 (isomerization of PM and FA) program package (Gaussian Inc., USA, Wallingford, Connecticut, 2009) (222) using the standard convergence criteria of 3.0×10^{-4}, 4.5×10^{-4}, 1.2×10^{-3} and 1.8×10^{-3}, for the gradients of the root mean square (RMS) force, maximum force, RMS displacement, and maximum displacement vectors, respectively. Computations were carried out at the B3LYP level of theory (223) using /6-31 G(d,p) basis set. The explicit-implicit solvent model was also included using the IEFPCM method (radii=UFF) (224) and seven explicit water molecules to model the aqueous media properly (225). The vibrational frequencies were computed at the same levels of theory, to properly confirm all structures as residing at the minima on their potential energy hypersurfaces. The thermodynamic functions *G*, *H*, and *S* were computed at 298.15 K. Computations were performed at Femtonics Ltd., Budapest, Hungary.

4.7 *In vitro* cytotoxic and cytostatic activity tests of isolated compounds on non-human primate Vero E6 cell culture

The cytostatic or cytotoxic effect of isolated PhEGs, cichoriin, and standard aesculin was measured on Vero E6 cells of non-human primate origin (kidney epithelia cells from *Chlorocebus aethiops*; ATCC No. CRL-1586) (226). The Vero E6 cells were kindly provided by Bernadett Pályi (National Biosafety Laboratory, National Public Health Institute, Hungary) and maintained in Dulbecco's Modified Eagle's Medium (Lonza™).

Cells were incubated with different concentrations of compounds for 24 h or 48 h in a 96-well plate and the cell viability was determined by a modified version of the classic (4,5-dimethylthiazol-2-yl)-2,5-diphenyltetrazolium bromide (MTT)-assay (221, 227) or by alamarBlue™ assay. A membrane-active cationic peptide (Transportan) or chloroquine diphosphate was used as a cytostatic or cytotoxic positive control,

respectively (221). All measurements were performed in quadruplicates and the mean cytostatic/cytotoxic % values, together with the standard error of the mean (SEM), were represented on the graphs. The *in vitro* experiments were conducted by the research group of Szilvia Bősze at the MTA-ELTE Research Group of Peptide Chemistry, Eötvös Loránd University, Hungarian Academy of Sciences, Budapest, Hungary.

DOI:10.14753/SE.2022.2639

5 RESULTS

5.1 Identification of compounds

During this work, 14 phenolic compounds were detected in the galls of *Fraxinus*, the underground parts of *Plantago*, as well as the fruits and leaves of *Forsythia* species (**Table 4**). Based on the comparison of our results with data available in the literature, compounds 1 – 7 were presumed to be PhEGs, compounds 8, 8a, and 10 to be coumarin derivatives, compound 9 to be a caffeic acid derivative, and compound 11 to be a flavonoid glycoside. Even though a high number of compounds is described in the investigated species, we only identified 14 compounds, since we focused on the presence of PhEGs.

DOI:10.14753/SE.2022.2639

Table 4: Identified compounds in galls of *Fraxinus*, underground parts of *Plantago*, and fruits and leaves of *Forsythia* species and their HR-MS/MS data, obtained by collision-induced dissociation (CID) using optimized fragmentation energy.

No.*	**Detected formula**	**Detected ion**	**Detected** *m/z*	Δ *ppm*	**Calculated** *m/z*	**MS/MS fragment ions** *m/z*	**Compound name**
1	$[M-H]^-$	$C_{29}H_{35}O_{15}$	623.19733	0.455	623.19705	135.04445; 161.02356; 179.03421; 461.16763; 623.19733	Forsythoside I[a]
2	$[M-H]^-$	$C_{29}H_{35}O_{16}$	639.19336	2.188	639.19196	135.04391; 161.02357; 179.03484; 315.11179; 477.16223; 639.19336	Plantamajoside[b]
3	$[M-H]^-$	$C_{29}H_{35}O_{15}$	623.19739	0.551	623.19705	135.04419; 161.02345; 179.03418; 461.16644; 623.19739	Forsythoside H[a]
4	$[M-H]^-$	$C_{29}H_{35}O_{15}$	623.19745	0.647	623.19705	135.04396; 161.02357; 179.03436; 461.16711; 623.19745	Forsythoside A[a]
5	$[M-H]^-$	$C_{29}H_{35}O_{15}$	623.19928	3.584	623.19705	135.04376; 161.02353; 179.03436; 315.10925; 461.16718; 623.19928	Acteoside[a, b, c]
5a	$[M-H]^-$	$C_{23}H_{25}O_{11}$	477.13959	0.943	477.13914	135.04388; 161.02341; 179.03407; 315.10867; 477.14044	Desrhamnosylacteoside[c]
6	$[M-H]^-$	$C_{29}H_{35}O_{16}$	639.19324	2.001	639.19196	135.04395; 161.02351; 179.03412; 315.10543; 477.16266; 639.19324	Isoplantamajoside[b]
7	$[M-H]^-$	$C_{29}H_{35}O_{15}$	623.19922	3.487	623.19705	135.04337; 161.02350; 179.03452; 315.10870; 461.16742; 623.19922	Isoacteoside[a, b, c]

DOI:10.14753/SE.2022.2639

7a	$[M-H]^-$	$C_{23}H_{25}O_{11}$	477.13956	0.880	477.13914	135.04404; 161.02341; 179.03403; 315.10895; 477.13914	Desrhamnosylisoacteoside[c]
8	$[M-H]^-$	$C_{15}H_{15}O_9$	339.07229	3.632	339.07106	-	Aesculin[c, -]
8a	$[M-H]^-$	$C_{15}H_{15}O_9$	339.07229	3.632	339.07106	-	Cichoriin[c, -]
9	$[M-H]^-$	$C_{16}H_{17}O_{19}$	353.08806	3.828	353.08671	135.04321; 179.03351; 191.05441; 353.08806	Chlorogenic acid[a, c]
10	$[M-H]^-$	$C_{16}H_{17}O_{10}$	369.08292	3.532	369.08162	-	Methoxy-dihydroxycoumarins[c]
11	$[M-H]^-$	$C_{27}H_{29}O_{16}$	609.14557	0.918	609.14501	-	Rutin[a]

[*] Numbers correspond to the retention order of compounds, determined by UHPLC.

[a] The compounds were detected in fruit and leaf samples of *Forsythia* species.

[b] The compounds were detected in underground parts of *Plantago* species

[c] The compounds were detected in gall samples of *Fraxinus* species

[-] The compounds were not studied.

5.1.1 Ultra high performance liquid chromatography separation of compounds

Compounds 1 – 7 could be effectively separated from each other by our UHPLC separation method (separation method 2; **Table 2, Figure 21**).

Among the PhEGs, compounds 5 and 7 were distributed throughout the samples of *Fraxinus*, *Plantago*, and *Forsythia* species (**Figure 22, Figure 24, Figure 25, Figure 26, Figure 27**), while compounds 2 and 6, as well as 1 and 4, were limited to the genera *Plantago* (**Figure 24**) and *Forsythia* (**Figure 25, Figure 26, Figure 27**), respectively. The presence of the PhEGs 5a and 7a was limited to *Fraxinus* species; furthermore, *Fraxinus* galls were characterized by the presence of compounds 8 and 8a, as well as their methoxy derivatives (10) (**Figure 22**), while 11 was limited to the fruits and leaves of *Forsythia* species (**Figure 25, Figure 26, Figure 27**). We detected compound 9 in gall samples of *Fraxinus* (**Figure 22**) and leaves of *Forsythia* (**Figure 25**) species, however, it was not ubiquitously present among the samples within each genus.

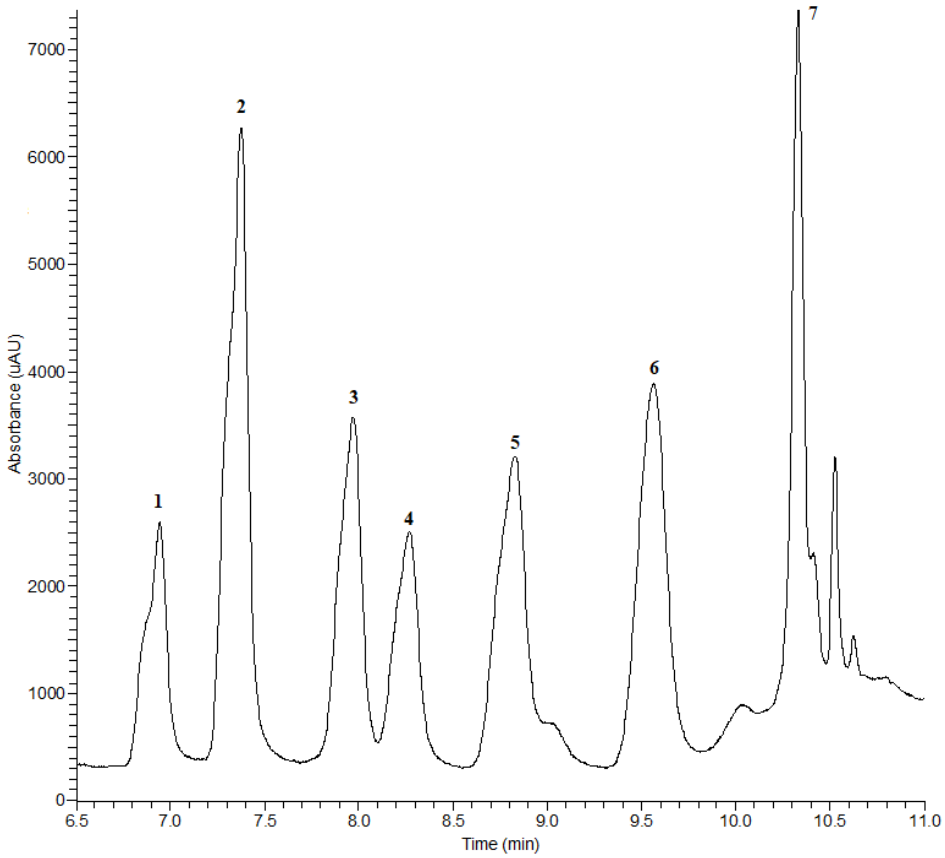

Figure 21: UHPLC separation of compounds 1 – 7, isolated from their optimum sources. The spectrum was recorded at λ = 270 – 370 nm. For assignment of numbers to the respective compounds refer to **Table 4**.

5.1.1.1 Compounds in galls of *Fraxinus* species

The UHPLC-UV-HR-MS separations of *Fr. angustifolia*, *Fr. excelsior*, and *Fr. ornus* gall extracts show similar metabolite compositions (**Figure 22**). Based on HR-MS data, compounds appearing with comparable retentions in the chromatograms of gall extracts of the three species are characterized by identical molecular formulas (**Table 4**). Comparing this data with that obtained for already identified compounds of *Fraxinus* species, coumarin glucosides (8, 8a) and a methoxy derivative of a coumarin glucoside (10), four PhEGs that differ from each other by the presence (5, 7) or absence (5a, 7a) of a rhamnosyl moiety, and an isomer of caffeoylquinic acid (9) were presumed to be present

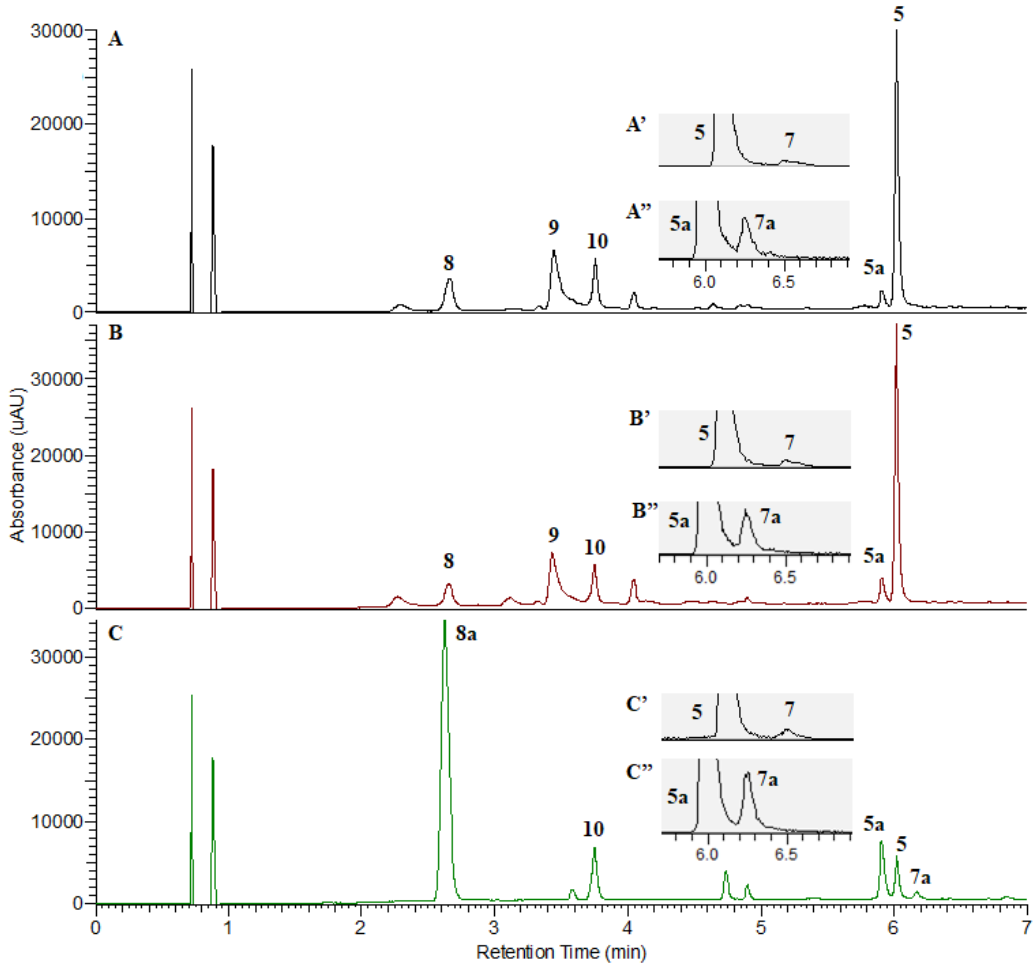

Figure 22: UHPLC separation of *Fr. angustifolia* gall sample 1 (A, A', A''), *Fr. excelsior* gall sample 1 (B, B', B'') and *Fr. ornus* gall sample 1 (C, C', C''). Full chromatograms (A, B, C) were recorded using UV detection (λ = 270 – 370 nm), and trace chromatograms (A', A'', B', B'', C', C'') were obtained by MS detection, monitoring the extracted ion current for *m/z* 623 (A', B', C') and *m/z* 477 (A'', B'', C'') corresponding to PhEGs. For assignment of numbers to the respective compounds refer to **Table 4**.

in *Fr. angustifolia*, *Fr. excelsior,* and *Fr. ornus* gall extracts. Since these compounds may all be present as regioisomers, further analyses, i.e., NMR, UHPLC-HR-MS/MS as well as computational conversion studies, were conducted to determine their constitutions.

Subsequent to the preparation of compounds related to 5 in galls of *Fraxinus* species (**chapter 4.3.2**), a preparative HPLC was performed as detailed in **chapter 4.4.2** to isolate compounds 5a, 7, and 7a (**Figure 23**).

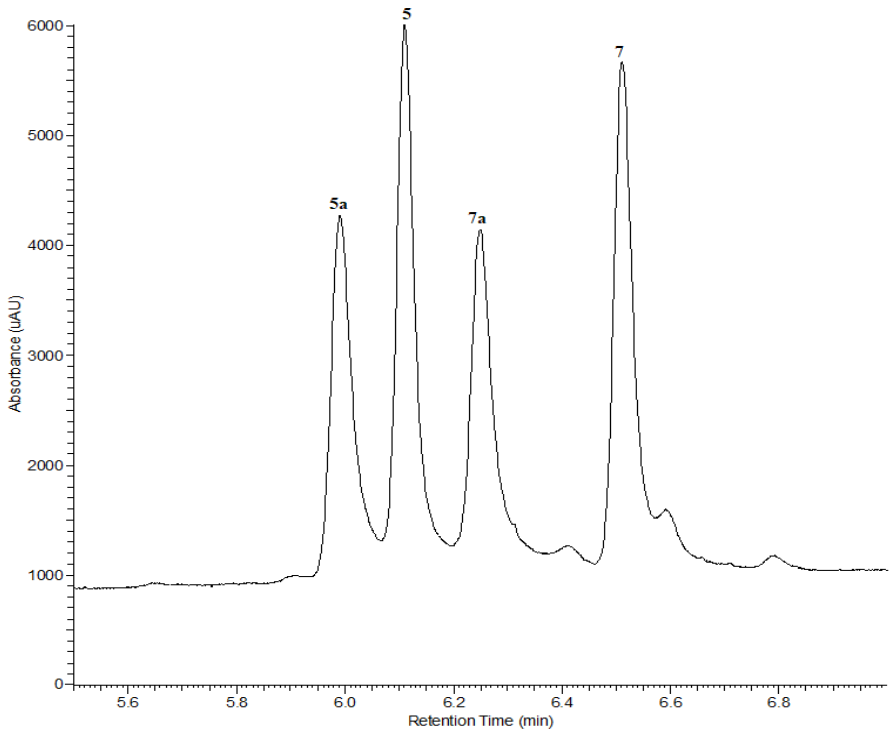

Figure 23: UHPLC separation of PhEGs in the gall of *Fr. excelsior* after consecutive DW and TFA treatments of the methanolic extract. The spectrum was recorded at λ = 270 – 370 nm. For assignment of numbers to the respective compounds refer to **Table 4**.

5.1.1.2 Compounds in underground parts of *Plantago* species

The UHPLC-DAD-UV separations of methanolic extracts of underground parts of *P. lanceolata, P. major,* and *P. media* showed a similar metabolic profile (**Figure 24**). Additional HR-MS data suggested the presence of four PhEGs in *Plantago* species, which contain a glucose (2, 6) or rhamnose (5, 7) unit as a second saccharide attached to the central β-D-glucose moiety of the PhEGs (**Table 4**). Similar to the analyses of *Fraxinus* gall extracts, further analyses, i.e., NMR, UHPLC-HR-MS/MS, and computational studies, were performed to elucidate the conformation of regioisomeric pairs.

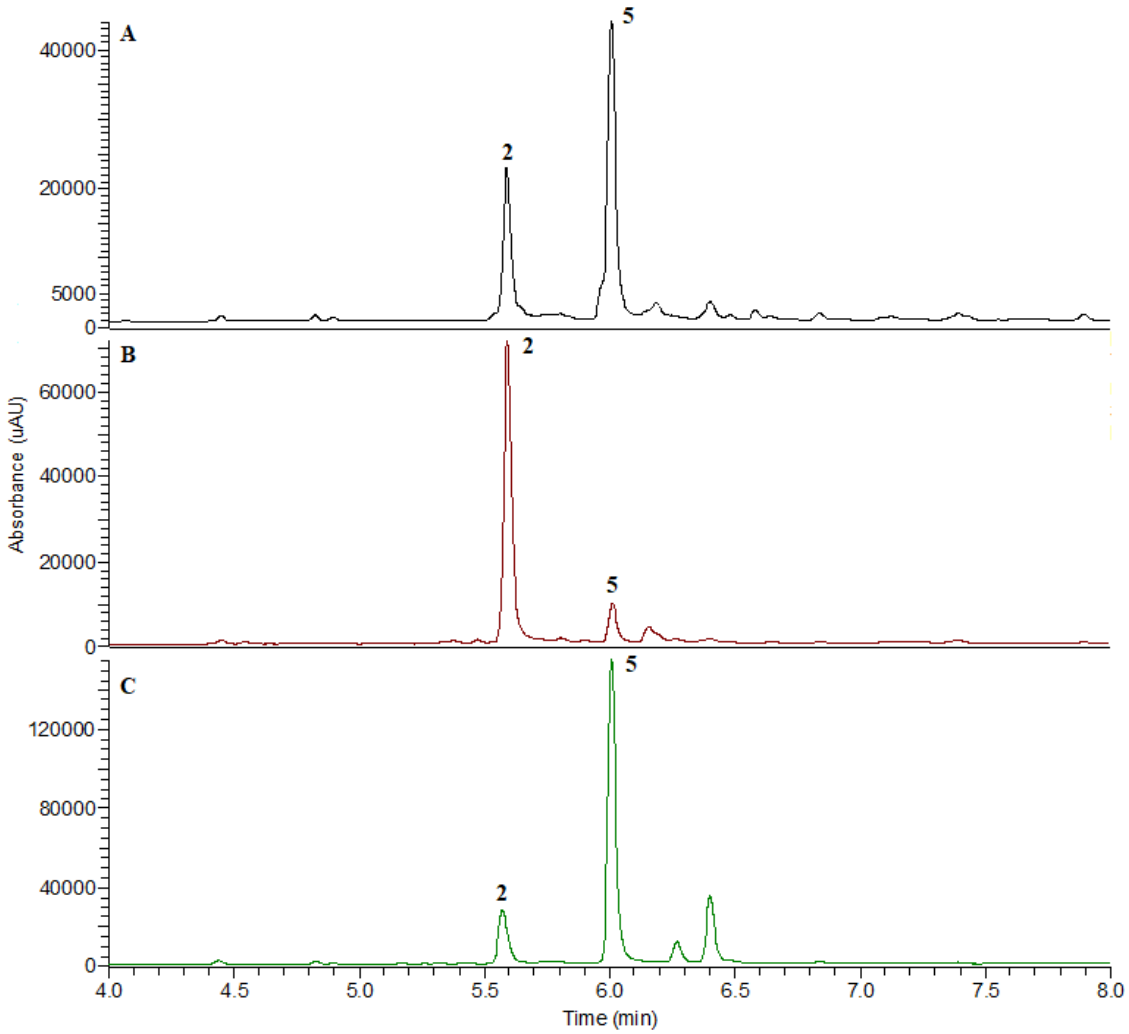

Figure 24: UHPLC separation of *P. lanceolata* several-year-old rhizome collection no. 1 (A), *P. major* complete young underground part collection no. 1 (B) and *P. media* old root collection no. 1 (C), showing the main components. The spectra were recorded at λ = 270 – 370 nm. For assignment of numbers to the respective compounds refer to **Table 4**.

5.1.1.3 Compounds in leaves and fruits of *Forsythia* species

The UHPLC-DAD-UV separations of methanolic leaf extract of *Fo. europaea*, *Fo. suspensa*, and various cultivars of *Fo.* × *intermedia* showed comparable metabolic profiles (**Figure 25**). While all extracts contained 11, they were distinguishable from each other based on the presence or absence of the PhEGs 4 and 5, identified by additional HR-MS data (**Table 4**). *Fo. europaea* leaves contained 5, while 4 was completely absent (**Figure 25A**). In contrast, the presence of 4 and the absence of 5 were indicative of the methanolic extract of *Fo. suspensa* leaves (**Figure 25B**). The leaves of various cultivars of *Fo.* × *intermedia* were characterized by the presence of both PhEGs (**Figure 25C**). Furthermore, an ester of caffeic and quinic acid (9) was found in the leaves of *Fo. europaea* and the cultivars of *Fo.* × *intermedia* (**Figure 25A, C**).

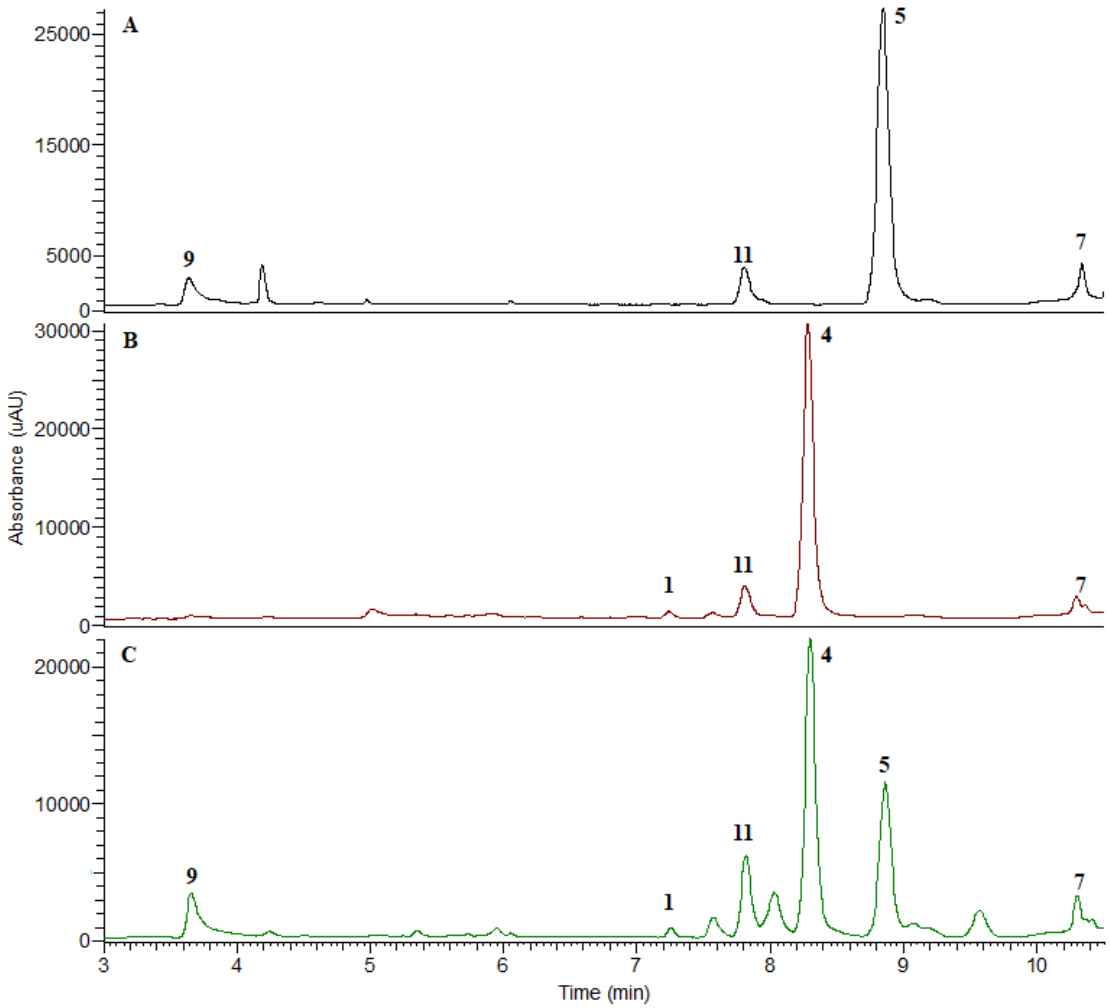

Figure 25: UHPLC separations of leaves of *Fo. europaea* collection no. 1 (A), *Fo. suspensa* collection no. 1 (B) and *Fo.* × *intermedia* 'Primulina' collection no. 2 (C). The spectra were recorded at λ = 270 – 370 nm. For assignment of numbers to the respective compounds refer to **Table 4**.

Based on their UHPLC-DAD-UV separations, the metabolic profile of *Forsythia'*s seed extracts (**Figure 26**) is much more limited than that of the corresponding leaves (**Figure 25**). The seeds of *Fo. europaea* were mainly characterized by the presence of compounds 11 and 5 (**Figure 26A**). In contrast, the presence of 4 was found to be characteristic for the methanolic seed extracts of *Fo. suspensa*, however, 11 was equally detected. Additionally, *Fo. suspensa* seed extracts contained 1, which was identified as a regioisomer of 4 based on additional HR-MS data. (**Figure 26B**)

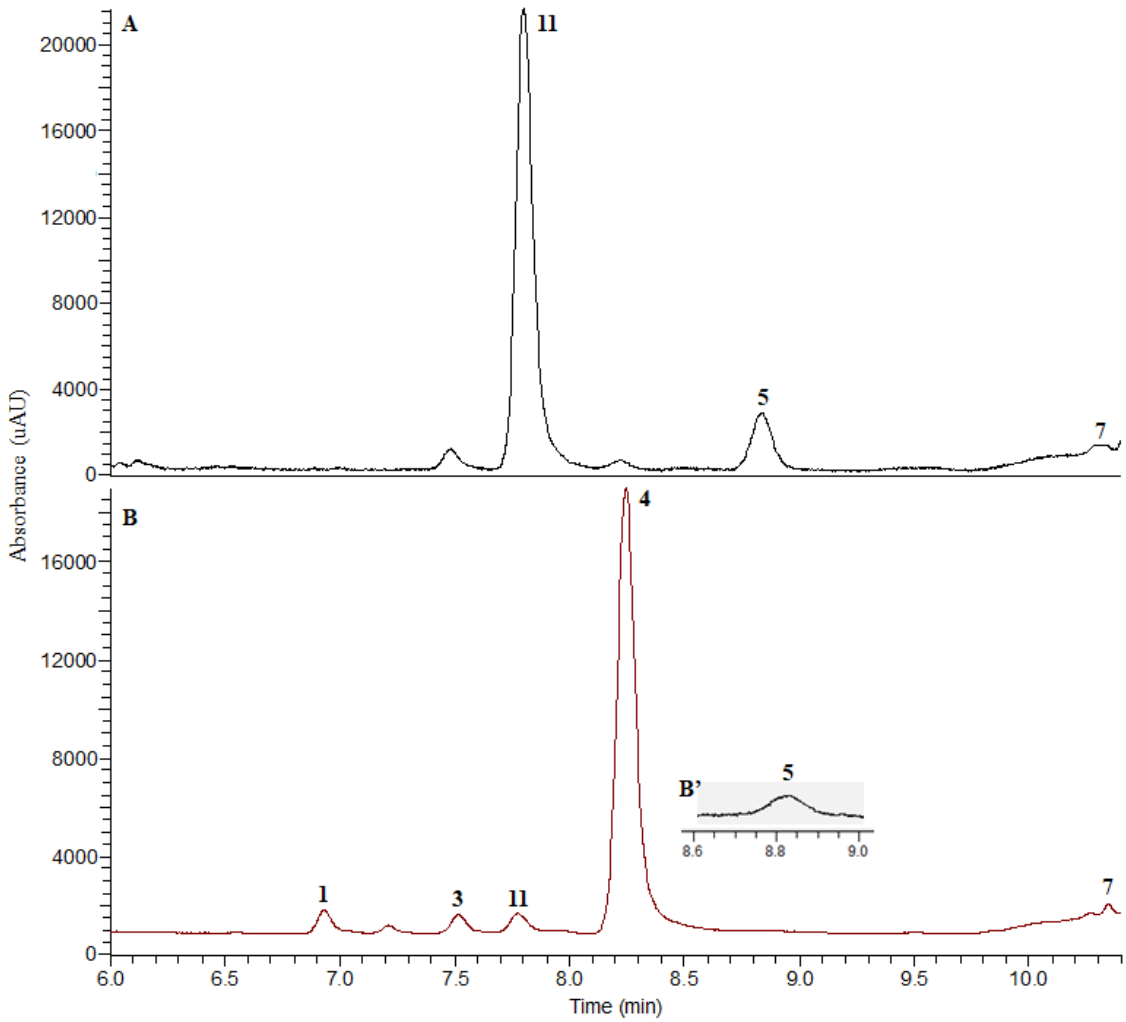

Figure 26: UHPLC separation of ripe seed samples of *Fo. europaea* collection no. 1 (A) and *Fo. suspensa* collection no. 1 (B). Full chromatograms (A, B) were recorded using UV detection at λ = 270 – 370 nm, and the trace chromatogram (A') was obtained by MS detection, monitoring the extracted ion current for *m/z* 623, corresponding to the PhEG. For assignment of numbers to the respective compounds refer to **Table 4**.

The phytochemical profile of fruit wall parts of *Forsythia* species is mainly characterized by the presence of the PhEGs 4 and 5. Furthermore, we showed that *Fo. suspensa* fruit wall contains PhEGs 1, 3, and 7, as well as compound 11 (**Figure 27**).

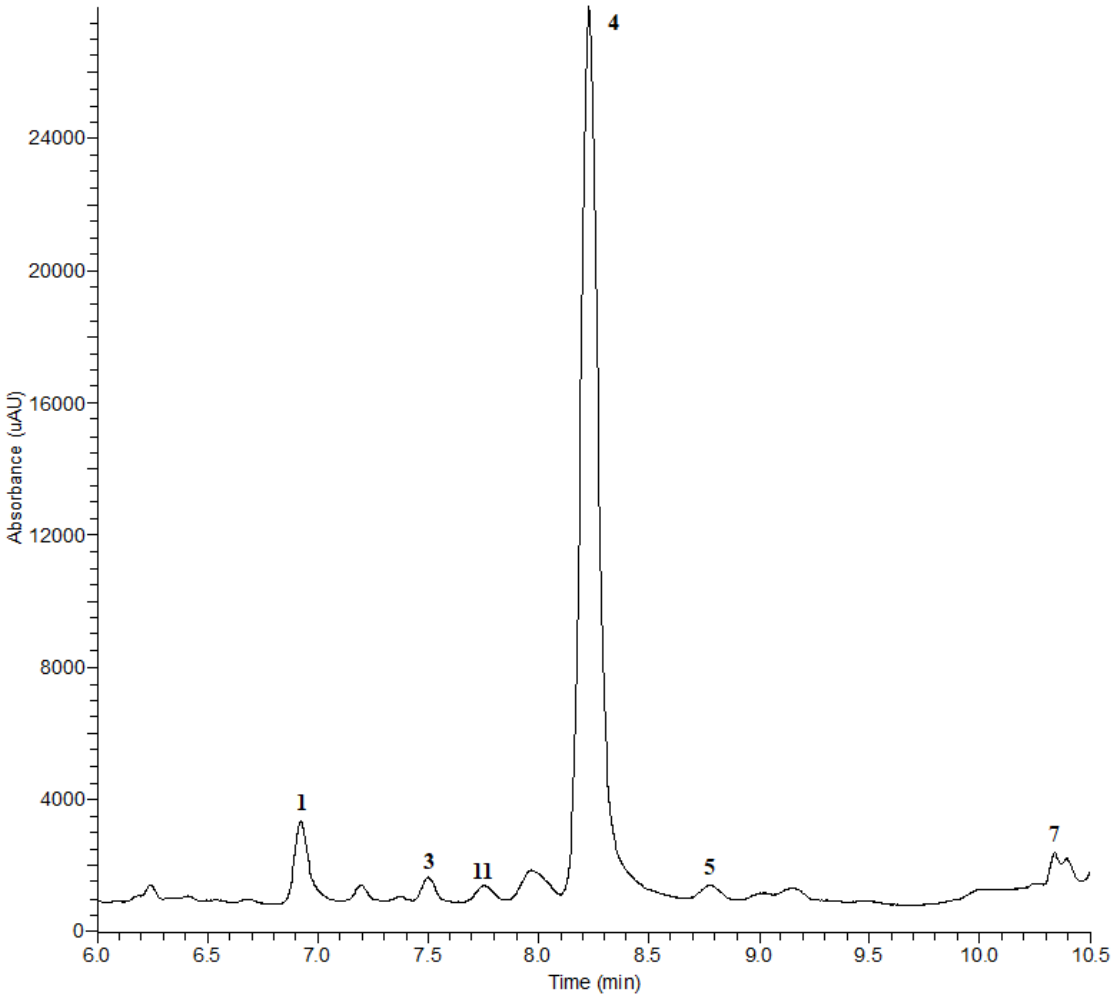

Figure 27: UHPLC separation of *Fo. suspensa* unripe fruit wall sample collection no. 1. The spectrum was recorded using UV detection at λ = 270 – 370 nm. For assignment of numbers to the respective compounds refer to **Table 4**.

DOI:10.14753/SE.2022.2639

5.1.2 Mass spectrometric studies

Compounds with identical elemental composition are indistinguishable by HR-MS analysis (**Figure 28**). Subsequent tandem mass spectra (MS/MS) of PhEGs characterized by the same molecular formula show comparable fragment ions after collision-induced dissociation (CID) using optimized fragmentation energy (**Figure 29**). Furthermore, we performed MS and MS/MS analyses of chlorogenic acid (**Figure 30**).

DOI:10.14753/SE.2022.2639

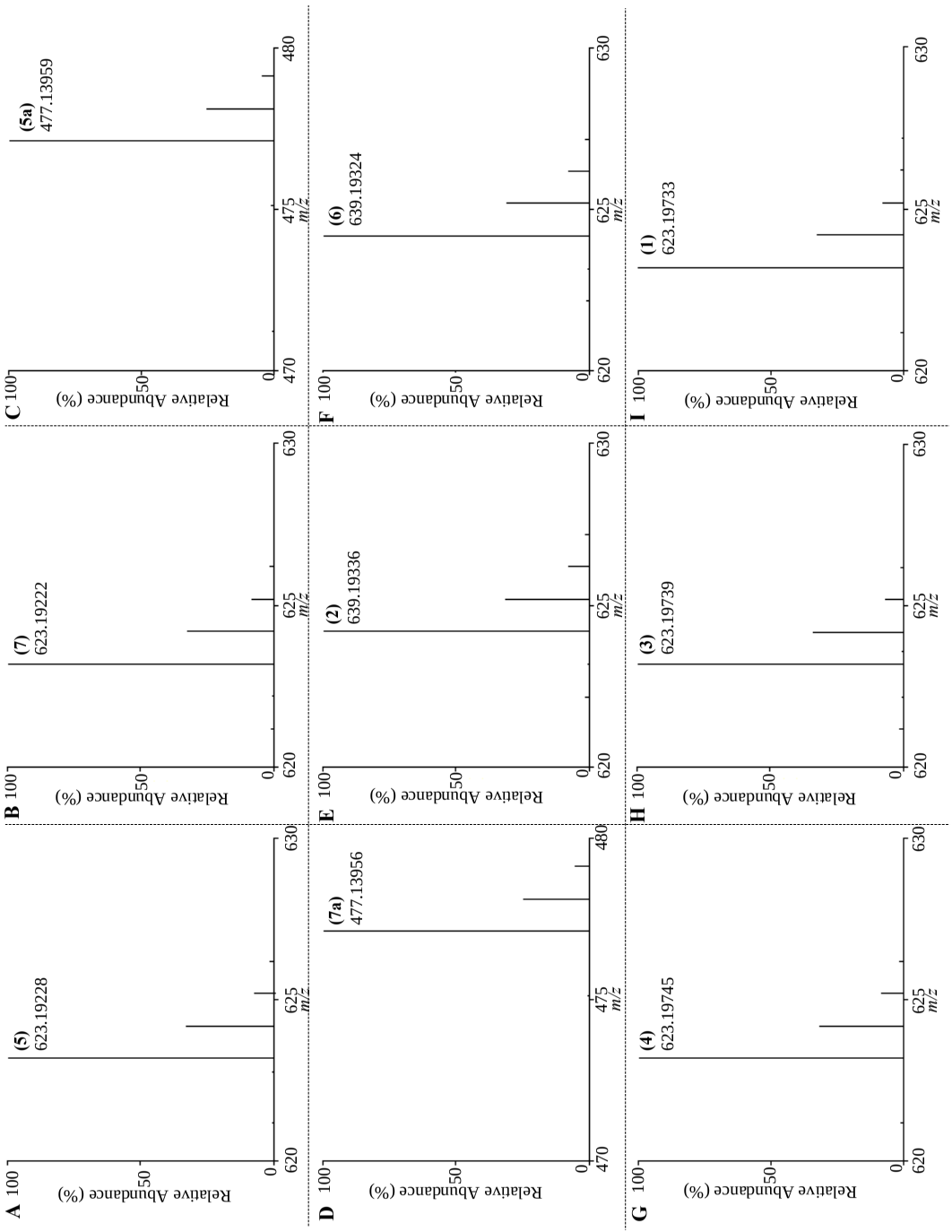

Figure 28: Mass spectra of PhEGs 1 – 7 (negative ionization) For assignment of numbers to the respective compounds refer to **Table 4**.

DOI:10.14753/SE.2022.2639

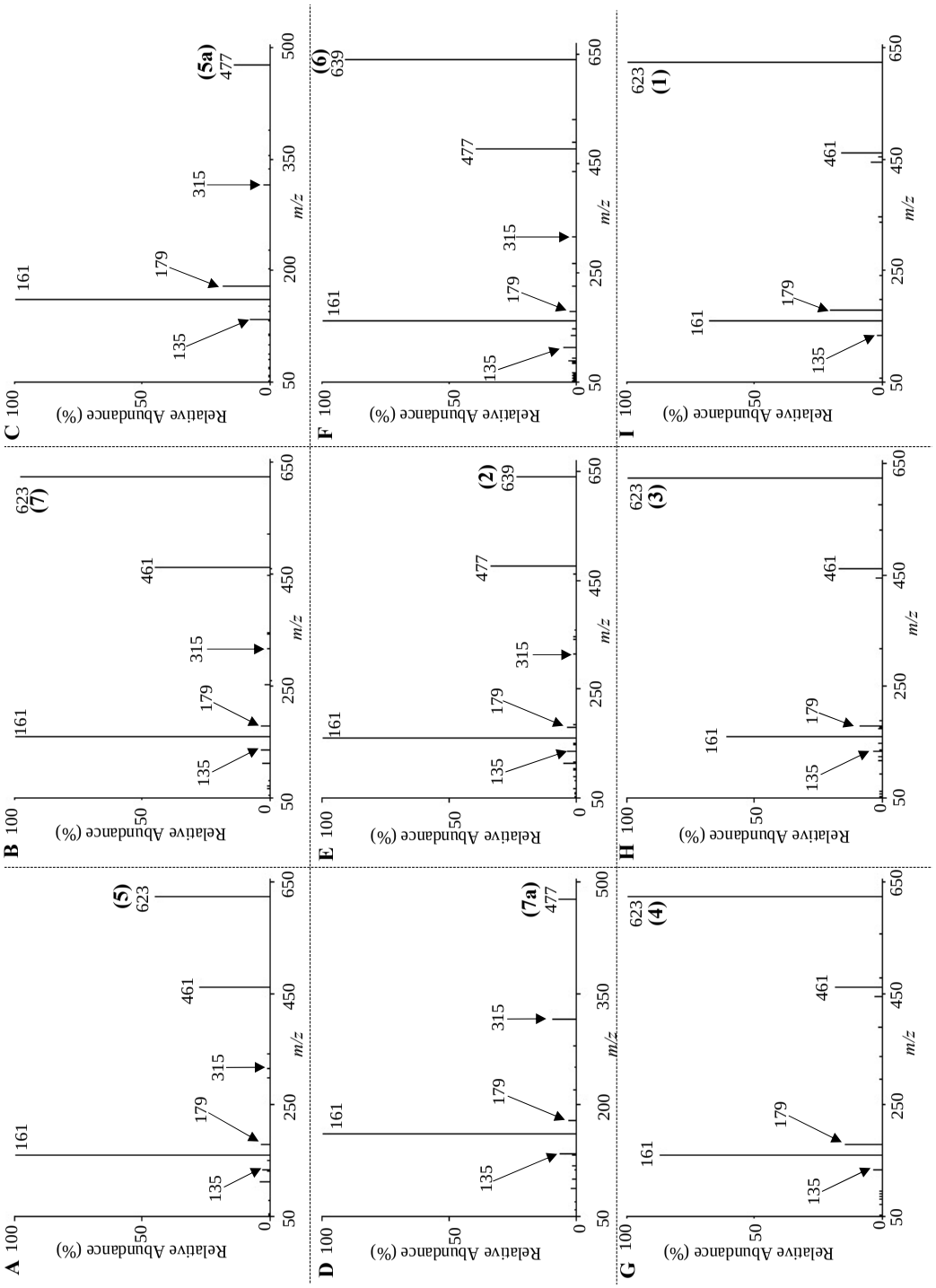

Figure 29: Tandem mass spectra (MS/MS, negative ionization) of the deprotonated molecular ions of PhEGs 1 – 7, obtained by CID at 30 eV (E, F) or 35 eV (A, B, C, D, G, H, I).

DOI:10.14753/SE.2022.2639

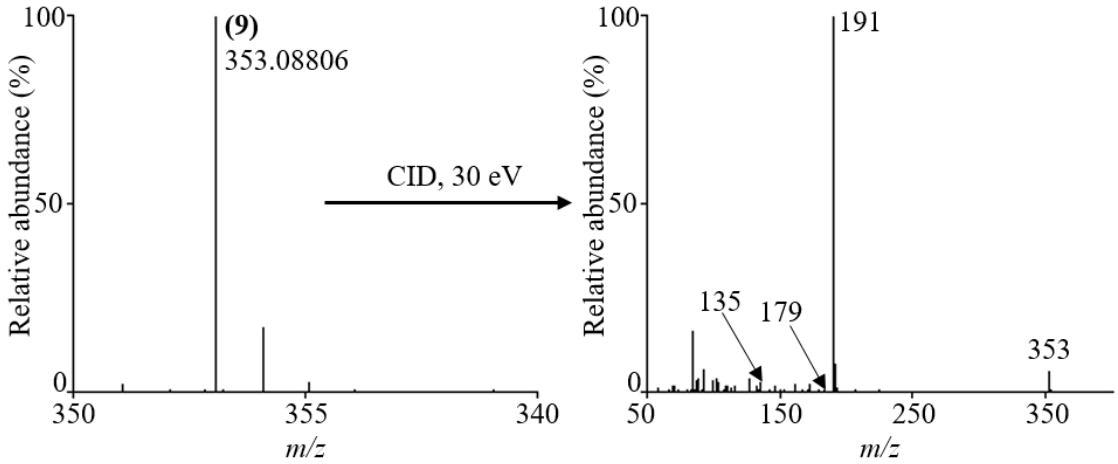

Figure 30: MS and MS/MS spectra (generated from the deprotonated molecular ion) of chlorogenic acid, obtained by CID at 30 eV.

5.2 Quantification of compounds

To quantify compounds by UHPLC-MS, extracted ion chromatograms (EICs) of their molecular ions were recovered from the total ion current chromatograms, and an external standard method was applied by using EICs. Linear regression analysis of the isolated PhEGs, as well as that of standards aesculin, rutin, and 5-CQA, was performed in the range of 0.057 – 10.0 ng of their injected amounts, resulting in appropriate r^2 values, higher than 0.9997. The amounts of cichoriin and methoxy-dihydroxycoumarin-glucoside were calculated using the calibration curve for standard aesculin.

5.2.1 Amounts of compounds in galls of *Fraxinus* species

The quantitative UHPLC-MS analyses of 15 gall samples collected from five different habitats of *Fr. angustifolia*, *Fr. excelsior*, and *Fr. ornus*, showed extraordinarily high amounts of AO (86.7 – 139.9 mg/g and 71.7 – 161.2 mg/g in galls of *Fr. angustifolia* and *Fr. excelsior*, respectively) and cichoriin (143.0 – 232.0 mg/g in galls of *Fr. ornus*) (**Table 5**). To confirm these remarkable results, triplicate parallels of methanol extracts of *Fr. angustifolia* (sample 1) and those of *Fr. ornus* (sample 3) galls were also analyzed using quantitative UHPLC-MS and qNMR spectroscopy. The differences were characterized by the relative standard deviation percentages of the three parallel tests: i) 128.0 mg/g (2.38 RSD%) and 119.3 mg/g (2.96 RSD%) AO in *Fr. angustifolia* (gall sample 1), and ii) 193.2 mg/g (3.02 RSD%) and 185.8 mg/g (2.24 RSD%) cichoriin in *Fr. ornus* (gall sample 3) were determined using UHPLC-MS and qNMR analyses, respectively.

DOI:10.14753/SE.2022.2639

Table 5: Composition of the dried gall samples of the three *Fraxinus* species, determined by UHPLC-MS. Corresponding chromatograms of *Fr. angustifolia* gall sample 1, *Fr. excelsior* gall sample 1, and *Fr. ornus* gall sample 1 are shown in **Figure 22**.

Fraxinus species	Gall samples (GSs)[a]	Amounts of compounds in the dried gall samples in mg/g[b]						
		Aesculin or cichoriin[c]	5-CQA	MeDCG	AO	IsAO	DeAO	DeIsAO
Fr. angustifolia	GS-1	14.2	38.6	13.5	128.0	1.06	8.09	0.556
	GS-2	6.05	30.1	8.52	101.3	2.25	3.34	0.482
	GS-3	13.3	30.6	11.3	112.4	0.985	4.63	0.494
	GS-4	10.3	24.9	7.18	86.7	0.706	4.82	0.400
	GS-5	18.0	41.0	15.5	139.9	1.86	8.08	0.822
	Average	12.4	33.0	11.2	113.7	1.37	5.79	0.551
Fr. excelsior	GS-1	12.1	39.8	15.2	161.2	1.73	15.0	1.15
	GS-2	17.9	24.8	18.8	122.5	0.996	21.3	1.04
	GS-3	10.8	18.3	9.50	88.7	0.887	20.7	2.01
	GS-4	4.65	6.43	15.9	71.7	2.79	15.6	4.95
	GS-5	16.0	24.2	16.3	132.1	0.991	15.0	1.01
	Average	12.3	22.7	15.1	115.2	1.48	17.5	2.03
Fr. ornus	GS-1	165.3	-	20.2	20.1	0.396	25.7	3.85
	GS-2	143.0	-	33.3	13.5	0.569	17.4	5.85
	GS-3	193.2	-	11.2	9.29	0.311	28.0	3.17
	GS-4	232.0	-	13.1	24.8	0.204	7.93	0.996

GS-5	170.7	-	10.1	8.59	0.374	31.2	2.99
Average	180.8	-	17.6	15.3	0.371	22.0	3.37

5-CQA: chlorogenic acid, MeDCG: methoxy-dihydroxycoumarin-glucoside, AO: acteoside, IsAO: isoacteoside, DeAO: desrhamnosyl-acteoside, DeIsAO: desrhamnosylisoacteoside.

[a] GSs 1-5 were collected from different localities of *Fraxinus* trees.

[b] Values are the averages of three separate extractions. Differences could be characterized by the relative standard deviation (RSD) values, ranging from 2.38% (AO in *Fr. angustifolia* GS-1) to 4.78% (CA in *Fr. excelsior* GS-2).

[c] GSs of *Fr. angustifolia* and *Fr. excelsior* contain aesculin and GSs of *Fr. ornus* contain cichoriin.

DOI:10.14753/SE.2022.2639

5.2.2 Amounts of compounds in underground parts of *Plantago* species

The underground organs of several-year-old *Plantago* plants can be separated into rhizome and root parts by manual dissection, allowing the comparison of their PhEG compositions. Since the rhizomes of young plants are undeveloped, only their root systems were analyzed.

The UHPLC-MS determination of PhEGs in 25 samples of underground parts of three *Plantago* species from different habitats revealed the high-yield accumulation of AO (53.0 – 99.7 mg/g) and PM (66.3 – 82.8 mg/g) in several-year-old rhizome of *P. media* and *P. major*, respectively. Furthermore, the analysis showed high amounts of IsAO (30.4 – 33.0 mg/g) and IsoPM (4.54 – 6.76 mg/g) in several-year-old roots of *P. media* (**Table 6**).

Table 6: Composition of the dried underground samples of three *Plantago* species, determined by UHPLC-MS. Corresponding chromatograms of *P. lanceolata* several-year-old rhizome collection no. 1, *P. major* young root collection no. 1, and *P. media* young root collection no. 1 are shown in **Figure 24**.

Plantago species	Organ sample[a]	Coll. no.[b]	Amounts of compounds in the dried samples in mg/g[c]			
			PM	IsoPM	AO	IsAO
P. major	root, young plants	1	60.5	3.64	7.34	1.24
		2	37.5	0.48	6.26	0.38
	rhizome, several-year-old plants	1	80.6	2.17	1.56	0.99
		2	82.8	2.09	6.00	0.58
		3	66.3	1.25	7.64	0.53
	root, several-year-old plants	1	20.2	3.24	14.1	1.97
		2	16.6	2.02	10.1	2.11
		3	18.0	0.29	10.4	0.55
P. lanceolata	root, young plants	1	7.75	0.91	29.2	1.13
		2	10.8	0.87	43.0	2.20
		3	8.35	0.25	38.0	2.30
	rhizome, several-year-old plants	1	15.1	1.68	30.3	3.73
		2	11.6	0.9	28.6	2.40
		3	8.09	0.13	13.9	0.52
	root, several-year-old plants	1	11.4	1.59	16.3	4.59
		2	6.98	0.79	9.45	2.21
		3	10.4	0.25	19.3	2.49
P. media	root, young plants	1	7.99	2.73	83.9	14.1
		2	10.7	3.56	73.5	10.1
	rhizome, several-year-old plants	1	17.0	3.56	86.8	16.1
		2	9.90	1.65	99.7	21.9
		3	5.22	2.07	53.0	18.1
	root, several-year-old plants	1	18.7	5.79	86.5	33.0
		2	18.8	6.76	86.7	30.5
		3	5.83	4.54	54.7	30.4

[a] Root system of young plants, which do not develop rhizomes, and separately collected roots and rhizomes of several-year-old plants were analyzed.
[b] Samples marked with 1 – 3 were harvested from different localities of *Plantago* plants.
[c] Values are the averages of three separate extractions. Differences could be characterized by the relative standard deviation percentages (RSD%), ranging from 3.2% (PM in *P. major* root of young plant, collection no. 2) to 6.8% (IsAO in *P. major* rhizome of several-year-old plant, collection no. 2)

DOI:10.14753/SE.2022.2639

5.2.3 Amounts of compounds in fruits and leaves of *Forsythia* species

We determined AO and FA to be the main components in the leaves of *Fo. europaea* and *Fo. suspensa*, with their highest amounts being 73.9 mg/g and 96.0 mg/g, respectively. The leaves of *Fo.* × *intermedia* cultivars are characterized by the simultaneous presence of AO and FA, with FA amounts being higher than those of AO. (**Table 7**)

The phytochemical composition in the seed and fruit wall parts of *Fo. suspensa* and *Fo. europaea* fruits was followed as a function of ripening time (**Table 8**). Similar to their leaf composition, fruit parts of *Fo. europaea* and *Fo. suspensa* accumulate mainly AO and FA, respectively. However, the amounts of these PhEGs show close correlation with the ripening process (as detailed in **chapter 6.5.2**).

DOI:10.14753/SE.2022.2639

Table 7: Composition of the dried leaf samples of three *Forsythia* species, including *Fo. europaea*, *Fo. suspensa* and 6 cultivars of *Fo.* × *intermedia*, determined by UHPLC-MS. Corresponding chromatograms of *Fo. europaea* collection no. 1, *Fo. suspensa* collection no. 1, and *Fo.* × *intermedia* 'Primulina' collection no. 2 are shown in **Figure 25**.

Forsythia species	Cultivar	Coll. no.[a]	Amounts of compounds in the dried leaves in mg/g[b]					
			5-CQA	Rutin	FA	FI	AO	IsAO
Fo. europaea	-	1	1.83	7.28	-	-	73.9	7.55
		2	11.09	4.17	-	-	73.2	5.81
Fo. suspensa	-	1	-	5.69	96.0	0.60	-	4.15
		2	-	4.75	80.6	0.42	-	3.03
Fo. × *intermedia*	'Lynwood'	1	1.04	3.8	25.6	0.11	10.1	0.25
		2	1.43	5.1	35.9	0.26	17.1	0.56
	'Melisa'	1	2.48	5.9	43.7	0.014	28.4	1.38
		2	0.52	2.1	12.0	0.008	5.90	0.19
	'Minigold'	1	2.09	11.4	45.1	0.013	19.8	0.56
		2	0.26	1.25	6.50	0.004	2.75	0.06
	'Primulina'	1	1.83	8.13	53.6	0.22	22.2	0.63
		2	2.22	8.44	66.4	0.28	24.6	0.50
	'Spectabilis'	1	0.78	3.19	18.3	0.007	9.69	0.25
		2	0.65	1.38	13.8	0.006	8.19	0.19

'Week End'	1	0.26	2.19	12.0	0.004	4.50	0.06
	2	1.94	0.31	36.1	0.013	16.3	0.44

[a] Collection numbers 1 and 2 correspond to two different individuals of *Forsythia* plants we sampled.

[b] Values are the averages of three separate extractions. Differences could be characterized by the relative standard deviation percentages (RSD%), ranging from 2.9% (FA in *Fo.* × *intermedia* 'Lynwood', collection no. 1) to 10.6% (FI in *Fo.* × *intermedia* 'Minigold', collection no. 2).

DOI:10.14753/SE.2022.2639

Table 8: Composition of the dried seed and fruit wall parts of *Fo. suspensa* and *Fo. europaea* fruits harvested at different maturity stages (StA, StB, and StC), determined by UHPLC-MS. Corresponding chromatograms for *Fo. europaea* ripe seed collection no. 1 and *Fo. suspensa* ripe seed collection no. 1, as well as *Fo. suspensa* unripe fruit wall collection no. 1 are shown in **Figure 26** and **Figure 27**, respectively.

Forsythia species	Tissue[a]	Maturity stage[b]	Coll. no.[c]	Amounts of compounds in the dried tissues in mg/g[d]						
				5-CQA	FA	FI	FH	AO	IsAO	Rutin
Fo. suspensa	Fruit wall	StA	1	-	87.0	5.93	0.41	2.72	3.33	0.82
			2	-	73.8	5.90	0.30	1.69	2.06	0.52
		StB	1	-	20.6	1.25	-	0.17	1.18	0.14
		StC	1	-	1.44	-	-	-	0.15	0.11
			2	-	1.88	-	-	-	0.062	0.023
	Seed	StA	1	-	58.2	3.68	0.13	0.32	2.00	1.00
			2	-	59.1	3.04	0.089	0.37	1.33	1.22
		StB	1	-	53.7	4.15	0.11	0.60	3.69	0.86
		StC	1	-	59.2	5.15	0.14	0.25	3.95	1.18
			2	-	64.1	4.03	0.074	-	1.35	1.51
Fo. europaea	Fruit wall	StA	1	26.5	-	-	-	77.3	11.6	2.14
			2	23.6	-	-	-	65.5	9.2	1.04
		StC	1	-	-	-	-	2.52	0.62	1.43
			2	-	-	-	-	2.31	0.58	0.44
	Seed	StA	1	3.13	-	-	-	19.3	1.81	4.76

DOI:10.14753/SE.2022.2639

	2	1.57	-	-	-	10.4	0.89	5.66
StC	1	-	-	-	-	1.97	0.13	2.43
	2	-	-	-	-	1.13	0.08	0.69

[a] Fruit wall and seed parts of the fruits were manually separated.

[b] Maturity stages (StA, StB and StC) correspond to unripe green, closed fruits (StA), ripe, yellow-brown, closed fruits (StB) and ripe, yellow-brown, opened fruits (StC).

[c] Collection numbers 1 and 2 correspond to two different individuals of *Forsythia* plants.

[d] Values are the averages of three separate extractions. Differences could be characterized by the relative standard deviation percentages (RSD%), ranging from 2.0% (FA in *Fo. suspensa* seed at maturity stage StA, collection no. 1) to 9.3% (IsAO in *Fo. suspensa* seed at maturity stage StC, collection no. 2).

5.3 Optimization of treatment parameters

5.3.1 Preparation of acteoside-related compounds

Starting with a sample containing AO, the other three related PhEGs, IsAO, DeAO, and DeIsAO, can also be prepared by consecutive DW and TFA treatments (**Figure 31**), however, treatment conditions, temperature, time, and acid concentration, need to be optimized to minimize unwanted decompositions. Acteoside treatment processes were therefore performed using DW and different concentrations of TFA (0.2 M, 0.6 M, and 2 M) at 50 °C and 100 °C, applying various heating times from 7 min to 600 min.

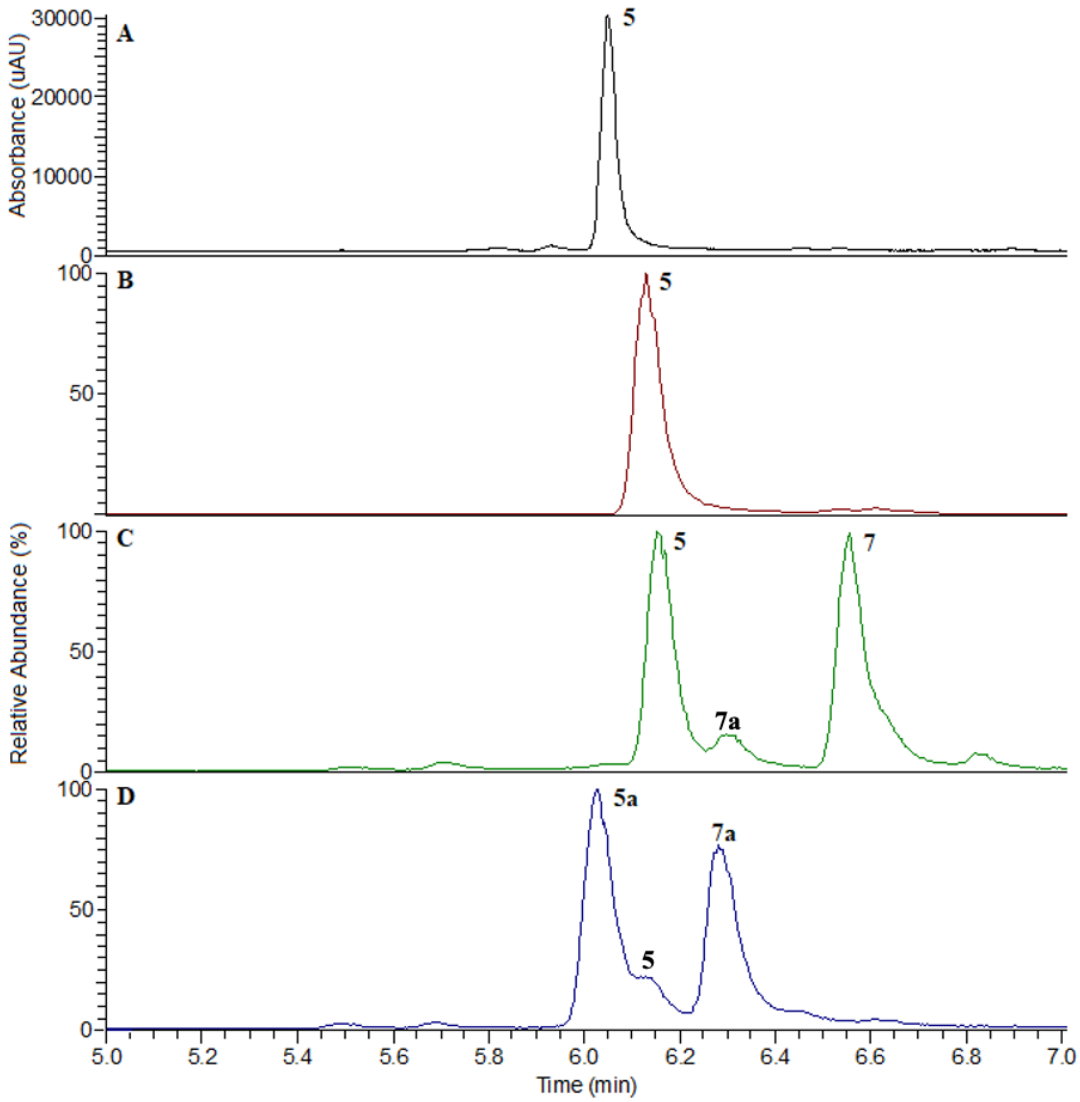

Figure 31: UHPLC-UV (λ = 270 – 370 nm) chromatogram (A) and extracted ion chromatograms (B – D) for *m/z* 623 and *m/z* 477 corresponding to PhEGs, obtained from the intact AO sample (A, B), and from the AO sample after DW (C; 100 °C, 120 min) and subsequent 2 M TFA (D; 100 °C, 15 min) treatments. **5**: acteoside, **5a**: desrhamnosylacteoside, **7**: isoacteoside, **7a**: desrhamnosylisoacteoside.

DOI:10.14753/SE.2022.2639

5.3.2 Preparation of isoplantamajoside

PM can be converted into IsoPM by DW treatment at 100 °C. However, treatment time needs to be optimized to avoid unwanted decomposition. Therefore, DW treatment of the PM-containing sample was performed using different incubation times, ranging from 120 min to 420 min (**Figure 32, Figure 40**).

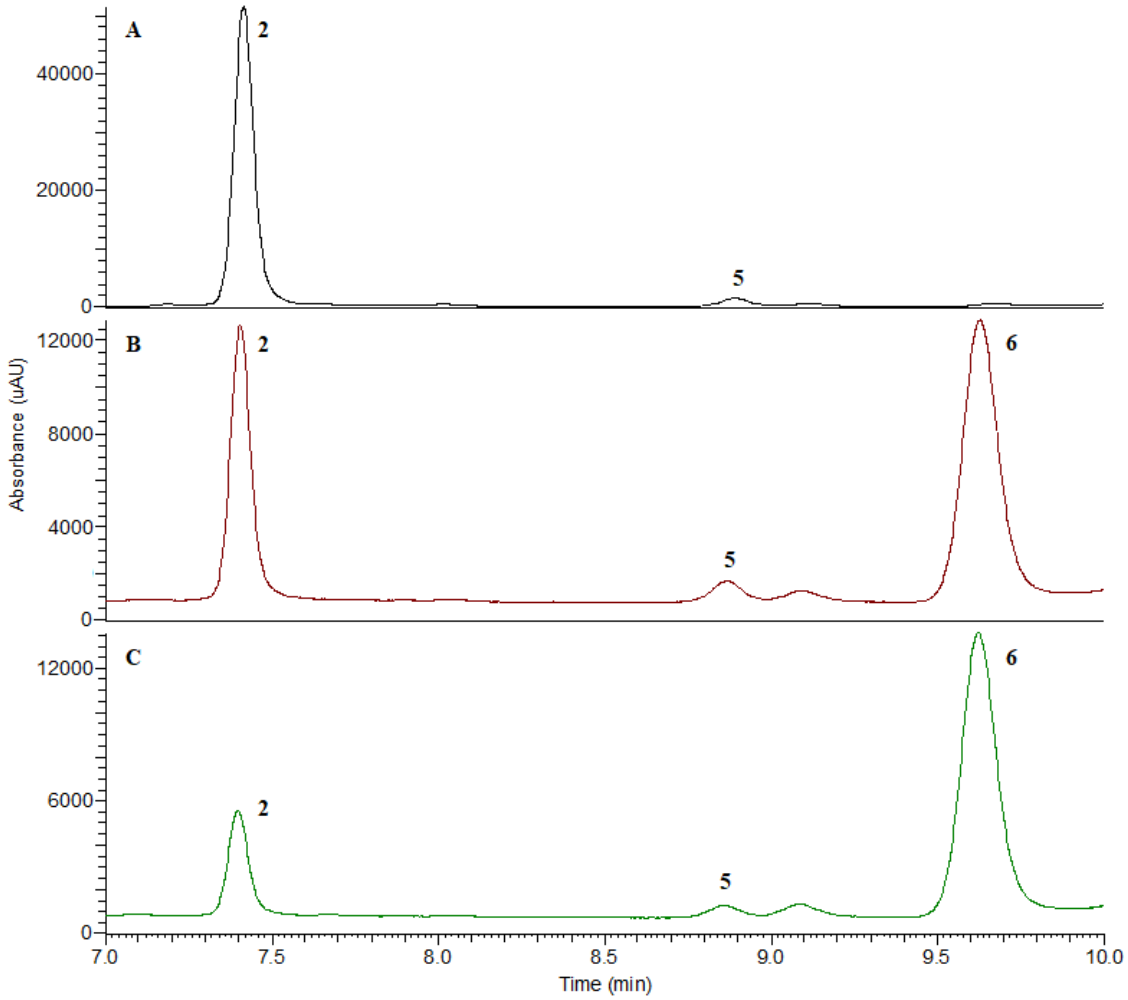

Figure 32: UHPLC-DAD-UV spectra of methanolic extract of *P. major* several-year-old rhizome (A), treated with distilled water at 100 °C for 120 min (B) and 420 min (C). The spectra were recorded at λ = 270 – 370 nm. **2**: plantamajoside, **5**: acteoside, **6**: isoplantamajoside.

DOI:10.14753/SE.2022.2639

5.3.3 Preparation of forsythoside A-related compounds

DW treatment of FA-containing samples resulted in the formation of FH and FI. To minimize unwanted decomposition, we subjected the FA containing green (unripe) fruit wall tissue of *Fo. suspensa* to increasing treatment periods ranging from 30 min to 420 min. Treatments were performed in DW at 100 °C. (**Figure 33**, **Figure 43**).

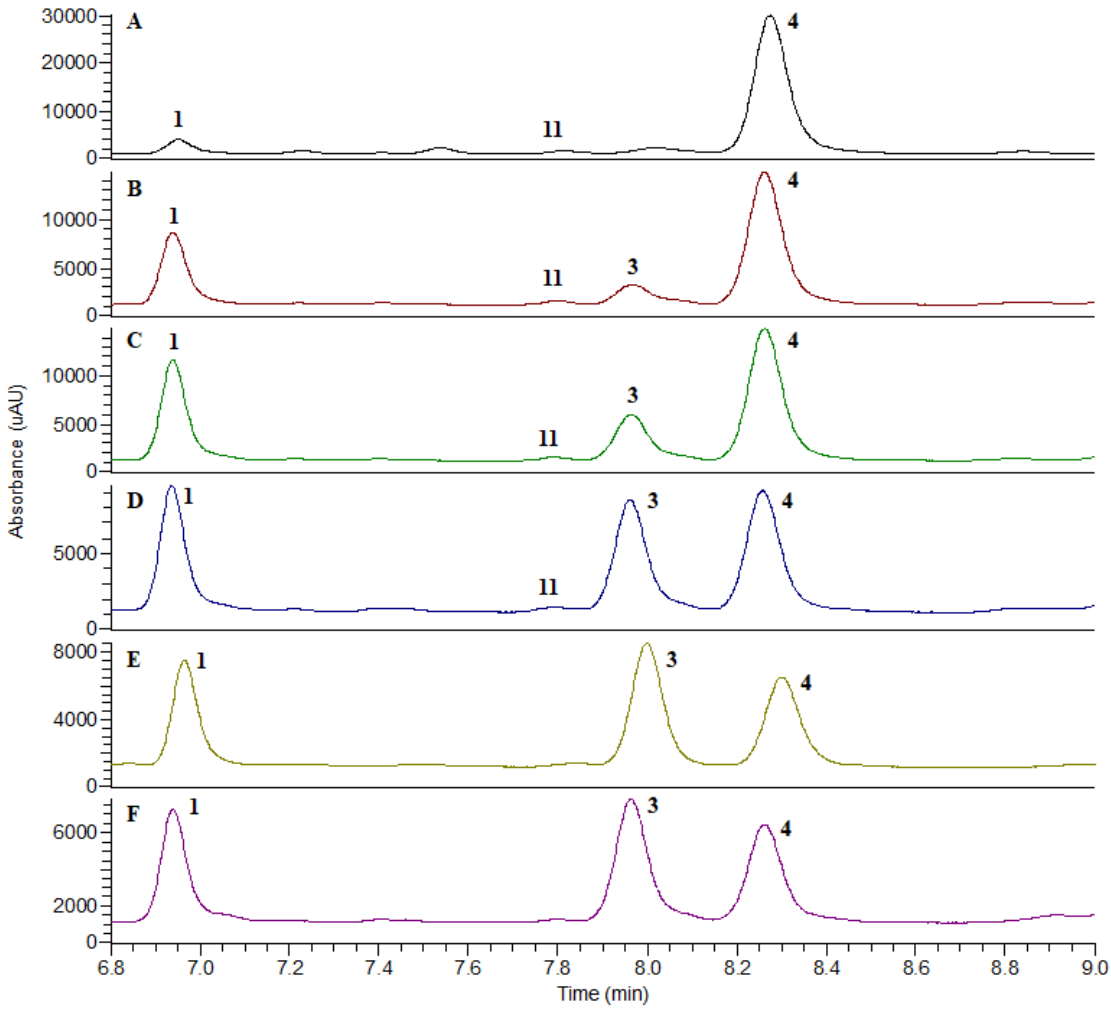

Figure 33: UHPLC-DAD-UV spectra of methanolic extract of *Fo. suspensa* unripe green fruit wall (A), treated with distilled water at 100°C for 30 min (B), 60 min (C), 180 min (D), 300 min (E), and 420 min (F). The spectra were recorded at λ = 270 – 370 nm. **1**: forsythoside I, **3**: forsythoside H, **4**: forsythoside A, **11**: rutin.

DOI:10.14753/SE.2022.2639

5.4 *In vitro* effects of compounds on Vero E6 cells

In vitro profiling of nine PhEGs (AO, IsAO, DeAO, DeIsAO, PM, IsoPM, FA, FH, and FI) and two coumarins (aesculin and cichoriin) was performed on Vero E6 cells.

No cytostatic or cytotoxic activity occurred on Vero E6 cells after treatment with the PhEGs and coumarins in the concentration range of 0.04 – 100 µM. Either a cationic membrane-active peptide (Transportan) or chloroquine was applied as a positive control. Transportan demonstrated relevant cytostatic activity on the Vero E6 cell culture (IC_{50} = 33.9 ± 5.5 µM), while 100 µM chloroquine exhibited time-dependent cytotoxicity, increasing from 30% after 24 h to 86% after 48 h exposure (**Figure 48, Figure 49**).

DOI:10.14753/SE.2022.2639

5.5 Computational modeling of the isomerization of phenylethanoid glycosides

The thermodynamic (driving force) and kinetic (reaction rate) aspects of the transformations of AO into IsAO, PM into IsoPM, as well as FA into FI and FH were studied using theoretical methods at the B3LYP/6-31 G(d,p) level of theory, with the IEFPCM solvent model by Gaussian09 (isomerization of AO) or Gaussian16 program package (isomerizations of PM and FA). During the transformation of AO into IsAO, the enthalpy (ΔH) and Gibbs free energy (ΔG) decrease equally by -1.0 kJ mol^{-1} and -2.8 kJ mol^{-1}, respectively, while entropy (ΔS) increases by +6.0 J mol^{-1} K^{-1} (**Figure 44**).

The transformation of PM into IsoPM was characterized by a much greater decrease of ΔH and ΔG of -24.2 kJ mol^{-1} and -26.2 kJ mol^{-1}, respectively. In contrast, ΔS increased by +6.7 J mol^{-1} K^{-1} (**Figure 45**).

During the transformations of FA into FI and FI into FH, ΔH and ΔG were near zero.

The calculated carbonylicity percentage values (*CA*%) of regioisomeric pairs were as follows: AO (52.8%), IsAO (53.0%), PM (52.2%), IsoPM (52.9%), FA (52.9%), FI (53.0%), and FH (52.5%).

The reaction mechanisms of the isomerizations of AO, PM, and FA were studied to estimate the reaction rate of the isomerization, using an explicit-implicit solvent model with 7 water molecules (**Figure 47**, **Table 10**).

6 DISCUSSION

6.1 Mass fragmentation study allowing phenylethanoid glycoside discrimination

Compounds characterized by the same molecular formula cannot be differentiated from each other based on their HR-MS analysis. However, in certain cases, differences in the relative intensities of selected fragment ions (SFIs), generated by CID can be used to discriminate these compounds. Thus, the difference in the relative ion intensities of two key fragment ions *m/z* 461 and *m/z* 179, corresponding to deprotonated hxdroxytyrosol rhamnosyl glucoside and caffeic acid moieties, allowed the discrimination between forsythoside isomers (FA, FI, FH) and acteoside isomers (AO, IsAO). The abundance ratios between *m/z* 461 and *m/z* 179 were calculated to be less than 1 for forsythoside isomers (0.80, 0.97, and 0.54 for FA, FH, and FI, respectively), while being higher than 5 for acteoside isomers (5.42 and 5.97 for AO and IsAO, respectively) (**Table 9**).

The discrimination of PhEGs from each other within their respective groups, i.e., forsythosides (FA, FH, FI), AO-related compounds (AO, IsAO, DeAO, DeIsAO), and plantamajosides (PM and IsoPM) is described in the following chapters (**chapters 6.3.1, 6.4.1, 6.5.1**).

Table 9: Relative intensities of selected fragment ions, generated from the molecular ions of isolated PhEGs by CID[a] followed by UHPLC-HR-MS/MS analyses of three injected amounts of the PhEGs.

Phenylethanoid glycosides	Injected amounts (ng)	Selected fragment ions, *m/z*							
		135	161	179	315	461	477	623	639
		Relative intensities (%)[b]							
Plantamajoside	10	1.5	57.2	1.53	1.10	-	17.8	-	13.3
	5	1.7	56.7	1.64	0.97	-	18.4	-	12.7
	1	2.2	54.9	1.54	0.72	-	17.6	-	12.5
	Average	1.8	56.3	1.57	0.93	-	**17.9**	-	**12.8**
Isoplanta-majoside	10	1.6	34.7	0.90	0.71	-	15.6	-	33.8
	5	1.1	35.0	0.78	0.66	-	15.0	-	34.1
	1	0.9	31.0	0.31	0.65	-	15.1	-	33.2
	Average	1.2	33.6	0.66	0.67	-	**15.2**	-	**33.7**

Forsythoside A	10	1.3	57.7	10.0	-	8.20	-	16.4	-
	5	1.2	52.8	10.8	-	8.45	-	14.6	-
	1	0.4	53.6	10.4	-	8.22	-	15.0	-
	Average	0.97	54.7	**10.4**	-	**8.29**	-	15.3	-
Forsythoside H	10	1.1	48.8	8.54	-	8.00	-	17.8	-
	5	1.2	50.3	8.67	-	8.57	-	19.2	-
	1	0.7	48.9	8.71	-	8.51	-	18.7	-
	Average	1.0	49.3	**8.64**	-	**8.36**	-	18.6	-
Forsythoside I	10	1.3	45.6	13.3	-	6.73	-	17.2	-
	5	1.3	43.5	12.1	-	6.24	-	15.7	-
	1	0.8	41.7	11.8	-	7.10	-	15.8	-
	Average	1.13	43.6	**12.4**	-	**6.69**	-	16.2	-
Acteoside	10	4.7	67.2	1.92	1.20	10.4	-	5.59	-
	5	4.7	68.7	1.96	1.17	11.0	-	6.00	-
	1	6.1	72.7	2.20	1.15	11.6	-	6.22	-
	Average	5.16	69.5	**2.03**	1.17	**11.0**	-	**5.94**	-
Isoacteoside	10	4.5	56.3	2.32	1.03	14.5	-	14.0	-
	5	4.2	60.6	2.61	1.00	15.6	-	14.1	-
	1	6.5	57.4	2.51	0.89	14.3	-	13.7	-
	Average	5.17	58.1	**2.48**	0.97	**14.8**	-	**13.9**	-
Desrhamnosyl-acteoside	6.4	5.0	63.2	12.6	1.5	-	11.3	-	-
	3.2	5.0	61.9	11.9	1.5	-	10.8	-	-
	0.64	5.1	71.0	14.0	1.9	-	11.5	-	-
	Average	5.03	65.37	**12.8**	**1.6**	-	11.2	-	-
Desrhamnosyl-isoacteoside	5.7	4.6	66.2	1.6	6.3	-	6.5	-	-
	2.85	4.0	71.6	1.6	6.5	-	5.7	-	-
	0.57	4.9	70.9	2.3	7.2	-	6.2	-	-
	Average	4.5	69.56	**1.8**	**6.67**	-	6.13	-	-

[a] An optimized CID energy of 30 eV was used for the fragmentation of PM and IsoPM, while fragmentation of FA, FH, FI, AO, IsAO, DeAO, and DeIsAO was performed using a CID energy of 35 eV

[b] Expressed as percentages of the sum of the total product ion current (FullMS2)

Bold printed data: average results of ion abundances, calculated from the three different injected amounts of PhEGs, allowing the discrimination of plantamajoside and isoplantamajoside, desrhamnosylacteoside and desrhamnosylisoacteoside as well as acteoside isomers and forsythosides, respectively.

6.2 Isolation strategy based on the amount of phenylethanoid glycosides

Due to the small amount of IsAO (**Table 5**), IsoPM (**Table 6**), FH (**Table 8**), and FI (**Table 7**) in the intact plant tissues investigated, their isolation from these tissues is a challenging task, requiring multi-step purification procedures and the extraction of high amounts of plant tissue. However, these minor compounds can also be prepared by subjecting tissues containing high amounts of AO, PM or FA to a heat treatment procedure followed by one-step preparative HPLC. Optimum conditions, such as starting tissues and treatment times need to be defined to avoid the presence of contaminants which are not separable from the PhEGs, to prepare the minor compounds in the highest yield possible and to minimize their unwanted decomposition.

6.3 Galls of *Fraxinus* species: sources of acteoside-related phenylethanoid glycosides

6.3.1 Identification of compounds in galls of *Fraxinus* species

As PhEGs are present in all organs of the European *Fraxinus* species investigated so far, we hypothesized the accumulation of these metabolites in the gall tissues as well. The galls of the *Fraxinus* species might thus be a novel source of these valuable SMs (16).

NMR spectral data of whole methanol extracts of *Fr. ornus* gall confirmed the identity of the main compound 8a as cichoriin, the 7-*O*-glucoside of dihydroxycoumarin. (228).

Unlike *Fr. ornus* gall, the galls of the other two *Fraxinus* species contained only a minor compound (peak 8 in **Figure 22**), which can be identified by the molecular formula $C_{15}H_{16}O_9$ (**Table 4**) and a retention time identical with that of cichoriin. However, the UV spectral data of cichoriin and 8, demonstrating characteristic differences in their wavelengths of absorption maxima (λ_{max}, 8a: 288 nm, 340 nm; 8: 293 nm, 334 nm), confirmed 8 to be the 6-*O*-glucoside of dihydroxycoumarin, as aesculin (**Figure 34**) (229).

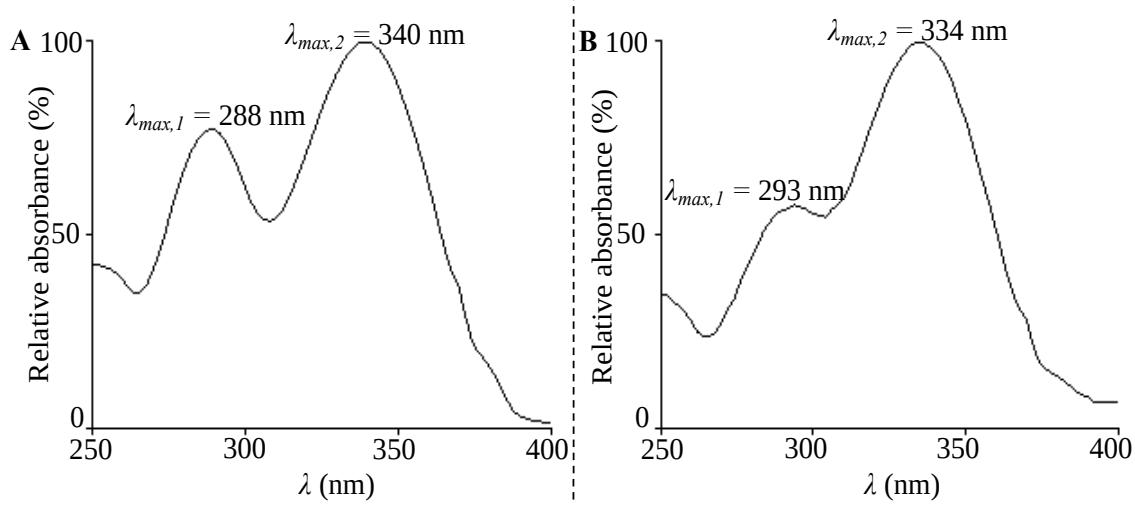

Figure 34: UV absorption spectra of cichoriin (panel A) and aesculin (panel B), determined in the galls of *Fr. angustifolia* and *Fr. excelsior* as well as *Fr. ornus*, respectively.

Compound 10 was determined as MeDCG by UHPLC-HR-MS, although without confirming its conformation.

The mass spectra of the molecular ion of the caffeoylquinic acid isomer 9 (*m/z* 353), obtained by UHPLC-HR-MS/MS, exhibited a base peak at *m/z* 191.06 and two low intensity peaks (< 5% relative to the base peak) at *m/z* 179.03 and *m/z* 135.04 (**Figure 30**). This result is consistent with recent experience (230), confirming the presence of 5-CQA in galls of *Fr. angustifolia* and *Fr. excelsior*. As further confirmation, standard 5-CQA was also analyzed by UHPLC-HR-MS/MS, resulting in comparable mass fragmentation and retention properties to those for compound 9.

The PhEG 5, identified as the main compound in *Fr. angustifolia* gall, was isolated using preparative HPLC for its precise identification. Solutions of 5 prepared in DW or TFA were heated at 100 °C for different periods of time and analyzed by UHPLC-HR-MS/MS (**Figure 31, Figure 37**). In fact, heating of 5 in DW and TFA resulted in the

formation of compounds appearing with longer (7, **Figure 31C**, DW treated sample) and shorter retentions (5a, **Figure 31D**, TFA treated sample) relative to 5, respectively. The molecular formula of 7 was determined as $C_{29}H_{36}O_{15}$, based on UHPLC-HR-MS results, which was the same as that of 5 (**Figure 28A, B, Table 4**). The chromatographic and MS data for 5 and 7 was comparable to that reported in the literature for AO and IsAO, respectively, thereby confirming the identity of 5 and 7 as these PhEG type regioisomers (53, 54). As further confirmations, i) computational calculations interpreting the isomerization of AO into IsAO at atomic level (**chapter 6.6**), and ii) NMR analysis of whole methanol extract of *Fr. angustifolia* gall sample, confirming the identity of AO, were also performed.

The difference between the molecular formulas of AO and 5a (**Table 4**) is consistent with the loss of a rhamnosyl moiety ($C_6H_{10}O_4$), and thus the formation of 5a from AO during TFA treatment can be explained by the hydrolysis of the glycosidic bond between rhamnose and glucose units of AO, forming the corresponding desrhamnosyl derivative of AO. A DW treated sample containing comparable amounts of AO and IsAO (**Figure 31C**), was also heated in TFA medium, resulting in the desrhamnosylation of both compounds. Compounds 5a (DeAO) and 7a (DeIsAO) were thus equally detected (**Figure 31D**).

AO and IsAO were detected in form of their deprotonated molecular ions $[M-H]^-$ (*m/z* 623). Subsequent CID at an optimized fragmentation energy of 35 eV resulted in the formation of ions $[C_9H_8O_4-H]^-$ (**a**; *m/z* 179) and $[C_{20}H_{30}O_{12}-H]^-$ (**b**; *m/z* 461), representing deprotonated caffeic acid and hydroxytyrosol rhamnosyl glucoside moieties. Fragment ion **a** lost H_2O and CO_2 molecules, forming $[C_9H_6O_3-H]$ (**c**; *m/z* 161) and $[C_8H_8O_2-H]^-$ (**d**; *m/z* 135). The loss of a glucosyl moiety of fragment ion **b** resulted in the formation of ion $[C_{14}H_{20}O_8-H]^-$ (**e**; *m/z* 315) (**Figure 35**). Based on the relative intensities of the deprotonated molecular ions of AO and IsAO, the two compounds can be discriminated from each other. The intensity ratio of the ion *m/z* 623 between IsAO and AO was calculated as 2.34 (**Table 9**, average results, calculated from the relative ion intensities of three different injected amounts of AO and IsAO) using a CID energy of 35 eV, confirming the greater stability of IsAO against fragmentation processes generated by CID.

DOI:10.14753/SE.2022.2639

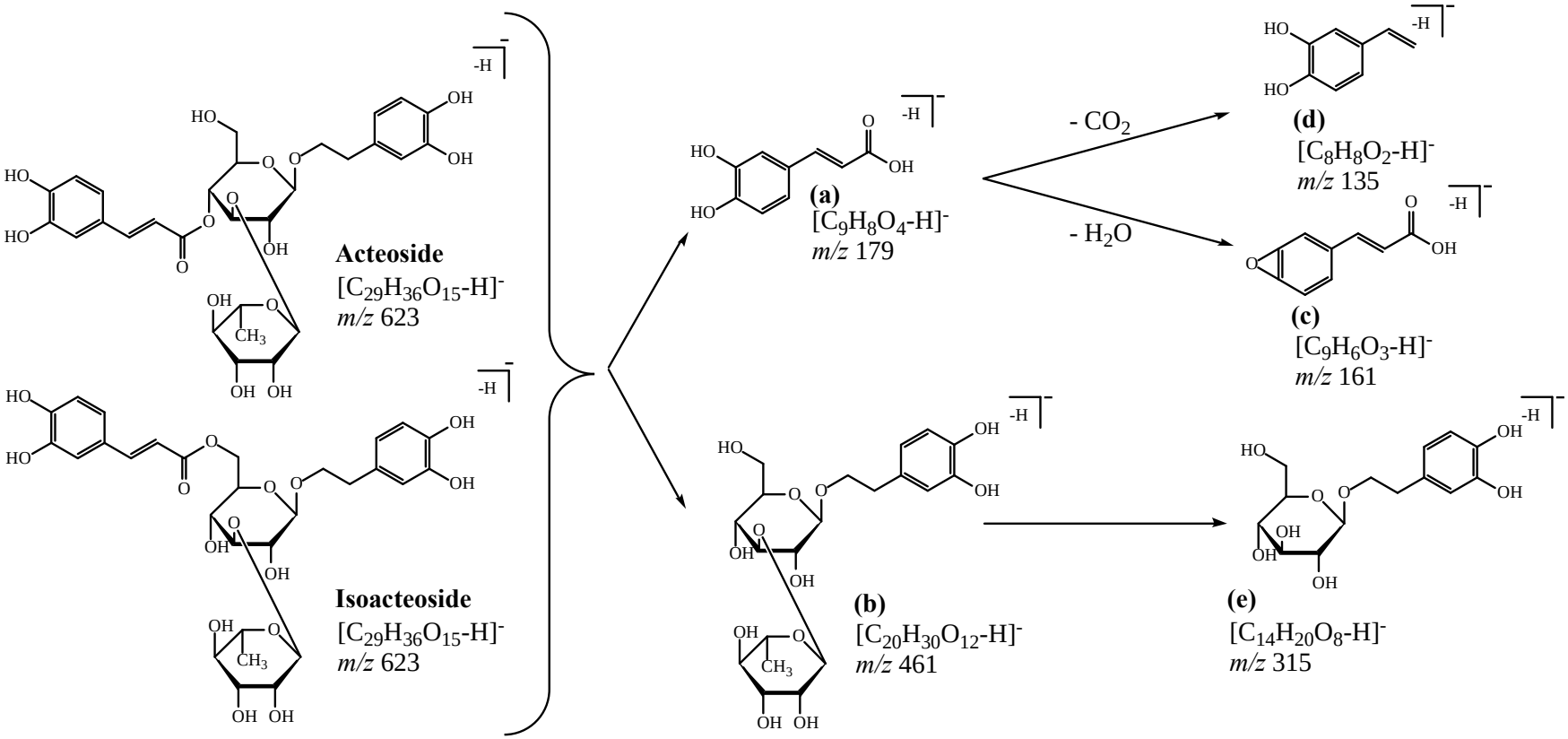

Figure 35: Fragmentation pattern of acteoside and isoacteoside.

DeAO and DeIsAO were detected in form of their deprotonated molecular ions $[M-H]^-$ (*m/z* 477), which were fragmented into $[C_9H_8O_4-H]^-$ (**a**; *m/z* 179) and $[C_{14}H_{20}O_8-H]^-$ (**b**; *m/z* 315) using CID at 35 eV. Subsequent loss of CO_2 and H_2O molecules from fragment ion **a** resulted in the formation of ions $[C_9H_6O_3-H]^-$ (**c**; *m/z* 161) and $[C_8H_8O_2-H]^-$ (**d**; *m/z* 135) (**Figure 36**).

In accordance with the literature (53, 54), identical fragment ions were observed for the regioisomeric pairs AO-IsAO and DeAO-DeIsAO, respectively (**Figure 29A–D, Table 4**); however, differences in the relative ion intensities of the two key fragment ions *m/z* 179 and *m/z* 315, corresponding to the deprotonated caffeic acid and hydroxytyrosol glucoside moieties, allowed the discrimination of DeAO and DeIsAO. Analyzing the fragment ion spectra generated from molecular ions of DeAO and DeIsAO using a CID with an optimized collision energy value (35 eV), ion abundance ratios *m/z* 179/315 were calculated as 8.0 and 0.27 for DeAO and DeIsAO, respectively (average results, calculated from the relative ion intensities of three different injected amounts of DeAO and DeIsAO) (**Table 9**).

Additional NMR spectral data for AO, IsAO, DeAO, and DeIsAO, isolated from their optimum sources (**chapter 6.3.3**), was comparable to that reported in the literature for these PhEGs, thereby unambiguously confirming their identity (111, 231).

DOI:10.14753/SE.2022.2639

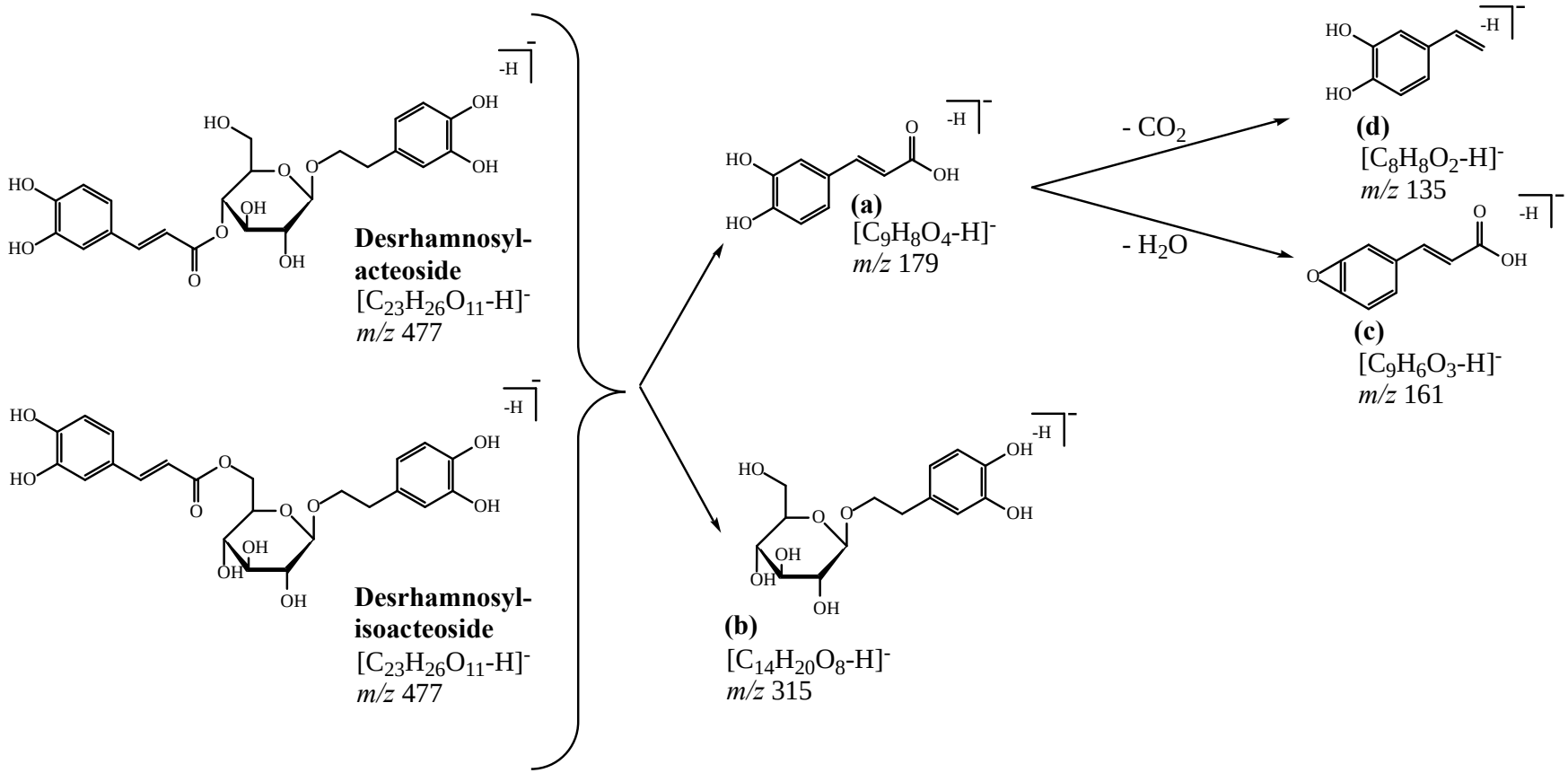

Figure 36: Fragmentation pattern of desrhamnosylacteoside and desrhamnosylisoacteoside.

6.3.2 Amounts of compounds in galls of *Fraxinus* species

The average AO contents in the galls of *Fr. angustifolia* (113.7 mg/g) and *Fr. excelsior* (115.2 mg/g) (**Table 5**) correspond to those reported as the highest in the plant kingdom (dried leaves of *Sesamum indicum*, 129 mg/g) (43), and the average cichoriin content in galls of *Fr. ornus* (180.8 mg) (**Table 5**) is six times higher than its highest amount found to date (30 mg/g, *Fr. ornus* flower) (149), thus highlighting the significance of *Fraxinus* galls in the production of these valuable metabolites.

The conventional taxonomic classification of *Fr. angustifolia, Fr. excelsior* and *Fr. ornus* trees (141) (**chapter 2.7.1**) showed close correlations with the phytochemical composition of their galls: i) the high-level accumulation of AO and the absence of cichoriin in the two representatives of the section *Fraxinus* (*Fr. angustifolia, Fr. excelsior*), and ii) the presence of cichoriin in *Fr. ornus* belonging to the section *Ornus*, were found to be characteristic.

6.3.3 Isolation of AO related compounds

AO conversions were performed using DW and different concentrations of TFA (0.2 M, 0.6 M, and 2 M) at 50 °C and 100 °C, applying various heating times from 7 min to 600 min. To demonstrate the conversions on a comparable basis, amounts of AO and conversion products are given in mM values as shown in **Figure 37**. At 50 °C, AO remained intact, and its conversion products could not be identified either in DW or TFA treated samples. However, at 100 °C, characteristic conversions occurred as a result of simultaneous isomerization, desrhamnosylation, and undefined degradation processes (**Figure 31**). The isomerization of AO into IsAO was detected in DW at 100 °C, accompanied by negligible desrhamnosylation and significant undesired degradation. The highest IsAO yield was determined after heating for 300 min 0.35 mM (**Figure 37A**). Comparing the ratios of IsAO and AO amounts between samples heated in DW at 100 °C for different periods of time, a maximum value of 1.2 was calculated after heating for 600 min (0.31 mM/0.26 mM = 1.2; **Figure 37A**). This result is in good accordance with data obtained using the computational method (as detailed in **chapter 6.6**), indicating that IsAO is slightly more stable in DW than AO.

In addition to isomerization and undesired degradation, the acid treatment at 100 °C led to intense desrhamnosylation, resulting in the formation of DeAO as a main

product. Its highest yield was determined in a 2 M TFA solution heated for 15 min (0.70 mM, **Figure 37D**). Similarly, when AO and IsAO were equally present (as the result of DW heating at 100 °C for 300 min), their 2 M TFA treatment (100 °C, 15 min) resulted in the formation of comparable amounts of DeAO and DeIsAO, as shown in **Figure 31D**. The following optimum treatment conditions were thus applied for the preparative isolation of selected PhEGs: i) DW heating (100 °C, 300 min) for IsAO, and ii) consecutive heating in DW (100 °C, 300 min) and 2 M TFA (100 °C, 15 min) for DeAO and DeIsAO isolation.

DOI:10.14753/SE.2022.2639

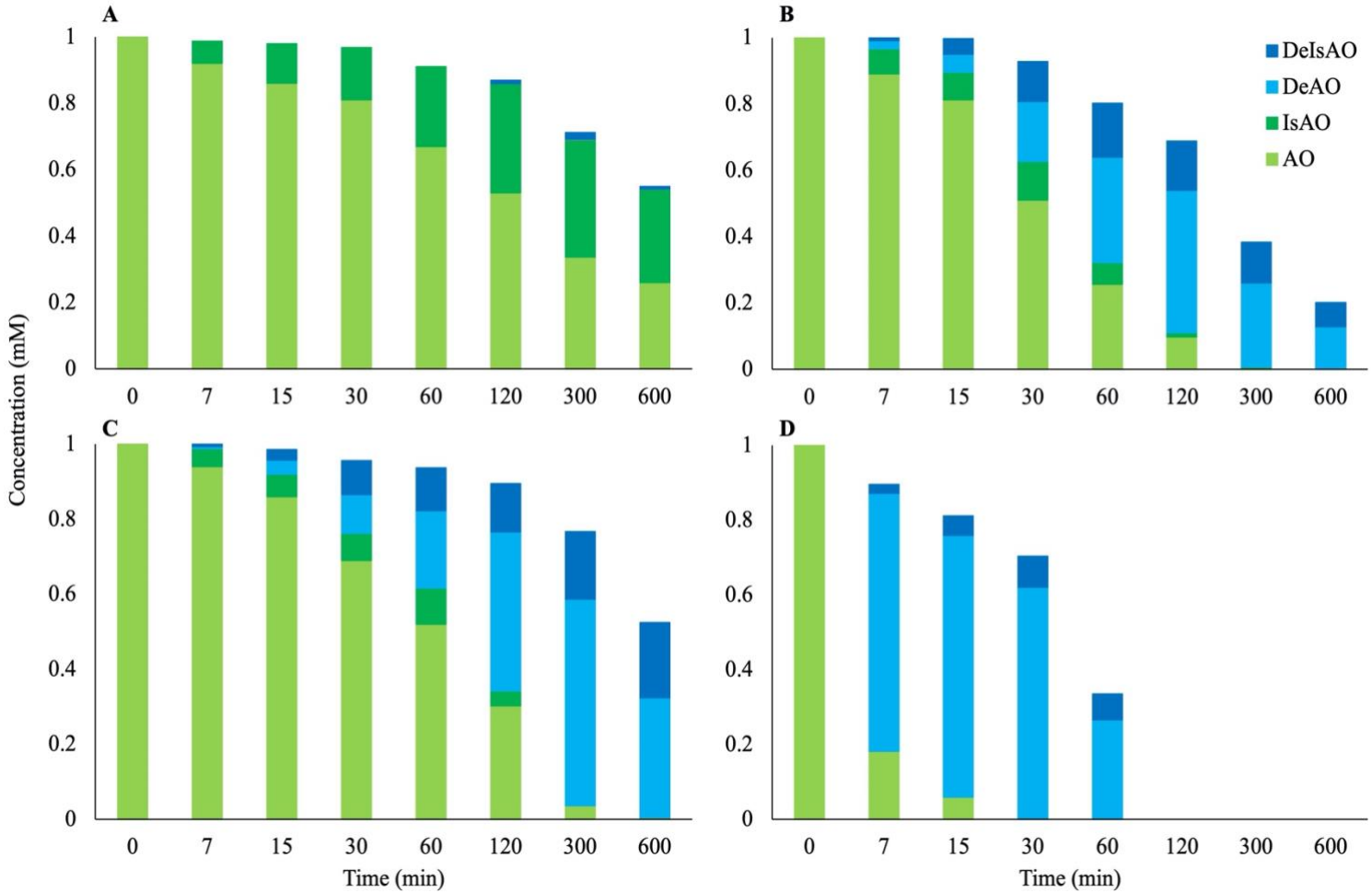

Figure 37: Comparison of the composition of PhEGs in isolated AO samples that were heated at 100 °C with DW (A), 0.2 M TFA (B), 0.6 M TFA (C), and 2 M TFA (D) for different periods of time. Corresponding chromatograms of samples treated with DW for 120 min and 2 M TFA for 15 min are shown in **Figure 31C** and **D**, respectively.

6.3.4 Practical utility of *Fraxinus* galls in the isolation of phenylethanoid glycosides and coumarins

Fr. angustifolia gall sample 1 was used to isolate PhEGs, as its AO content (124.0 mg/g, average of UHPLC-MS and NMR quantitations) represents a mean value among *Fr. angustifolia* and *Fr. excelsior* galls (**Table 5**). Accordingly, 12.4 mg AO could be isolated as the theoretical maximum yield (TMY) from methanol extract of 100.0 mg gall sample 1. The isolation procedure could be regarded as effective, according to a comparison of the TMY of AO (12.4 mg) with the amount of AO isolated by preparative HPLC (8.5 mg), resulting in the highest isolated yield of AO (85 mg/g) among plants, thus confirming the significance of *Fraxinus* galls in AO production (47).

Starting from the 100.0 mg sample 1: i) 4.7 mg IsAO after optimized DW treatment (100 °C, 300 min), and ii) 0.97 mg DeAO and 1.3 mg DeIsAO after consecutive, optimized DW (100 °C, 300 min) and TFA (2 M TFA, 100 °C, 15 min) treatments were isolated. A review of the content of these three PhEGs among plants found that 37.3 mg/g of IsAO (48), 0.8 mg/g of DeAO (49), and 2.5 mg/g of DeIsAO (50) were the highest amounts, in *Castilleja tenuiflora* (dried root culture), *Isoplexis sceptrum* (fresh leaf) and *Nematanthus wettsteinii* (fresh plant), respectively. Thus, the amounts of IsAO, DeAO, and DeIsAO, isolated from *Fr. angustifolia* galls, were 1.3, 12.1, and 5.2 times higher than those reported as the highest for these compounds in the plant kingdom to date.

An evaluation of the harvestable gall yield is also needed to confirm the practical significance of *Fraxinus* galls in the large-scale production of these valuable metabolites. Since gall production is the result of a mite infection, the occurrence of galls is not guaranteed on all *Fraxinus* trees, however, if this frequently occurring infection is present, extraordinarily high numbers of galls may be collected, without harming the host plant itself. In fact, the maximum yields harvested from ≈1 m^3 crown of *Fr. angustifolia*, *Fr. excelsior,* and *Fr. ornus* are 0.6 kg, 0.9 kg, and 0.4 kg, respectively, therefore suggesting the potential for the industrial-scale isolation of PhEGs and cichoriin (**Figure 13**).

6.4 Underground parts of *Plantago* species: abundant sources of acteoside- and plantamajoside-related phenylethanoid glycosides

6.4.1 Identification of compounds in underground parts of *Plantago* species

Compound 2, identified as the main metabolite in the underground organs of *P. major*, was isolated from several-year-old rhizomes of this plant by preparative HPLC for its structural identification. The difference between the molecular formulas of AO and 2 is consistent with the substitution of AO's rhamnosyl moiety ($C_6H_{10}O_4$) by a glucosyl group ($C_6H_{10}O_5$), therefore identifying 2 as the PhEG PM. Based on UHPLC-UV-HR-MS measurements, the molecular formulas of PM and 6 were determined to be identical ($C_{29}H_{36}O_{16}$) (**Table 4**). In addition, the increased yield of compound 6 after DW treatment of several-year-old rhizomes (**Figure 32**), suggested 6 to be the isomer of PM, namely IsoPM. Furthermore, chromatographical and MS data of compounds 2 and 6 were comparable to that of PM and IsoPM described in the literature, therefore identifying 2 and 6 as these PhEGs (62). NMR spectral data of PM and IsoPM were comparable to those reported in the literature, thus confirming their identity unambiguously (57, 94).

Figure 38 shows the proposed fragmentation pathway of these two regioisomers. Compounds PM and IsoPM were detected in form of their molecular ions $[M\text{-}H]^-$ (*m/z* 639). CID at an optimized fragmentation energy of 30 eV led to the formation of ions $[C_9H_8O_4\text{-}H]^-$ (**a**; *m/z* 179) and $[C_{20}H_{30}O_{13}\text{-}H]^-$ (**b**; *m/z* 477), representing deprotonated caffeic acid and hydroxytyrosol glucosyl glucoside moieties, respectively. Fragment ion **a** lost H_2O and CO_2 molecules, subsequently forming $[C_9H_6O_3\text{-}H]$ (**c**; *m/z* 161) and $[C_8H_8O_2\text{-}H]^-$ (**d**; *m/z* 135). The loss of a glucosyl moiety of fragment ion **b** resulted in the formation of ion $[C_{14}H_{20}O_8\text{-}H]^-$ (**e**; *m/z* 315).

Concordant with the literature, MS/MS analysis of PM and IsoPM led to the formation of identical fragment ions (**Figure 29E, F, Table 4**). However, by analyzing the respective fragment ion spectra of PM and IsoPM, generated by CID, the two regioisomers can be differentiated from each other using the difference in the intensities of two key fragment ions *m/z* 639 and *m/z* 477, corresponding to deprotonated precursor ions and decaffeoyl moieties (**Figure 38**). Accordingly, using an optimized collision energy value of 30 eV, the ion abundance ratios between ions *m/z* 639 and *m/z* 477 were calculated to be 0.72 and 2.22 for PM and IsoPM, respectively (average results, calculated

DOI:10.14753/SE.2022.2639

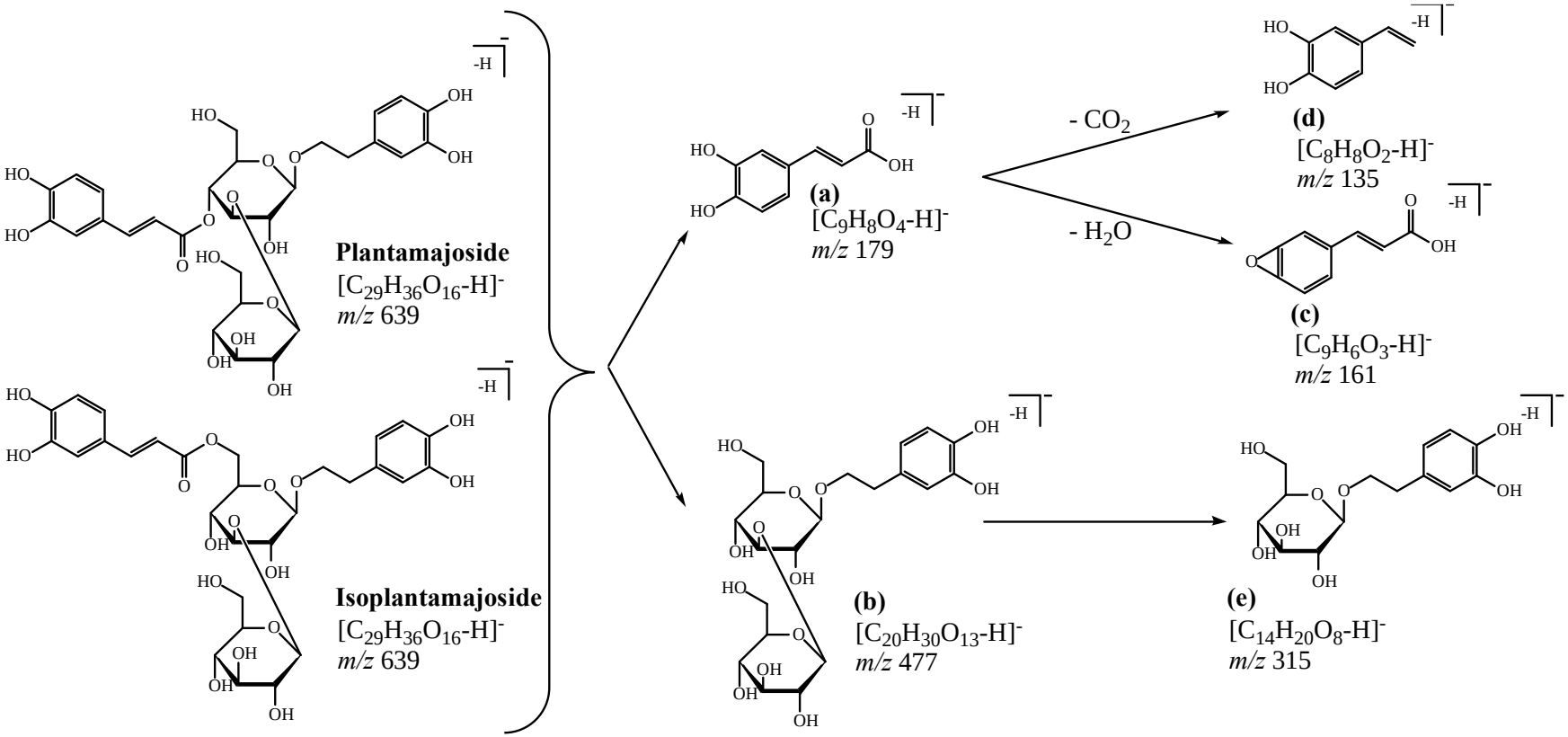

Figure 38: Fragmentation pattern of plantamajoside and isoplantamajoside.

from the relative ion intensities of three different injected amounts of PM and IsoPM), confirming IsoPM to be more stable against fragmentation processes than PM (**Table 9**). This result was in accordance with the computational modeling of the isomerization (**chapter 6.6**), confirming the greater stability of IsoPM.

AO and IsAO in underground parts of *Plantago* species were identified based on their comparable chromatographical and MS data obtained during the analysis of *Fraxinus* galls. Furthermore, their structures were also confirmed by NMR analyses.

6.4.2 Amounts of compounds in underground parts of *Plantago* species

Manually separated rhizome and root parts of several-year-old *Plantago* species were compared regarding their PhEG composition (**Figure 17**). The rhizomes of young plants are undeveloped, therefore, only their root systems were analyzed. The PhEG PM was determined as the main compound in the underground organs of *P. major*, reaching its highest level in the rhizome. The average PM content of the rhizome (76.6 mg/g) (**Table 6**) corresponds to the highest amount of PM reported in the plant kingdom (30 – 80 mg/g, determined in the *in vitro* root culture of *P. lanceolata*) (37). Comparing the average PM contents between the several-year-old rhizomes (76.6 mg/g) and roots (18.27 mg/g), an organ-specific accumulation of PM was confirmed, thus highlighting the significance of *P. major* rhizomes in the production of this valuable natural PhEG (**Figure 39**).

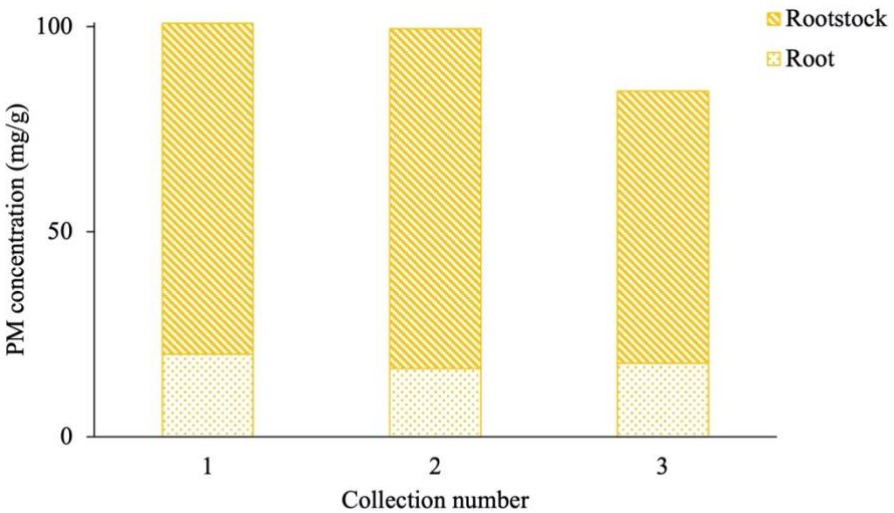

Figure 39: Accumulation of plantamajoside in several-year-old rhizomes and roots of wild-grown *P. major* harvested from three different locations, marked with collection numbers 1, 2, and 3 (corresponding amounts of plantamajoside can also be found in **Table 6**).

The amounts of AO were significantly higher than those of PM in all analyzed samples of *P. lanceolata* and *P. media* (**Table 6**). However, previous studies confirmed the dominance of PM in the roots of *P. lanceolata* and *P. media*, grown *in vitro* (59, 232). Since the PhEG biosynthesis could be influenced by various stress stimuli (e.g., microbial attack) (37-39), we assume that interactions between wild-grown *Plantago* roots and microorganisms result in the change in the quantitative ratio of AO and PM, characteristic for roots grown *in vitro* under sterile conditions.

To the best of our knowledge, we analyzed the PhEG composition of underground organs of wild-grown *Plantago* species for the first time, confirming their significance in the production of PhEGs (18).

6.4.3 Isolation of plantamajoside isomers

Aiming to isolate the minor metabolite IsoPM, there is a need to increase its yield by a simple method. Pursuant to the findings during the isomerization of AO into IsAO, PM-containing samples may also be used to increase the yield of IsoPM. Thus, *P. major* several-year-old rhizome was selected since it contained the highest amount of PM among tested *Plantago* samples. Accordingly, tissue suspensions, prepared from the selected powdered plant tissue, were heated in DW at 100 °C for various heating times ranging from 120 min to 420 min and analyzed by UHPLC-UV-HR-MS, confirming simultaneous isomerization and degradation processes (**Figure 32**). As a result of these processes, an equilibrium mixture was formed with 85% IsoPM and 15% PM contents after heating the solution for 300 min (**Figure 40**), indicating greater stability of IsoPM.

Further heating resulted in significant degradation of both compounds without affecting the equilibrium. This result correlates to the computational modeling of this isomerization (**chapter 6.6**).

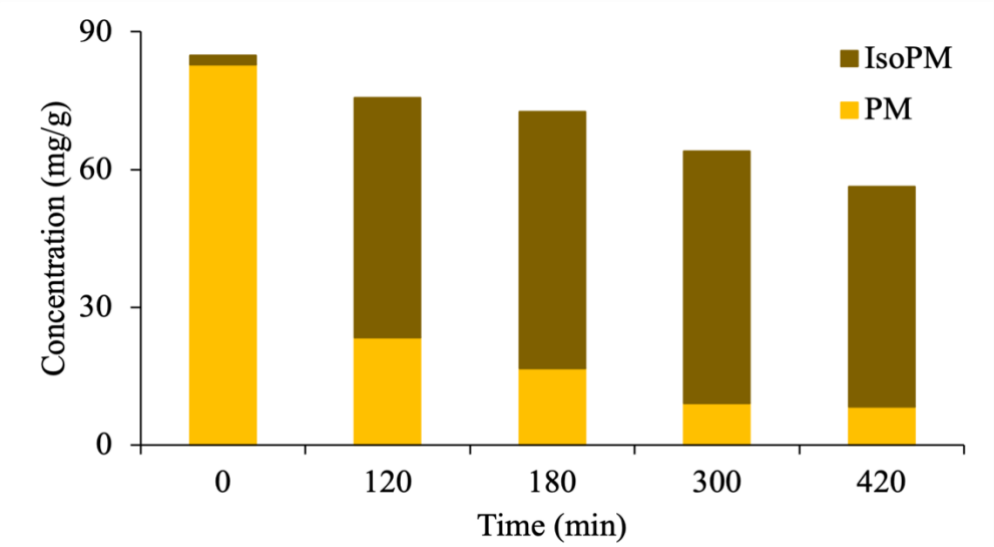

Figure 40: Comparison of the compositions of PM and IsoPM in rhizome samples of *P. major* that were heated at 100 °C in DW for different periods of time. Values are the averages of three parallel heat treatments and differences could be characterized by the RSD% values, ranging from 3.7% (PM in unheated intact sample) to 10.1% (PM in sample heated for 420 min). Corresponding chromatograms of unheated samples and those of samples heated for 120 min and 420 min are shown in **Figure 32**.

6.4.4 Practical utility of *Plantago* underground parts in the isolation of plantamajoside isomers

Starting from 1 g plant tissue, 24.0 mg IsoPM of 86% purity was isolated after 300 min heat treatment of *P. major* rhizome. A review of the IsoPM content among plants showed that 0.67 mg/g of IsoPM was its highest amount detected in the whole plant of *P. asiatica* (57). Therefore, the amount of IsoPM isolated after optimized heat treatment was 36 times higher than that reported as the highest in the plant kingdom to date.

Since the equilibrium mixture, prepared through 300 min heating of *P. major* rhizome suspension, contained a relatively small amount of PM (15% PM vs. 85% IsoPM, **Figure 40**), the untreated intact *P. major* rhizome was used to isolate PM. Thus, 56.1 mg PM of 96% purity could be isolated from 100.0 mg *P. major* rhizome. This isolated yield was comparable to the highest amount of PM determined among plants so far (80 mg/g, determined in the *in vitro* root culture of *P. lanceolata*) (37).

These results highlight the significance of *P. major* in the isolation of PhEGs PM and IsoPM after optimized heat treatments, as easily available, new raw materials for these pharmacologically important metabolites.

Furthermore, we also detected a high-level accumulation of AO in the underground parts of *P. media* (78.1 mg/g (**Table 6**), which corresponds to the highest amount in the plant kingdom (16), thus highlighting the significance of these plant tissues in the production of the valuable PhEG-type metabolite AO.

6.5 Fruits and leaves of *Forsythia* species: sources of acteoside- and forsythoside A-related phenylethanoid glycosides

6.5.1 Identification of compounds in fruits and leaves of *Forsythia* species

Next to AO and IsAO, the fruits of *Fo. suspensa* and *Fo.* × *intermedia* cultivars contained three additional compounds 1, 3, and 4, which were identified by the molecular formula $C_{29}H_{36}O_{15}$ (**Table 4**). Heating of unripe green fruit wall of *Fo. suspensa* (containing a high amount of compound 4) in DW at 100 °C for various periods of time resulted in the formation of two compounds with identical molecular formulas and shorter retention times relative to 4, i.e., 1 and 3 (**Figure 33**). These results suggest an isomeric relationship between compounds 1, 3, and 4. Comparable chromatographic and MS data of 1, 3, and 4 to those reported in the literature for FI, FH, and FA identified 1, 3, and 4 as these PhEGs, respectively (64, 65). Based on the fragment ion spectra of FA, FH, and FI, the differentiation of these three related compounds is not possible. However, additional NMR investigations unambiguously identified compounds 1, 3, and 4 as forsythosides I, H, and A, respectively (71).

Figure 41 shows the identical fragmentation pathway of the three forsythoside regioisomers. FA, FH, and FI were detected in form of their molecular ions $[M\text{-}H]^-$ (*m/z* 623). CID at optimized fragmentation energy of 35 eV led to the formation of ions $[C_9H_8O_4\text{-}H]^-$ (**a**; *m/z* 179) and $[C_{20}H_{30}O_{11}\text{-}H]^-$ (**b**; *m/z* 461), representing deprotonated caffeic acid and hydroxytyrosol rhamnosyl glucoside moieties, respectively. Fragment ion **a** lost H_2O and CO_2 molecules, subsequently forming $[C_9H_6O_3\text{-}H]$ (**c**; *m/z* 161) and $[C_8H_8O_2\text{-}H]^-$ (**d**; *m/z* 135). The presence of 5-CQA in leaves of *Fo. europaea* and *Fo.* × *intermedia* cultivars was confirmed by comparison of obtained chromatographical and MS data with those reported in the literature (230).

DOI:10.14753/SE.2022.2639

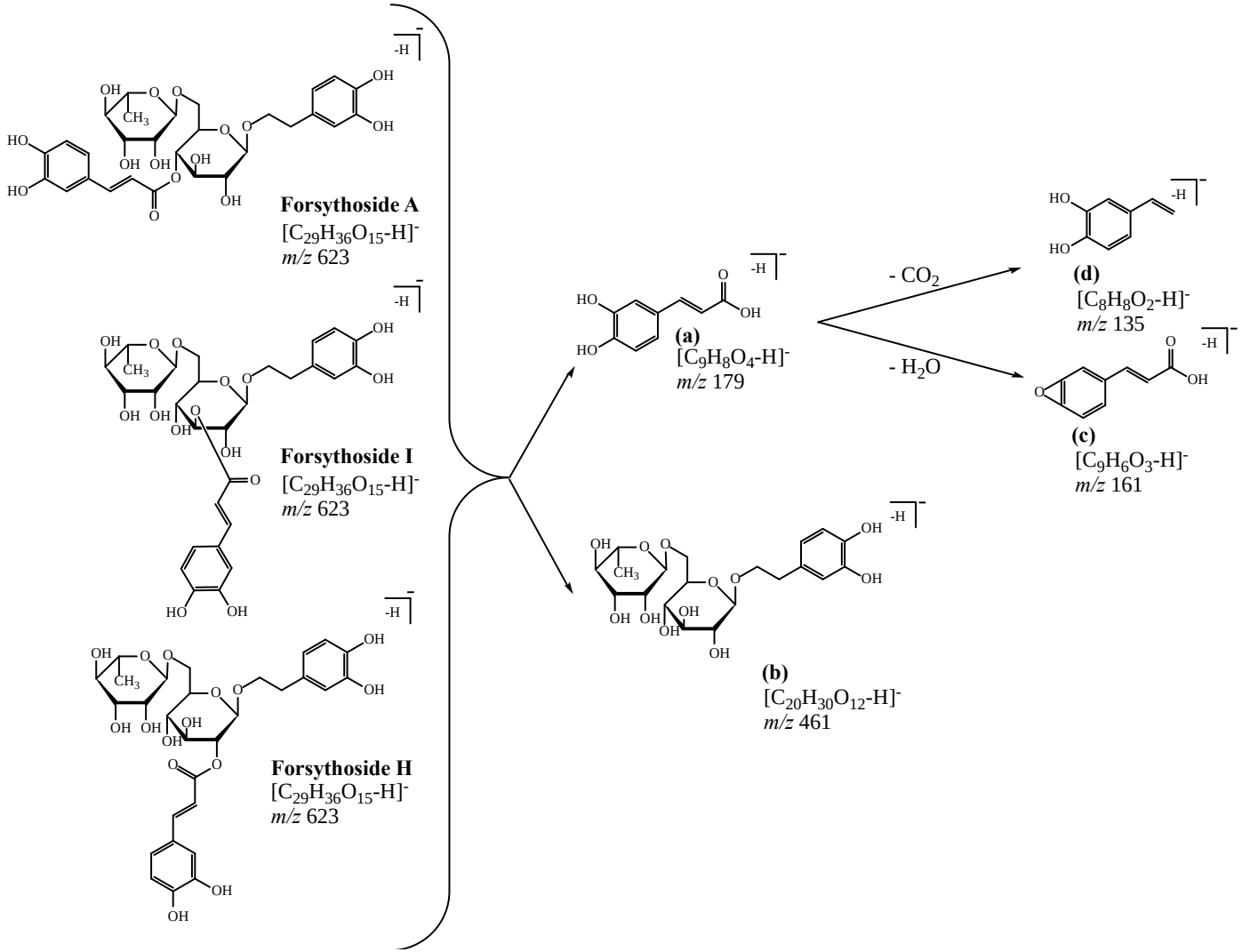

Figure 41: Fragmentation pattern of forsythosides A, I and H.

6.5.2 Amounts of compounds in fruits and leaves of *Forsythia* species

As *Fo.* × *intermedia* generally do not form fruits in temperate climates, more attention has been paid to the analysis of the phytochemical composition of their leaves (233). However, only unspecified cultivars have already been analyzed, confirming the co-occurrence of the PhEGs FA and AO (233, 234) in their leaves. The ratios of FA and AO amounts, calculated from HPLC quantitation data (49 mg/g FA and 15 mg/g AO dry weight) and isolated yields (0.16 mg/g FA and 0.11 mg/g AO, dried leaf) were 3.3 and 1.4, respectively (233, 234). We compared the metabolite composition in the leaves of six *Fo.* × *intermedia* cultivars, confirming for the first time that the PhEGs FA and AO were the main compounds in each cultivar. Their amounts were found to be highly variable between the cultivars as well as between the individuals of the same cultivars. However, the ratios of FA and AO amounts in the leaf samples proved to be nearly constant, varying from 1.5 (cultivar 'Melisa', individual I; 43.7 mg/g FA divided by 28.4 mg/g AO = 1.5) to 2.7 (cultivar 'Primulina', individual II; 66.4 mg/g FA divided by 24.6 mg/g AO = 2.7) (**Table 7**). These ratios are in good accordance with those obtained from the literature, indicating the dominance of FA over AO to be characteristic for the leaves of *Fo.* × *intermedia* cultivars.

As shown in the literature, the main PhEG compound in the leaf and fruit samples of *Fo. europaea,* collected from two Far Eastern and one European botanical gardens, was identified to be either FA (in the Far Eastern leaf and fruit samples) (70, 234), or AO (in the European fruit sample) (212). The results of our study performed on Hungarian *Fo. europaea* leaves and fruits (**Table 7, Table 8**), confirmed AO as the main compound in these organs. These data suggest a chemical diversity among *Fo. europaea* plants, living in different habitats since FA and AO were found to be the main compounds in the Far Eastern and European *Fo. europaea* plant tissues, respectively.

Based on the literature results, FA was determined as being the main PhEG compound in the fruit and leaf samples of *Fo. suspensa*. In accordance with previous results (64, 234), *Fo. suspensa* leaf samples contained high levels of FA (88.3 mg/g, dry weight, average of leaf samples collected from two individuals) (**Table 7**).

Great attention was paid to the determination of PhEGs accumulated by the unripe and ripe fruits of *Fo. suspensa*. The FA contents of the unripe fruits were 5-fold or 15-fold higher than those of the ripe fruits (65, 235). Furthermore, high levels of FA were

determined in the separated seeds, obtained from the unripe fruits of *Fo. suspensa* (47 mg/g dry weight) (65), highlighting the need to follow FA accumulation in both separated fruit parts, i.e., seed and fruit wall, during the fruit ripening of *Fo. suspensa* and *Fo. europaea*.

While analyzing the metabolite composition of both fruit parts (i.e., seed and fruit wall) during the fruit ripening of *Fo. europaea* and *Fo. suspensa*, a fruit part specific accumulation and decomposition of PhEGs, was confirmed for the first time (**Table 8**). In fact, the unripe fruit wall of *Fo. europaea* and *Fo. suspensa* accumulated high amounts of AO (71.4 mg/g, dry weight) and FA (80.4 mg/g, dry weight), respectively (data are the average of unripe fruit wall samples (StA) collected from two individuals) (**Table 8**). However, the amounts of these PhEGs were negligible in the corresponding fruit walls obtained from the fully ripe fruits (marked with StC in **Table 8**), confirming a decomposition of AO and FA, taking place in the fruit walls during their ripening processes. In addition to the unripe fruit wall of *Fo. suspensa*, the seeds of this plant, isolated from the unripe and ripe fruits, were also rich in FA (ripe seed: 61.7 mg/g, marked with StC in **Table 8, Figure 42**; unripe seed: 58.7 mg/g, marked with StA in **Table 8**; dry weight, average data of seed samples collected from two individuals). Thus, FA was found to be stable in the seeds of *Fo. suspensa* during the fruit ripening. Based on these results and considering that 1) *Forsythia* fruit consists of nearly equal amounts of fruit wall and seed parts, and 2) the ripe fruit splits open to release their seeds we can explain the differences between the ratios of the FA amounts measured in unripe and ripe *Fo. suspensa* fruits as described earlier. Namely, the FA content ratio between the unripe and ripe fruit should approximately be between 2 and 3 (139.1 mg/g divided by 67.1 mg/g = 2.25) as a minimum value, if all the FA containing seeds have remained in the fruit. However, the value of this ratio might also be extremely high, reaching a value of around 40, as the result of a significant seed loss.

Both isomers of FA, namely FI and FH, occur in very low amounts in *Forsythia* tissues (71-74). Our analyses revealed that the unripe fruit wall of *Fo. suspensa* contains the highest levels of FA and FI. However, during the ripening process, these PhEGs are degraded in the fruit wall, while their amounts do not significantly change in the seeds (**Figure 42, Table 8**).

DOI:10.14753/SE.2022.2639

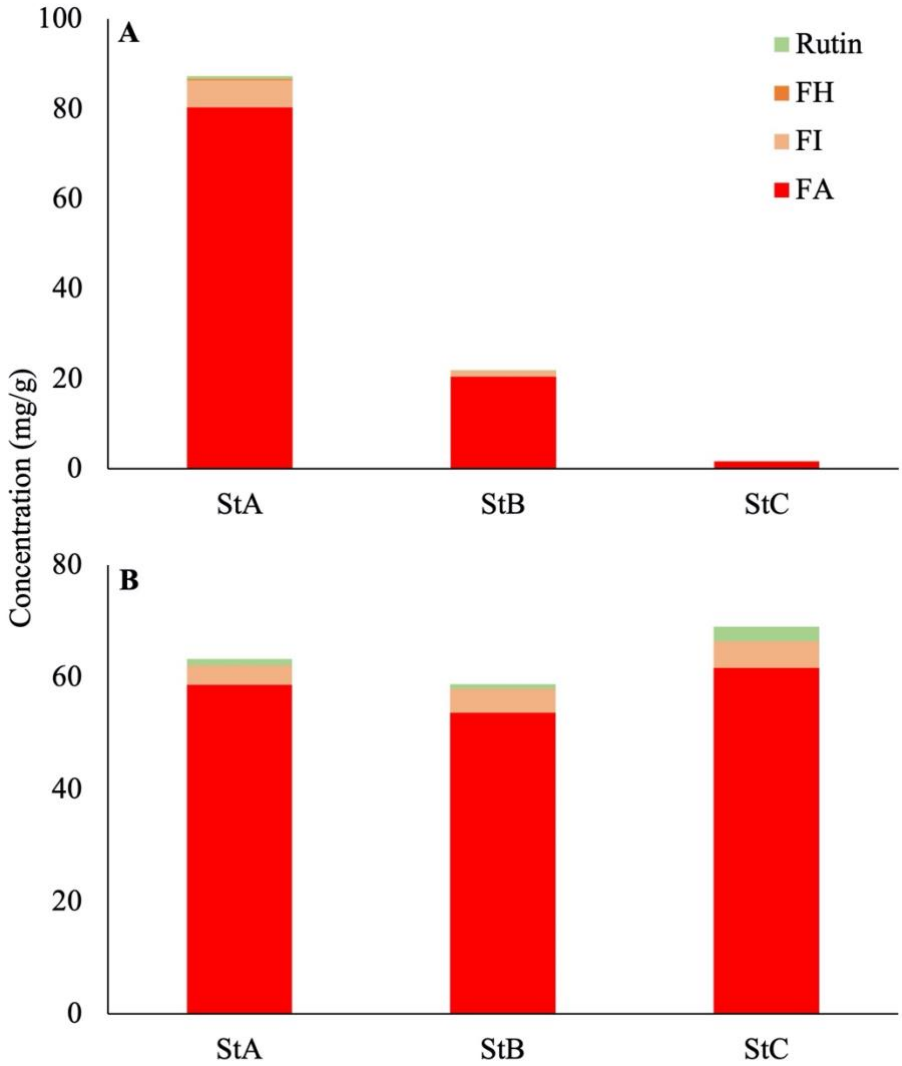

Figure 42: Composition of the dried fruit wall (A) and seed parts (B) of *Fo. suspensa* fruits in different developmental stages of the fruits. Maturity stages (StA, StB and StC) correspond to unripe, green, closed fruits (StA), ripe, yellow-brown, closed fruits (StB) and ripe, yellow-brown, opened fruits (StC). Data are the average of samples collected from two individuals marked with 1 and 2 in **Table 8**.

DOI:10.14753/SE.2022.2639

6.5.3 Isolation of forsythosides

The regioisomers of FA, i.e., FH and FI, are rarely occurring compounds in the plant kingdom and their isolable amount is extremely limited (literature data in **chapter 2.5**). Pursuant to our findings during the isomerization of AO and PM into IsAO and IsoPM, respectively, the amount of FH and FI may be increased by subjecting FA-containing samples to a DW treatment. To minimize unwanted decomposition and avoid the presence of compounds disturbing the isolation of FH and FI, we performed DW treatments on the unripe fruit wall sample of *Fo. suspensa*, applying various heating times ranging from 30 to 420 min at 100 °C (**Figure 43**). The unripe fruit wall of *Fo. suspensa* was chosen over the leaves of *Fo. suspensa* since it contains significantly lower amounts of rutin (**Table 7, Table 8**). Thus, this flavonoid closely eluting with FH did not disturb the isolation of the PhEG (**Figure 33**). As a result of isomerization and degradation processes, an equilibrium mixture of FI, FH, and FA (with 31% FI, 35% FH, and 34% FA) was formed after 300 min heating. This result shows good concordance with the data obtained during the computational method (**chapter 6.6**). Longer treatment times resulted in the degradation of PhEGs without affecting the equilibrium composition (**Figure 43**).

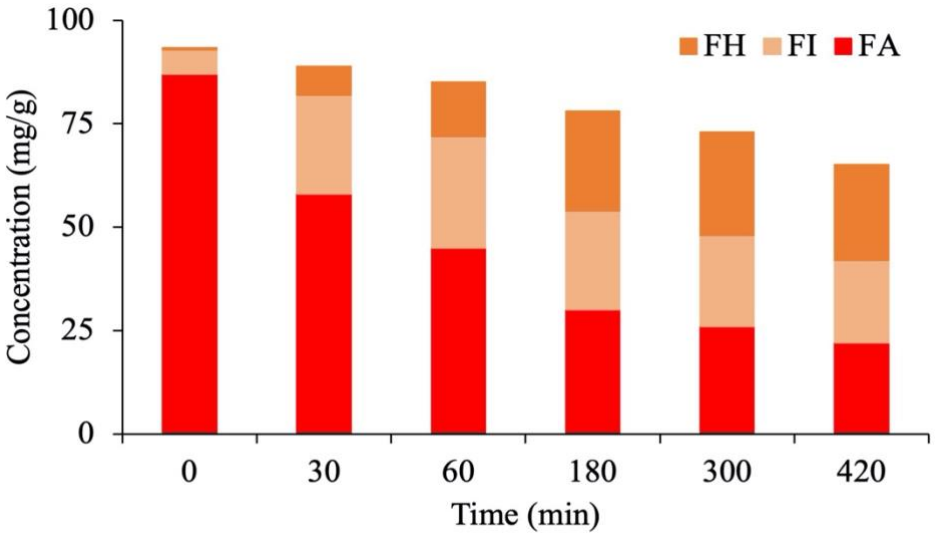

Figure 43: Comparison of the composition of FA, FA, and FI in the unripe fruit wall sample of *Fo. suspensa* that were heated at 100 °C in DW for different periods of time. Values are the averages of three parallel heat treatments and differences could be characterized by the RSD% values, ranging from 3.4% (FA in unheated intact sample) to 11.0% (FH in sample heated for 420 min). Corresponding chromatograms of unheated samples and those heated for 300 min are shown in **Figure 33A, D**.

6.5.4 Practical utility of *Forsythia* fruits and leaves in the isolation of forsythoside A related compounds

Starting from 1 g plant tissue, 4.6 mg FI and 5.6 mg FH of 96% and 85% purity, respectively (and 3.6 mg FA of 92% purity) were isolated after 300 min heat treatment of *Fo. suspensa* unripe fruit wall. A review of the content of these PhEGs among plants showed that 0.22 mg/g of FI and 0.012 mg/g of FH (in *Fo. suspensa*, ripe fruit) (72) were the highest amounts isolated to date. Therefore, the amounts of FI and FH isolated after optimized heat treatment, were 21 and 470 (!) times higher than those reported as the highest for these compounds in the plant kingdom to date.

These results highlight the significance of selected plant tissues, i.e., *Fo. suspensa* unripe fruit wall in the isolation of PhEGs (FA, FH, and FI) after optimized heat treatments, as easily available, new raw materials for these pharmacologically important metabolites.

Furthermore, we also detected a high-level accumulation of AO in the leaves (73.6 mg/g, average amount) (**Table 7**) and unripe fruit walls of *Fo. europaea* (sample StA: 71.4 mg/g, average amount) (**Table 8**), corresponding to the highest amount reported in the plant kingdom (16), thus highlighting the significance of these plant tissues in the production of the valuable PhEG-type metabolite AO.

6.6 Computational modeling of the isomerization processes

The isomerizations of AO into IsAO, PM into IsoPM, and FA into FI and FH were confirmed to be intramolecular acyl transfer reactions, where the caffeoyl ester moiety migrates from the C4 position to neighboring hydroxy groups. Acyl transfer reactions can be characterized by the change of carbonylicity percentage (*CA*%), where the increase of this value, i.e., $\Delta CA\% > 0$, during the reaction implies a beneficial, exothermic process. (236-238).

6.6.1 Kinetic and thermodynamic aspects of the isomerizations

The kinetic (reaction rate) and thermodynamic (driving force) aspects of the isomerizations were studied by theoretical methods at the B3LYP/6-31(d,p) level of

theory (223), with the IEFPCM solvent model (224) by Gaussian09 (isomerization of AO) or Gaussian16 program package (isomerization of PM and FA) (222).

The calculated *CA*% values of AO (52.8%) and IsAO (53.0%), PM (52.2%) and IsoPM (52.9%), as well as FA (52.9%), FI (53.0%) and FH (52.5%) confirmed the absence of an internal driving force during these transformations (**Figure 44, Figure 45, Figure 46**).

From a thermodynamic point of view, the transformation of AO into IsAO is slightly exothermic as the enthalpy (Δ*H*) and Gibbs free energy (Δ*G*) decrease equally by -1.0 kJ mol^{-1} and -2.8 kJ mol^{-1}, respectively. The beneficial entropy change (Δ*S*, +6.0 J mol^{-1} K^{-1}), deriving from the sterically less hindered and more freely rotating side chain supports the exothermic nature of the transformation as well. The values suggest an equilibrium constant (*K*) of 0.4 between AO and IsAO (**Figure 44**).

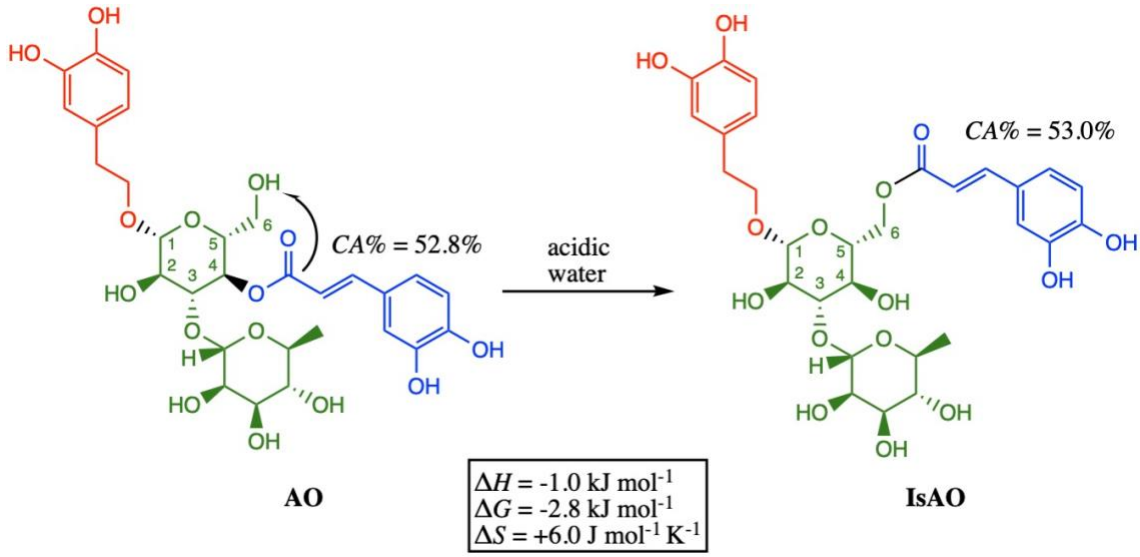

Figure 44: The isomerization of AO into IsAO by acyl transfer reaction. The enthalpy (Δ*H*, in kJ mol^{-1}), Gibbs free energy (Δ*G*, in kJ mol^{-1}), and entropy (Δ*S*, in J mol^{-1} K^{-1}), together with the carbonylicity percentages (*CA*%) are illustrated.

The decrease of Δ*H* and Δ*G* values during the transformation of PM into IsoPM (-24.2 kJ mol^{-1} and -26.2 kJ mol^{-1}, respectively) show the nature of this process to be significantly exothermic from a thermodynamic point of view, which is also supported by the beneficial entropy change (Δ*S*, +6.7 J mol^{-1} K^{-1}). Similar to the transformation of AO into IsAO, this entropy factor may result from the formation of a sterically less hindered, more freely rotating side chain. Theoretically, another isomer can also be considered as a possible product of the transformation, however, the computed enthalpy

DOI:10.14753/SE.2022.2639

value in this case is significantly endothermic, thus excluding the existence of this product (**Figure 45**).

The transformations of FA into FI and FI into FH are almost thermoneutral, as ΔH and ΔG are near zero, referring to a chemical equilibrium between the three isomers (**Figure 46**).

DOI:10.14753/SE.2022.2639

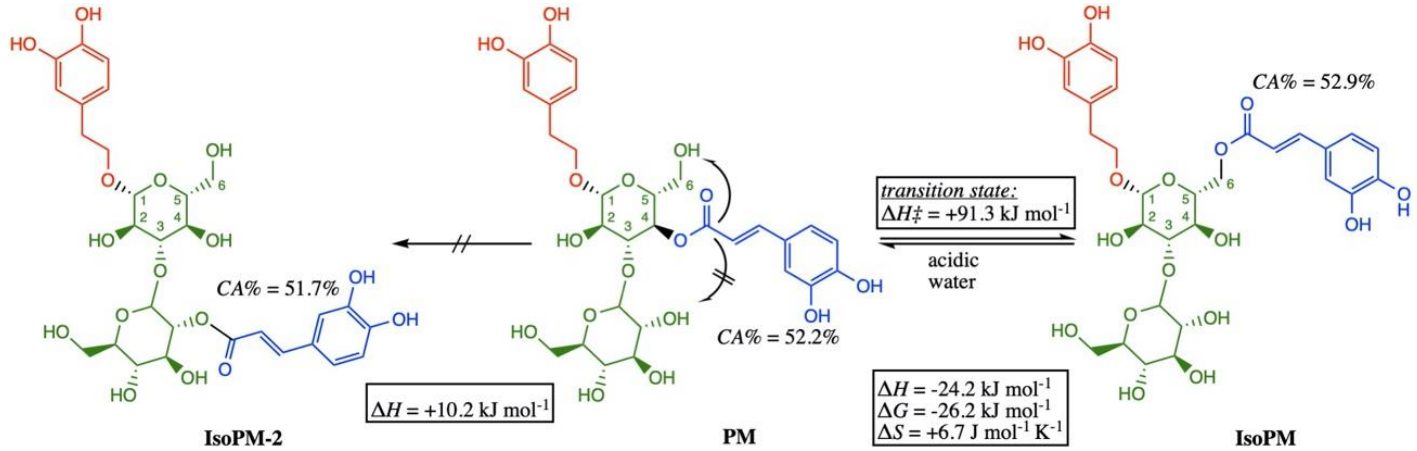

Figure 45: The isomerization of PM into IsoPM by acyl transfer reaction. The enthalpy (Δ*H*, in kJ mol^{-1}), Gibbs free energy (Δ*G*, in kJ mol^{-1}), and entropy (Δ*S*, in J mol^{-1} K^{-1}), together with the carbonylicity percentages (*CA*%) are illustrated.

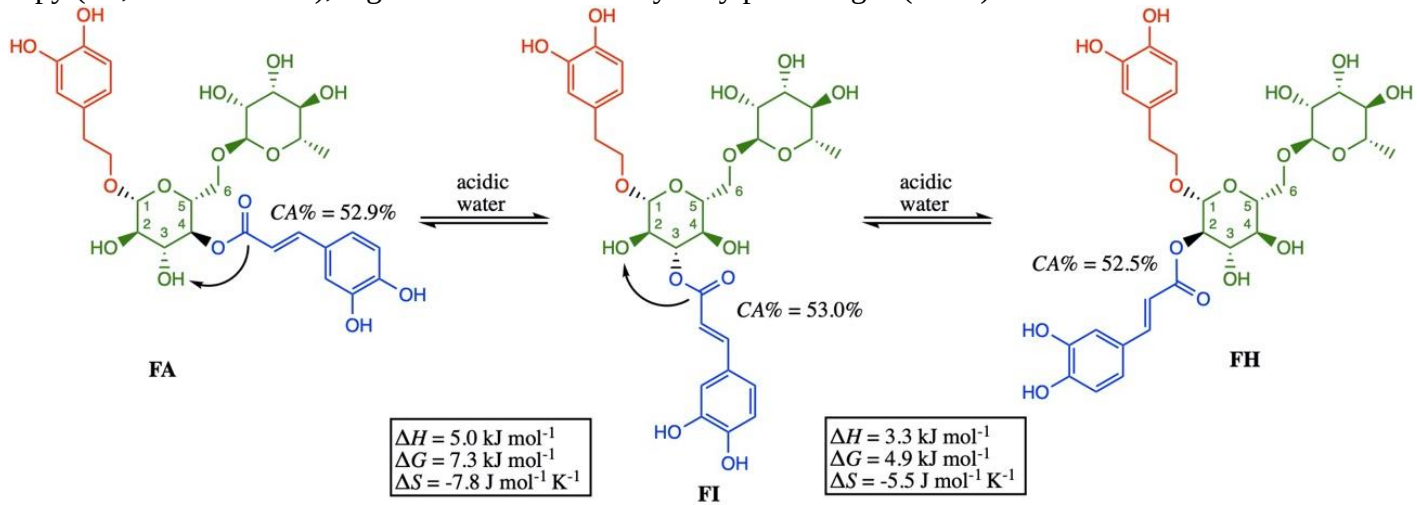

Figure 46: The isomerization of FA into FI and FH by acyl transfer reaction. The enthalpy (Δ*H*, in kJ mol^{-1}), Gibbs free energy (Δ*G*, in kJ mol^{-1}), and entropy (Δ*S*, in J mol^{-1} K^{-1}), together with the carbonylicity percentages (*CA*%) are illustrated**.**

6.6.2 Reaction mechanisms of the isomerizations

The reaction mechanisms of AO, PM, and FA isomerizations were studied using an explicit-implicit solvent model (225). In all cases, the model confirmed that the isomerization processes consist of two elementary steps, allowing a relatively fast reaction rate at elevated temperature (**Figure 47**). Structures involved are the starting and ending states (A and D), a ring-closed intermediate (with sp3 carbon) with two forms of solvation (B and C), and two transition states (TS1 and TS2). Despite the structural differences of forsythosides compared to AO and PM, i.e., sugar substitution at C6-OH instead of C3-OH of the central glucose moiety, we showed that the acyl transfer follows the same generalized reaction mechanism as shown below.

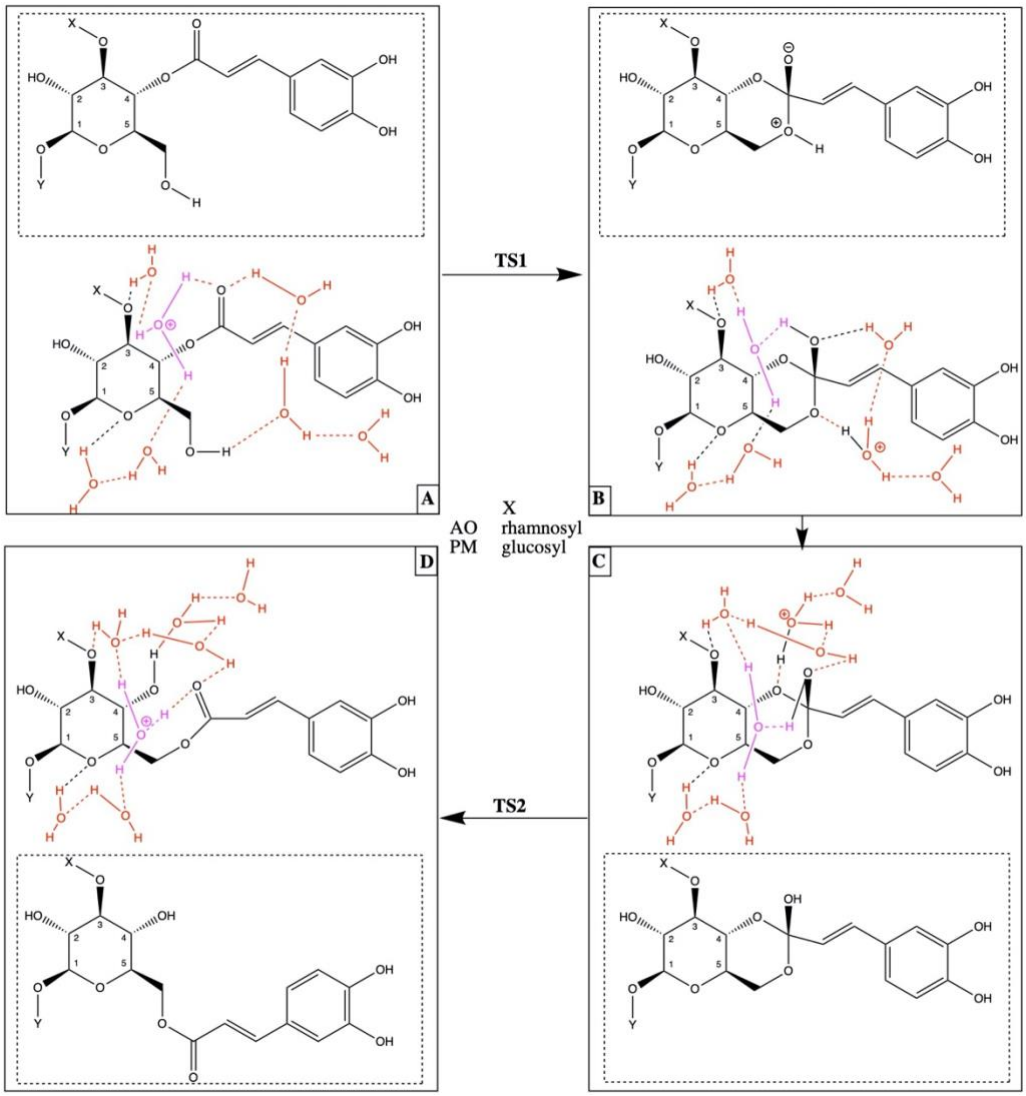

Figure 47: Generalized reaction mechanism of the acyl transfer reaction, determined by computational method using an explicit-implicit solvent model with 7 water molecules. The computed enthalpies of structures A, B, C, and D and activation enthalpies of transition states TS1 and TS2 are found in **Table 10**.

Furthermore, the isomer proportions of 85:15 for IsoPM and PM, 31:35:33 for FI, FH and FA and 54:46 for IsAO and AO, determined after heating in water medium for 300 min are supported by the computed data of the solvent model.

Table 10: Computed enthalpies (ΔH) of structures A, B, C and D and activation enthalpies ($\Delta H_{\ddagger}^{\ddagger}$) of transition states TS1 and TS2 during the isomerizations of AO, P and FA.

Isomerization	Enthalpies of structures and activation enthalpies of transition states in kJ mol^{-1} [a]					
	A	TS1	B	C	TS2	D
AO → IsAO	0.0	82.1	59.4	34.4	61.3	-14.7
PM → IsoPM	0.0	91.3	63.8	18.2	64.7	-15.9
PM → IsoPM-2	0.0	117.6	78.9	26.4	80.6	+25.5
FA → FI	0.0	86.1	66.7	22.4	59[b]	-4.2
FI → FH	-4.2	92.4	64.1	38.8	61[b]	+6.8

[a] Structures A, B, C and D can be found in **Figure 47**.

[b] Estimated values obtained by scanning along the reaction coordinates (± 3 – 4 kJ mol^{-1}).

6.7 *In vitro* activity

The PhEGs isolated from *Fraxinus* sp. (AO, IsAO, DeAO, DeIsAO) have significant antioxidant (77-79) and antiproliferative (52, 77) effects. AO and IsAO also exhibited neuroprotective (79), anti-inflammatory (103), immune-enhancing (130), and xanthine oxidase inhibitory (54) activity, and cichoriin expressed hepatoprotective (239) and antibacterial (240) effects. The main PhEG compounds of *Plantago* and *Forsythia* plants might be responsible, at least partly, for their medicinal activity as detailed in **chapter 2.6**. Accordingly, the wound healing activity of PM and the anti-inflammatory activity of FA were confirmed. Furthermore, their antiproliferative, antibacterial, and antioxidant properties have also been described (94, 241). The remarkable antiviral activity of FA against influenza (91) and avian bronchitis viruses (90) and that of AO against the respiratory syncytial virus (87) and Dengue virus 2 (88) has also been

confirmed, highlighting the relevance of testing all PhEGs for their antiviral potency against other viruses such as the severe acute respiratory syndrome coronavirus type 2 (SARS-CoV-2). Furthermore, the antiviral activity of DeAO and DeIsAO against HIV was reported (89).

The bioactivity of the minor PhEGs in *Plantago* and *Forsythia* species, IsoPM, FH, and FI, has been less frequently studied due to their limited availability. The antioxidant properties of these metabolites (28, 74, 80) as well as the antibacterial effects of FH and FI (28, 74), and the antihypertensive (122) and cardioprotective (123) effects of IsoPM, have already been confirmed.

However, prior to performing further efficacy studies with these PhEGs and coumarins, their *in vitro* side effects on mammalian cells, such as the cytostatic and cytotoxic activity on the Vero E6 cell line, should also be investigated. To perform *in vitro* antiviral tests, kidney epithelial cells isolated from *Chlorocebus aethiops* (Vero E6 cells) are often used as a host cell model for a class of intracellular pathogens such as slow-growing viruses and bacteria. In this model, promising antiviral drug candidates should not exhibit cytotoxic or cytostatic effects on Vero E6 cells. (221)

Recently, AO alone was tested for its cytotoxicity against Vero E6 cells and its non-toxicity in the concentration range applied (0 – 200 ug/mL) was confirmed (88). Also, the non-toxicity of PM on hamster ovary cells (101) and FA on canine kidney (91) and chicken embryo kidney cells (90) have been confirmed. However, the cytotoxicity of AO derivatives (IsAO, DeAO, and DeIsAO), PM isomers (PM and IsoPM), forsythosides A, H, I, and coumarins aesculin and cichoriin has not yet been tested against normal healthy cells such as Vero E6 cells. Thus, we analyzed the *in vitro* activity of these PhEGs and cichoriin (isolated from their optimum sources) and standard aesculin on Vero E6 cells for the first time (16, 18).

Neither cytostatic nor cytotoxic activity occurred on Vero E6 cells after treatment with the PhEGs (AO, IsAO, DeAO, DeIsAO, PM, IsoPM, FA, FH, and FI) and coumarins (aesculin and cichoriin) in the concentration range of 0.04 – 100 µM. In contrast, the positive control peptide Transportan demonstrated relevant cytostatic activity on the Vero E6 cell culture (IC_{50} = 33.9 ± 5.5 µM), while 100 µM chloroquine exhibited time-dependent cytotoxicity, increasing from 30% after 24 h to 86% after 48 h exposure (**Figure 48**, **Figure 49**).

DOI:10.14753/SE.2022.2639

Consequently, based on our results confirming the absence of cytotoxicity of PhEGs on Vero E6 cells, antiviral tests of PhEGs against SARS-CoV-2 virus can be performed using Vero E6 cells.

DOI:10.14753/SE.2022.2639

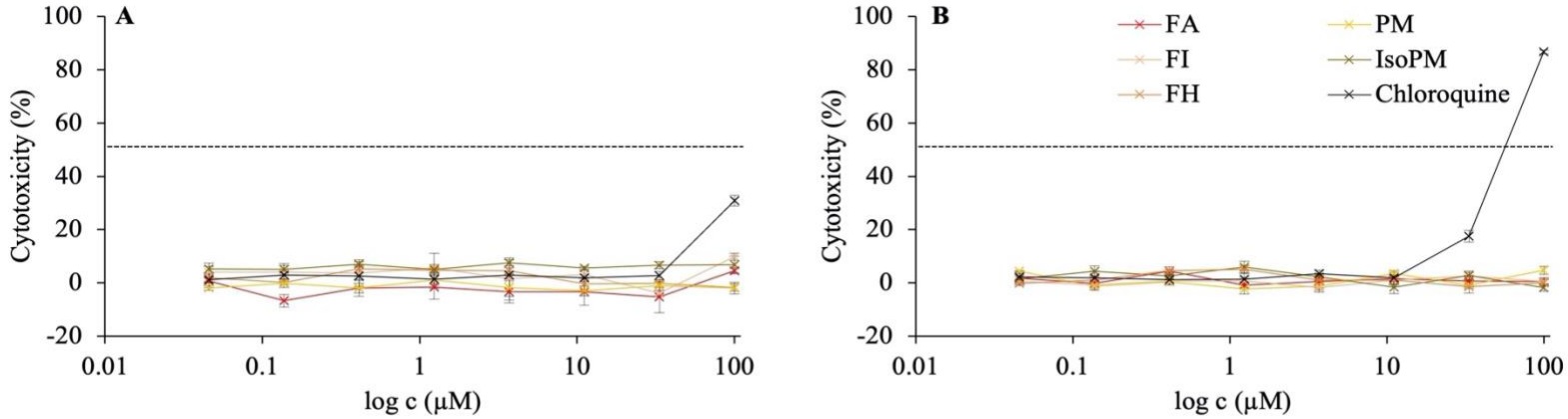

Figure 48: *In vitro* cytotoxic activity of PhEGs isolated from *Forsythia* and *Plantago* species (FA, FH, FI, PM, IsoPM) and that of the positive control chloroquine on Vero E6 cells after treatment periods of 24 h (panel A) and 48 h (panel B).

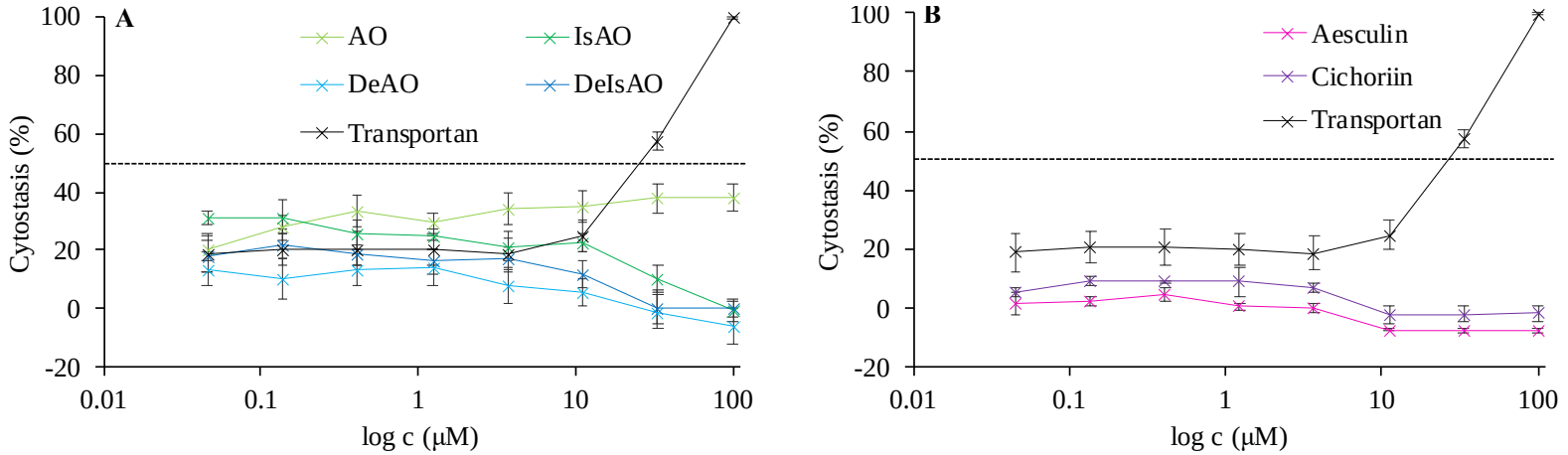

Figure 49: *In vitro* cytostatic activity of PhEGs (AO, IsAO, DeAO, DeIsAO; panel A) and coumarins (aesculin, cichoriin; panel B) isolated from *Fraxinus* species together with that of the positive control Transportan on Vero E6 cells.

DOI:10.14753/SE.2022.2639

7 CONCLUSION

In this thesis, new sources of valuable PhEG-type metabolites were determined, allowing their high-yield isolation:

1) Analysis of the gall composition of the three European *Fraxinus* species performed for the first time confirmed an extraordinarily high amount of the PhEG AO (in the galls of *Fr. angustifolia* and *Fr. excelsior*) and that of the coumarin glucoside cichoriin (in the galls of *Fr. ornus*).
2) Tissue- and age-specific accumulation of the PhEGs PM and AO were analyzed and confirmed in the underground parts of widely distributed *Plantago* species (*P. lanceolata, P. major,* and *P. media*) for the first time. The several-year-old rhizome of *P. major* was determined as the most important source of PM known to date.
3) A comprehensive phytochemical study on the leaves and separated fruit parts during the fruit development of three *Forsythia* species (*Fo. europaea, Fo. suspensa,* and various cultivars of *Fo.* × *intermedia*) revealed the unripe fruit wall of *Fo. suspensa* to be the optimum source of the PhEG FA, allowing its impurity-free, high-yield isolation.
4) In addition to the main PhEGs AO, PM, and FA, optimized heat treatments of their optimum sources resulted in their characteristic conversions. This allowed the isolation of rarely occurring PhEG-type compounds IsAO, DeAO, DeIsAO, IsoPM, FH, and FI in the highest yield reported in the plant kingdom so far

As a novelty in the analysis of PhEGs:

1) Molecular modeling was conducted to interpret the isomerization processes.
2) UHPLC-HR Orbitrap-MS/MS fragmentation studies of the closely related compounds confirmed characteristic differences between the ion intensities of key fragment ions. Thus, the regioisomeric pairs DeAO-DeIsAO and PM-IsoPM could be distinguished from each other. Forsythosides could not be differentiated from each other, however, they were distinguishable from the isomeric pair AO-IsAO.

As to the medicinal significance of the PhEGs (AO, IsAO, DeAO, DeIsAO, PM, IsoPM, FA, FH, and FI) and coumarins (aesculin and cichoriin):

1) they showed no cytostatic activity on Vero E6 cells, therefore supporting the safe use of these compounds as natural medicines and allowing to perform further *in vitro* profiling on different systems (such as against intracellular pathogens). Thus, their antiviral potency (e.g., against SARS-CoV-2) can also be tested.

DOI:10.14753/SE.2022.2639

8 SUMMARY

Representatives of *Fraxinus*, *Plantago*, and *Forsythia* genera are officially mentioned as natural medicines in the Ph. Eur. or used as agents in TCM; however, phytochemical knowledge on these plants is limited to the parts used as phytotherapeutic agents and, therefore, the phytochemical composition of other parts is mostly unknown.

In this thesis, 14 phenolic compounds were determined in previously not analyzed plant tissues, i.e., in the galls of three European *Fraxinus* species (*Fr. angustifolia*, *Fr. excelsior* and *Fr. ornus*), in the underground parts of three wild-grown *Plantago* species (*P. lanceolata*, *P. major* and *P. media*), and in the leaves and separated fruit parts during fruit development of three *Forsythia* species (*Fo. europaea*, *Fo. suspensa* and *Fo.* × *intermedia*). Most of the compounds were determined by a combination of UHPLC-UV-HR-MS/MS and NMR analyses as well as computational modeling as being PhEGs.

Optimum tissues could be selected for the impurity-free isolation of the main PhEGs AO, PM, and FA. Heat treatments performed in DW and TFA media revealed their characteristic conversions, forming regioisomeric and desrhamnosylated products of PhEGs. Tissue-specific accumulation of PhEGs and optimized heat treatments of selected tissues allowed the isolation of 9 PhEGs (AO, IsAO, DeAO, DeIsAO, FA, FH, FI, PM, and IsoPM) in the highest yield reported in the plant kingdom so far. The isomerization of PhEGs can be interpreted by computational modeling.

Differentiation of compounds characterized by the same molecular formula from each other is not possible based on their HR-MS analyses. Nevertheless, the relative intensities of SFIs, generated by CID may be used to help identify the respective compounds in certain cases.

Prior to performing further efficacy studies with investigated PhEGs, their *in vitro* side effects on mammalian cells, such as the cytostatic activity on the Vero E6 cell line, need to be investigated. The identified PhEGs exhibited no cytostatic or cytotoxic activity on Vero E6 cells, supporting their safe use as natural medicines and allowing to perform further *in vitro* profiling on different systems, such as against intracellular pathogens. Thus, their antiviral potency (e.g., against SARS-CoV-2) can also be tested.

DOI:10.14753/SE.2022.2639

9 ÖSSZEFOGLALÁS

Az aranyfa (*Forsythia*), a kőris (*Fraxinus*) és az útifű (*Plantago*) nemzetségek néhány faját természetes gyógyszerként említik az Európai Gyógyszerkönyvben vagy alapanyagként használják a Kínai Hagyományos Orvoslásban. Ezek a növények fitokémiai ismerete főleg a gyógyászati célra eddig felhasznált szerveire korlátozódik, ugyanakkor egyéb részei növénykémiai összetétele többnyire ismeretlen.

Jelen doktori tézisben 14, a fenoloidok csoportjába tartozó másodlagos anyagcsereterméket határoztuk meg az említett nemzetségek fajainak olyan szerveiben, melyeket eddig még nem vizsgáltak kémiai szempontból. Így jellemző összetevőkként feniletanoid-glikozidokat (FeGL) azonosítottunk három kőris fajon (*Fr. angustifolia, Fr. excelsior* és *Fr. ornus*) kialakult gubacsokból, három útifű faj (*P. lanceolata, P. major* és *P. media*) fölbeli szerveiből, valamint három aranyfa faj (*Fo. europaea, Fo. suspensa* és *Fo.* × *intermedia*) leveleiből és a termésérés különböző szakaszaiban begyűjtött terméfal és mag részeiből. Az összetevők szerkezetét és mennyiségét UHPLC-UV-HR-MS/MS, NMR és számítógépes molekulamodellezés módszerek egymást kiegészítő és megerősítő eredményeinek falhasználásával bizonyítottuk.

A fő összetevők, az akteozid, a plantamajozid és a forszitozid A tiszta formában való izolálásához optimális kiindulási nyersanyagot (elkülönített szerveket) találtunk. A kiválasztott növényi szövetek vizes vagy savas közegben optimalizált hőkezelése a fő összetevők specifikus átalakulási folyamatait eredményezték. Ennek során a FeGL-ok izomerizációja (regioizomerek keletkezése) és a ramnoz cukorrészük hidrolízissel történő kilépése volt jellemző. A FeGL-ok szövet-specifikus felhalmozódása és a kiválasztott növényi szövetek optimalizált hőkezelésének eredményképpen összesen 9 FeGL összetevőt ismereteink szerint az eddigi legnagyobb hozamban izoláltuk.

Az azonos összegképlettel jellemezhető FeGL regioizomerek tömegspektrometriás megkülönböztetésére alkalmas analitikai lehetőségeket találtunk az ütközés indukált disszociáció által generált fragmentionok relatív intenzitásának felhasználásával.

Az izolált FeGL-ok további hatékonysági vizsgálatainak elvégzése előtt meg kell vizsgálni az emlős sejtekre gyakorolt *in vitro* mellékhatásait. Az izolált FeGL-ok se citotoxikus se citosztatikus hatással nem rendelkeznek normál Vero E6 sejtekre, ami alátámasztja természetes gyógyszerkénti biztonságos felhasználásukat, valamint lehetővé teszi további antivirális hatásuk bizonyítására irányuló tesztek elvégzését is.

10 BIBLIOGRAPHY

1. Jiménez C, Riguera R. (1994) Phenylethanoid glycosides in plants: structure and biological activity. Nat Prod Rep, 11 (6): 591-606.
2. Hoskins JA. (1984) The occurrence, metabolism and toxicity of cinnamic acid and related compounds. J Appl Toxicol, 4 (6): 283-292.
3. Lafay S, Gil-Izquierdo A. (2007) Bioavailability of phenolic acids. Phytochem Rev, 7 (2): 301-311.
4. Das AB, Goud VV, Das C. Phenolic Compounds as Functional Ingredients in Beverages. In: Grumezescu AM, Holban AM (Eds.), Value-Added Ingredients and Enrichments of Beverages. Academic Press, Duxford, 2019: 285-323.
5. Dewick PM. Medicinal Natural Products: A Biosynthetic Approach. John Wiley & Sons, Ltd., Chichester, West Sussex, 2009: 7-9.
6. Garbe D. Cinnamic Acid. In: Wiley-VCH (Ed.), Ullmann's Encyclopedia of Industrial Chemistry. Wiley-VCH Verlag GmbH & Co. KGaA, Hoboken, NY, 2000: 193-196.
7. Yin Z, Wong W, Ye W, Li N. (2003) Biologically active cis-cinnamic acid occurs naturally in Brassica parachinensis. Chin Sci Bull, 48 (6): 555-558.
8. Hänsel R, Sticher O. Pharmakognosie - Phytopharmazie. Springer Medizin Verlag, Heidelberg, 2007: 1156.
9. Clifford MN, Jaganath IB, Ludwig IA, Crozier A. (2017) Chlorogenic acids and the acyl-quinic acids: discovery, biosynthesis, bioavailability and bioactivity. Nat Prod Rep, 34 (12): 1391-1421.
10. Vogt T. (2010) Phenylpropanoid Biosynthesis. Mol Plant, 3 (1): 2-20.
11. Alipieva K, Korkina L, Orhan IE, Georgiev MI. (2014) Verbascoside — A review of its occurrence, (bio)synthesis and pharmacological significance. Biotechnol Adv, 32 (6): 1065-1076.
12. Xue Z, Yang B. (2016) Phenylethanoid Glycosides: Research Advances in Their Phytochemistry, Pharmacological Activity and Pharmacokinetics. Molecules, 21 (8): 991.
13. Fu G, Pang H, Wong YH. (2008) Naturally occurring phenylethanoid glycosides: potential leads for new therapeutics. Curr Med Chem, 15 (25): 2592-2613.

14. Çaliş İ. Biodiversity of Phenylethanoid Glycosides. In: Şener B (Ed.), Biodiversity: Biomolecular Aspects of Biodiversity and Innovative Utilization. Springer US, Boston, MA, 2002: 137-149.
15. Gormann R, Kaloga M, Ferreira D, Marais JPJ, Kolodziej H. (2006) Newbouldiosides A–C, phenylethanoid glycosides from the stem bark of Newbouldia laevis. Phytochemistry, 67 (8): 805-811.
16. Zürn M, Tóth G, Kraszni M, Sólyomváry A, Mucsi Z, Deme R, Rózsa B, Fodor B, Molnár-Perl I, Horváti K, Bősze S, Pályi B, Kis Z, Béni S, Noszál B, Boldizsár I. (2019) Galls of European Fraxinus trees as new and abundant sources of valuable phenylethanoid and coumarin glycosides. Ind Crop Prod, 139: 111517.
17. Bedir E, Manyam R, Khan IA. (2003) Neo-clerodane diterpenoids and phenylethanoid glycosides from Teucrium chamaedrys L. Phytochemistry, 63 (8): 977-983.
18. Zürn M, Tóth G, Ausbüttel T, Mucsi Z, Horváti K, Bősze S, Sütöri-Diószegi M, Pályi B, Kis Z, Noszál B, Boldizsár I. (2021) Tissue-Specific Accumulation and Isomerization of Valuable Phenylethanoid Glycosides from Plantago and Forsythia Plants. Int J Mol Sci, 22 (8): 3880.
19. Ming DS, Yu DQ, Yu SS. (1999) Two New Caffeyol Glycosides from Forsythia suspensa. J Asian Nat Prod Res, 1 (4): 327-335.
20. Ishikawa T, Kondo K, Kitajima J. (2003) Water-Soluble Constituents of Coriander. Chem Phar Bull, 51 (1): 32-39.
21. Chang J, Case R. (2005) Phenolic glycosides and ionone glycoside from the stem of Sargentodoxa cuneata. Phytochemistry, 66 (23): 2752-2758.
22. Takenaka Y, Okazaki N, Tanahashi T, Nagakura N, Nishi T. (2002) Secoiridoid and iridoid glucosides from Syringa afghanica. Phytochemistry, 59 (7): 779-787.
23. Gu W, Zhang Y, Hao XJ, Yang FM, Sun QY, Morris-Natschke SL, Lee KH, Wang YH, Long CL. (2014) Indole Alkaloid Glycosides from the Aerial Parts of Strobilanthes cusia. J Nat Prod, 77 (12): 2590-2594.
24. Warashina T, Nagatani Y, Noro T. (2005) Further constituents from the bark of Tabebuia impetiginosa. Phytochemistry, 66 (5): 589-597.

25. Tanahashi T, Takenaka Y, Akimoto M, Okuda A, Kusunoki Y, Suekawa C, Nagakua N. (1997) Six Secoiridoid Glucosides from Jasminum polyanthum. Chem Pharm Bull, 45 (2): 367-372.
26. Tanahashi T, Takenaka Y, Nagakura N. (1997) Three Secoiridoid Glucosides Esterified with a Linear Monoterpene Unit and a Dimeric Secoiridoid Glucoside from Jasminum polyanthum. J Nat Prod, 60 (5): 514-518.
27. Franzyk H, Olsen CE, Jensen SR. (2004) Dopaol 2-Keto- and 2,3-Diketoglycosides from Chelone obliqua. J Nat Prod, 67 (6): 1052-1054.
28. Kuang HX, Xia YG, Liang J, Yang BY, Wang QH. (2011) Lianqiaoxinoside B, a Novel Caffeoyl Phenylethanoid Glycoside from Forsythia suspensa. Molecules, 16 (7): 5674-5681.
29. Jo Y, Kim M, Shin MH, Chung HY, Jung JH, Im KS. (2006) Antioxidative Phenolics from the Fresh Leaves of Ternstroemia japonica. J Nat Prod, 69 (10): 1399-1403.
30. Xue Z, Yan R, Yang B. (2016) Phenylethanoid glycosides and phenolic glycosides from stem bark of Magnolia officinalis. Phytochemistry, 127: 50-62.
31. Cole TCH, Hilger HH, Stevens P. (2019) Angiosperm phylogeny poster (APP) – Flowering plant systematics, 2019. PeerJ Prepr, 7: e2320v2326.
32. Rønsted N, Gøbel E, Franzyk H, Jensen SR, Olsen CE. (2000) Chemotaxonomy of Plantago. Iridoid glucosides and caffeoyl phenylethanoid glycosides. Phytochemistry, 55 (4): 337-348.
33. Dewick PM. Medicinal Natural Products: A Biosynthetic Approach. John Wiley & Sons, Ltd., Chichester, West Sussex, 2009: 137.
34. Kim SY, Song MK, Jeon JH, Ahn JH. (2018) Current Status of Microbial Phenylethanoid Biosynthesis. J Microbiol Biotechnol, 28 (8): 1225-1232.
35. Dewick PM. Medicinal Natural Products: A Biosynthetic Approach. John Wiley & Sons. Ltd., Chichester, West Sussex, 2009: 149.
36. Gálvez M, Martín-Cordero C, Ayuso MJ. Pharmacological Activities of Phenylpropanoids Glycosides. In: Atta ur R (Ed.), Studies in Natural Products Chemistry. Elsevier, Amsterdam, 2006: 675-718.

37. Fons F, Tousch D, Rapior S, Gueiffier A, Roussel JL, Gargadennec A, Andary C. (1999) Phenolic profiles of untransformed and hairy root cultures of Plantago lanceolata. Plant Physiol Biochem, 37 (4): 291-296.
38. Sakihama Y, Cohen MF, Grace SC, Yamasaki H. (2002) Plant phenolic antioxidant and prooxidant activities: phenolics-induced oxidative damage mediated by metals in plants. Toxicology, 177 (1): 67-80.
39. Dixon RA, Paiva NL. (1995) Stress-Induced Phenylpropanoid Metabolism. Plant Cell, 7 (7): 1085-1097.
40. Piątczak E, Grąbkowska R, Wysokińska H. Production of Iridoid and Phenylethanoid Glycosides by In Vitro Systems of Plants from the Buddlejaceae, Orobanchaceae, and Scrophulariaceae Families. In: Pavlov A, Bley T (Eds.), Bioprocessing of Plant In Vitro Systems. Springer International Publishing, Cham, 2016: 1-23.
41. Lamaison J, Petitjean Freytet C, Carnat A. (1993) Verbascoside, major phenolic compound of ash leaves (Fraxinus excelsior) and Vervain (Aloysia triphylla). Plantes médicinales et phytothérapie, 26 (3): 225-233.
42. Li L, Xu L, Peng Y, He Z, Shi R, Xiao P. (2012) Simultaneous determination of five phenylethanoid glycosides in small-leaved Kudingcha from the Ligustrum genus by UPLC/PDA. Food Chem, 131 (4): 1583-1588.
43. Fuji Y, Uchida A, Fukahori K, Chino M, Ohtsuki T, Matsufuji H. (2018) Chemical characterization and biological activity in young sesame leaves (Sesamum indicum L.) and changes in iridoid and polyphenol content at different growth stages. PLoS One, 13 (3): e0194449.
44. Tóth G, Sólyomváry A, Boldizsár I, Noszál B. (2014) Characterization of enzyme-catalysed endogenous β-hydroxylation of phenylethanoid glycosides in Euphrasia rostkoviana Hayne at the molecular level. Process Biochem, 49 (9): 1533-1537.
45. Tóth G, Alberti Á, Sólyomváry A, Barabás C, Boldizsár I, Noszál B. (2015) Phenolic profiling of various olive bark-types and leaves: HPLC–ESI/MS study. Ind Crop Prod, 67: 432-438.

46. Tóth G, Barabás C, Tóth A, Kéry Á, Béni S, Boldizsár I, Varga E, Noszál B. (2016) Characterization of antioxidant phenolics in Syringa vulgaris L. flowers and fruits by HPLC-DAD-ESI-MS. Biomed Chromatogr, 30 (6): 923-932.
47. Nishimura H, Sasaki H, Inagaki N, Masao C, Chen Z, Mitsuhashi H. (1991) Nine phenethyl alcohol glycosides from Stachys sieboldii. Phytochemistry, 30 (3): 965-969.
48. Gómez-Aguirre YA, Zamilpa A, González-Cortazar M, Trejo-Tapia G. (2012) Adventitious root cultures of Castilleja tenuiflora Benth. as a source of phenylethanoid glycosides. Ind Crop Prod, 36 (1): 188-195.
49. Taskova RM, Gotfredsen CH, Jensen SR. (2005) Chemotaxonomic markers in Digitalideae (Plantaginaceae). Phytochemistry, 66 (12): 1440-1447.
50. Jensen SR. (1996) Caffeoyl phenylethanoid glycosides in Sanango racemosum and in the Gesneriaceae. Phytochemistry, 43 (4): 777-783.
51. Mazzutti S, Salvador Ferreira SR, Herrero M, Ibañez E. (2017) Intensified aqueous-based processes to obtain bioactive extracts from Plantago major and Plantago lanceolata. J Supercrit Fluids, 119: 64-71.
52. Nagao T, Abe F, Okabe H. (2001) Antiproliferative Constituents in the Plants 7. Leaves of Clerodendron bungei and Leaves and Bark of C. trichotomum. Biol Pharm Bull, 24 (11): 1338-1341.
53. Keefover-Ring K, Holeski LM, Bowers MD, Clauss AD, Lindroth RL. (2014) Phenylpropanoid glycosides of Mimulus guttatus (yellow monkeyflower). Phytochem Lett, 10: 132-139.
54. Chen X, Deng Z, Huang X, Geng C, Chen J. (2018) Liquid chromatography–mass spectrometry combined with xanthine oxidase inhibition profiling for identifying the bioactive constituents from Cistanche deserticola. Int J Mass Spectrom, 430: 1-7.
55. Kelly MT, Lykke AM, Mondolot L, Ravin HW. (2018) Growth conditions modify the concentrations of bioactive caffeic acid derivatives, amino acids and the structure of Plantago leaves. Int J Biol Chem Sci, 12 (5): 2244-2257.
56. Yang X, Yuan J, Wan J. (2012) Cytotoxic phenolic glycosides from Boschniakia himalaica. Chem Nat Compd, 48 (4): 555-558.

57. Miyase T, Ishino M, Akahori C, Ueno A, Ohkawa Y, Tanizawa H. (1991) Phenylethanoid glycosides from Plantago asiatica. Phytochemistry, 30 (6): 2015-2018.
58. Zhou BN, Bahler BD, Hofmann GA, Mattern MR, Johnson RK, Kingston DGI. (1998) Phenylethanoid Glycosides from Digitalis purpurea and Penstemon linarioides with PKCα-Inhibitory Activity. J Nat Prod, 61 (11): 1410-1412.
59. Fons F, Gargadennec A, Gueiffier A, Roussel JL, Andary C. (1998) Effects of cinnamic acid on polyphenol production in Plantago lanceolata. Phytochemistry, 49 (3): 697-702.
60. Fons F, Rapior S, Gueiffier A, Roussel JL, Gargadennec A, Andary C. (1998) (E)-p-coumaroyl-1-O-β-D-glucopyranoside accumulation in roots of Plantago lanceolata cultures. Acta Bot Gallica, 145 (3): 249-255.
61. Zubair M, Nybom H, Lindholm C, Rumpunen K. (2011) Major polyphenols in aerial organs of greater plantain (Plantago major L.), and effects of drying temperature on polyphenol contents in the leaves. Sci Hort, 128 (4): 523-529.
62. Li C, Liu Y, Abdulla R, Aisa HA, Suo Y. (2014) Characterization and identification of chemical components in Neopicrorhiza scrphulariiflora roots by liquid chromatography-electrospray ionization quadrupole time-of-flight tandem mass spectrometry. Anal Methods, 6 (11): 3634-3643.
63. Kitagawa S, Hisada S, Nishibe S. (1984) Phenolic compounds from Forsythia leaves. Phytochemistry, 23 (8): 1635-1636.
64. Jiao J, Gai QY, Luo M, Wang W, Gu CB, Zhao CJ, Zu YG, Wei FY, Fu YJ. (2013) Comparison of main bioactive compounds in tea infusions with different seasonal Forsythia suspensa leaves by liquid chromatography–tandem mass spectrometry and evaluation of antioxidant activity. Food Res Int, 53 (2): 857-863.
65. Qu H, Li B, Li X, Tu G, Lü J, Sun W. (2008) Qualitative and quantitative analyses of three bioactive compounds in different parts of Forsythia suspensa by high-performance liquid chromatography-electrospray ionization-mass spectrometry. Microchem J, 89 (2): 159-164.
66. Shoyama Y, Matsumoto M, Nishioka I. (1986) Four caffeoyl glycosides from callus tissue of Rehmannia glutinosa. Phytochemistry, 25 (7): 1633-1636.

67. Di Fabio A, Bruni A, Poli F, Garbarino JA, Chamy MC, Piovano M, Nicoletti M. (1995) The distribution of phenylpropanoid glycosides in Chilean Calceolaria Spp. Biochem Syst Ecol, 23 (2): 179-182.
68. Marchetti L, Pellati F, Graziosi R, Brighenti V, Pinetti D, Bertelli D. (2019) Identification and determination of bioactive phenylpropanoid glycosides of Aloysia polystachya (Griseb. et Moldenke) by HPLC-MS. J Pharmaceut Biomed Anal, 166: 364-370.
69. Wang Z, Xia Q, Liu X, Liu W, Huang W, Mei X, Luo J, Shan M, Lin R, Zou D, Ma Z. (2018) Phytochemistry, pharmacology, quality control and future research of Forsythia suspensa (Thunb.) Vahl: A review. J Ethnopharmacol, 210: 318-339.
70. Kitagawa S, Nishibe S, Benecke R, Thieme H. (1988) Phenolic Compounds from Forsythia Leaves. II. Chem Pharm Bull, 36 (9): 3667-3670.
71. Wang FN, Ma ZQ, Liu Y, Guo YZ, Gu ZW. (2009) New Phenylethanoid Glycosides from the Fruits of Forsythia Suspense (Thunb.) Vahl. Molecules, 14 (3): 1324-1331.
72. Li C, Dai Y, Duan YH, Liu ML, Yao XS. (2014) A new lignan glycoside from Forsythia suspensa. Chin J Nat Med, 12 (9): 697-699.
73. Kuang HX, Xia YG, Yang BY, Liang J, Zhang QB, Li GY. (2009) A New Caffeoyl Phenylethanoid Glycoside from the Unripe Fruits of Forsythia suspensa. Chin J Nat Med, 7 (4): 278-282.
74. Qu H, Zhang Y, Chai X, Sun W. (2012) Isoforsythiaside, an antioxidant and antibacterial phenylethanoid glycoside isolated from Forsythia suspensa. Bioorg Chem, 40 (1): 87-91.
75. Qi M, Zhao S, Zhou B, Zhang M, Zhang H, Wang Y, Hu P. (2019) Probing the degradation mechanism of forsythiaside A and simultaneous determination of three forsythiasides in Forsythia preparations by a single marker. J Sep Sci, 42 (23): 3503-3511.
76. Bao J, Ding RB, Liang Y, Liu F, Wang K, Jia X, Zhang C, Chen M, Li P, Su H, Wan JB, Wang Y, He C. (2017) Differences in Chemical Component and Anticancer Activity of Green and Ripe Forsythiae Fructus. Am J Chin Med, 45 (7): 1513-1536.

77. Harput US, Genc Y, Saracoglu I. (2012) Cytotoxic and antioxidative activities of Plantago lagopus L. and characterization of its bioactive compounds. Food Chem Toxicol, 50 (5): 1554-1559.
78. Bardakci H, Skaltsa H, Milosevic-Ifantis T, Lazari D, Hadjipavlou-Litina D, Yeşilada E, Kırmızıbekmez H. (2015) Antioxidant activities of several Scutellaria taxa and bioactive phytoconstituents from Scutellaria hastifolia L. Ind Crop Prod, 77: 196-203.
79. Li M, Xu T, Zhou F, Wang M, Song H, Xiao X, Lu B. (2018) Neuroprotective Effects of Four Phenylethanoid Glycosides on H_2O_2-Induced Apoptosis on PC12 Cells via the Nrf2/ARE Pathway. Int J Mol Sci, 19 (4): 1135.
80. Ahn JH, Jo YH, Kim SB, Turk A, Oh KE, Hwang BY, Lee KY, Lee MK. (2018) Identification of antioxidant constituents of the aerial part of Plantago asiatica using LC–MS/MS coupled DPPH assay. Phytochem Lett, 26: 20-24.
81. Wang H, Sun Y, Ye WC, Xiong F, Wu JJ, Yang CH, Zhao SX. (2004) Antioxidative Phenylethanoid and Phenolic Glycosides from Picrorhiza scrophulariiflora. Chem Phar Bull, 52 (5): 615-617.
82. Huang CK, Lin Y, Su H, Ye D. (2015) Forsythiaside Protects Against Hydrogen Peroxide-Induced Oxidative Stress and Apoptosis in PC12 Cell. Neurochem Res, 40 (1): 27-35.
83. Lu T, Piao XL, Zhang Q, Wang D, Piao XS, Kim SW. (2010) Protective effects of Forsythia suspensa extract against oxidative stress induced by diquat in rats. Food Chem Toxicol, 48 (2): 764-770.
84. Ge Y, Wang Y, Chen P, Wang Y, Hou C, Wu Y, Zhang M, Li L, Huo C, Shi Q, Gao H. (2016) Polyhydroxytriterpenoids and Phenolic Constituents from Forsythia suspensa (Thunb.) Vahl Leaves. J Agric Food Chem, 64 (1): 125-131.
85. Wang P, Kang J, Zheng R, Yang Z, Lu J, Gao J, Jia Z. (1996) Scavenging effects of phenylpropanoid glycosides from Pedicularis on superoxide anion and hydroxyl radical by the Spin trapping method(95)02255-4. Biochem Pharmacol, 51 (5): 687-691.
86. Heilmann J, Çaliş İ, Kirmizibekmez H, Schühly W, Harput S, Sticher O. (2000) Radical Scavenger Activity of Phenylethanoid Glycosides in FMLP Stimulated

Human Polymorphonuclear Leukocytes: Structure-Activity Relationships. Planta Med, 66 (8): 746-748.

87. Kernan MR, Amarquaye A, Chen JL, Chan J, Sesin DF, Parkinson N, Ye Z, Barrett M, Bales C, Stoddart CA, Sloan B, Blanc P, Limbach C, Mrisho S, Rozhon EJ. (1998) Antiviral phenylpropanoid glycosides from the medicinal plant Markhamia lutea. J Nat Prod, 61 (5): 564-570.
88. Brandão GC, Kroon EG, Souza DER, Souza Filho JD, Oliveira AB. (2013) Chemistry and Antiviral Activity of Arrabidaea pulchra (Bignoniaceae). Molecules 18 (8): 9919-9932.
89. Kim HJ, Yu YG, Park H, Lee YS. (2002) HIV gp41 binding phenolic components from Fraxinus sieboldiana var. angustata. Planta Med, 68 (11): 1034-1036.
90. Li H, Wu J, Zhang Z, Ma Y, Liao F, Zhang Y, Wu G. (2011) Forsythoside A inhibits the avian infectious bronchitis virus in cell culture. Phytother Res, 25 (3): 338-342.
91. Law AHY, Yang CLH, Lau ASY, Chan GCF. (2017) Antiviral effect of forsythoside A from Forsythia suspensa (Thunb.) Vahl fruit against influenza A virus through reduction of viral M1 protein. J Ethnopharmacol, 209: 236-247.
92. Deng L, Pang P, Zheng K, Nie J, Xu H, Wu S, Chen J, Chen X. (2016) Forsythoside A Controls Influenza A Virus Infection and Improves the Prognosis by Inhibiting Virus Replication in Mice. Molecules, 21 (5): 524.
93. Maquiaveli CC, Lucon-Júnior JF, Brogi S, Campiani G, Gemma S, Vieira PC, Silva ER. (2016) Verbascoside Inhibits Promastigote Growth and Arginase Activity of Leishmania amazonensis. J Nat Prod, 79 (5): 1459-1463.
94. Ravn H, Brimer L. (1988) Structure and antibacterial activity of plantamajoside, a caffeic acid sugar ester from Plantago major subsp. major. Phytochemistry, 27 (11): 3433-3437.
95. Ravn H, Andary C, Kovács G, Mølgaard P. (1989) Caffeic acid esters as in vitro inhibitors of plant pathogenic bacteria and fungi. Biochem Syst Ecol, 17 (3): 175-184.
96. Qu H, Zhang Y, Wang Y, Li B, Sun W. (2008) Antioxidant and antibacterial activity of two compounds (forsythiaside and forsythin) isolated from Forsythia suspensa. J Pharm Pharmacol, 60 (2): 261-266.

97. Inoue M, Sakuma Z, Ogihara Y, Saracoglu I. (1998) Induction of Apoptotic Cell Death in HL-60 Cells by Acteoside, A Phenylpropanoid Glycoside. Biol Pharm Bull, 21 (1): 81-83.

98. Ohno T, Inoue M, Ogihara Y, Saracoglu I. (2002) Antimetastatic Activity of Acteoside, a Phenylethanoid Glycoside. Biol Pharm Bull, 25 (5): 666-668.

99. Li X, Chen D, Li M, Gao X, Shi G, Zhao H. (2018) Plantamajoside inhibits lipopolysaccharide-induced epithelial-mesenchymal transition through suppressing the NF-κB/IL-6 signaling in esophageal squamous cell carcinoma cells. Biomed Pharmacother, 102: 1045-1051.

100. Xiang Y, Jing Z, Haixia W, Ruitao Y, Huaixiu W, Zenggen L, Lijuan M, Yiping W, Yanduo T. (2017) Antiproliferative Activity of Phenylpropanoids Isolated from Lagotis brevituba Maxim. Phytother Res, 31 (10): 1509-1520.

101. Pei S, Yang X, Wang H, Zhang H, Zhou B, Zhang D, Lin D. (2015) Plantamajoside, a potential anti-tumor herbal medicine inhibits breast cancer growth and pulmonary metastasis by decreasing the activity of matrix metalloproteinase-9 and -2. BMC Cancer, 15 (1): 965.

102. Sanchez PM, Villarreal ML, Herrera-Ruiz M, Zamilpa A, Jiménez-Ferrer E, Trejo-Tapia G. (2013) In vivo anti-inflammatory and anti-ulcerogenic activities of extracts from wild growing and in vitro plants of Castilleja tenuiflora Benth. (Orobanchaceae). J Ethnopharmacol, 150 (3): 1032-1037.

103. Díaz AM, Abad MJ, Fernández L, Silván AM, De Santos J, Bermejo P. (2004) Phenylpropanoid glycosides from Scrophularia scorodonia: In vitro anti-inflammatory activity. Life Sci, 74 (20): 2515-2526.

104. Nakamura T, Okuyama E, Tsukada A, Yamazaki M, Satake M, Nishibe S, Deyama T, Moriya A, Maruno M, Nishimura H. (1997) Acteoside as the Analgesic Principle of Cedron (Lippia triphylla), a Peruvian Medicinal Plant. Chem Pharm Bull, 45 (3): 499-504.

105. Wang Y, Zhao H, Lin C, Ren J, Zhang S. (2016) Forsythiaside A Exhibits Anti-inflammatory Effects in LPS-Stimulated BV2 Microglia Cells Through Activation of Nrf2/HO-1 Signaling Pathway. Neurochem Res, 41 (4): 659-665.

106. Cheng G, Zhao Y, Li H, Wu Y, Li X, Han Q, Dai C, Li Y. (2014) Forsythiaside attenuates lipopolysaccharide-induced inflammatory responses in the bursa of

Fabricius of chickens by downregulating the NF-κB signaling pathway. Exp Ther Med, 7 (1): 179-184.

107. Cheng L, Li F, Ma R, Hu X. (2015) Forsythiaside inhibits cigarette smoke-induced lung inflammation by activation of Nrf2 and inhibition of NF-κB. Int Immunopharmacol, 28 (1): 494-499.
108. Qian J, Ma X, Xun Y, Pan L. (2017) Protective effect of forsythiaside A on OVA-induced asthma in mice. Eur J Pharmacol, 812: 250-255.
109. Ma C, Ma W. (2018) Plantamajoside Inhibits Lipopolysaccharide-Induced MUC5AC Expression and Inflammation through Suppressing the PI3K/Akt and NF-κB Signaling Pathways in Human Airway Epithelial Cells. Inflamm, 41 (3): 795-802.
110. Wu H, Zhao G, Jiang K, Chen X, Zhu Z, Qiu C, Li C, Deng G. (2016) Plantamajoside ameliorates lipopolysaccharide-induced acute lung injury via suppressing NF-κB and MAPK activation. Int Immunopharmacol, 35: 315-322.
111. Oh JW, Lee JY, Han SH, Moon YH, Kim YG, Woo ER, Kang KW. (2005) Effects of phenylethanoid glycosides from Digitalis purpurea L. on the expression of inducible nitric oxide synthase. J Pharm Pharmacol, 57 (7): 903-910.
112. Guroff G. PC12 Cells as a Model of Neuronal Differentiation. In: Bottenstein JE, Sato G (Eds.), Cell Culture in the Neurosciences. Springer US, Boston, MA, 1985: 245-272.
113. Wei W, Lu M, Lan X, Liu N, Wang H, Du J, Sun T, Li Y, Yu J. (2019) Neuroprotective effect of Verbascoside on hypoxic-ischemic brain damage in neonatal rat. Neurosci Lett, 711: 134415.
114. Li M, Zhou F, Xu T, Song H, Lu B. (2018) Acteoside protects against 6-OHDA-induced dopaminergic neuron damage via Nrf2-ARE signaling pathway. Food Chem Toxicol, 119: 6-13.
115. Wang HM, Wang LW, Liu XM, Li CL, Xu SP, Farooq AD. (2013) Neuroprotective effects of forsythiaside on learning and memory deficits in senescence-accelerated mouse prone (SAMP8) mice. Pharmacol Biochem Behav, 105: 134-141.
116. Kim SH, Kim DH, Choi JJ, Lee JG, Lee CH, Park SJ, Jung WY, Park DH, Ko KH, Lee SH, Ryu JH. (2009) Forsythiaside, a constituent of the fruits of Forsythia

suspense, ameliorates scopolamine-induced memory impairment in mice. Biomol Ther, 17 (3): 249-255.

117. Chen L, Yan Y, Chen T, Zhang L, Gao X, Du C, Du H. (2019) Forsythiaside prevents β-amyloid-induced hippocampal slice injury by upregulating 2-arachidonoylglycerol via cannabinoid receptor 1-dependent NF-κB pathway. Neurochem Int, 125: 57-66.
118. Yan X, Chen T, Zhang L, Du H. (2017) Protective effects of Forsythoside A on amyloid beta-induced apoptosis in PC12 cells by downregulating acetylcholinesterase. Eur J Pharmacol, 810: 141-148.
119. Kang DG, Lee YS, Kim HJ, Lee YM, Lee HS. (2003) Angiotensin converting enzyme inhibitory phenylpropanoid glycosides from Clerodendron trichotomum. J Ethnopharmacol, 89 (1): 151-154.
120. Martin-Nizard F, Sahpaz S, Kandoussi A, Carpentier M, Fruchart JC, Duriez P, Bailleul F. (2004) Natural phenylpropanoids inhibit lipoprotein-induced endothelin-1 secretion by endothelial cells. J Pharm Pharmacol, 56 (12): 1607-1611.
121. He ZD, Huang Y, Yao X, Lau CW, Law WI, Chen ZY. (2001) Purification of Phenylethanoids from Brandisia hancei and the Antiproliferative Effects on Aortic Smooth Muscle. Planta Med, 67 (6): 520-522.
122. Geng F, Yang L, Chou G, Wang Z. (2010) Bioguided isolation of angiotensin-converting enzyme inhibitors from the seeds of Plantago asiatica L. Phytother Res, 24 (7): 1088-1094.
123. Kim DS, Woo ER, Chae SW, Ha KC, Lee GH, Hong ST, Kwon DY, Kim MS, Jung YK, Kim HM, Kim HK, Kim HR, Chae HJ. (2007) Plantainoside D protects adriamycin-induced apoptosis in H9c2 cardiac muscle cells via the inhibition of ROS generation and NF-κB activation. Life Sci, 80 (4): 314-323.
124. Iizuka T, Nagai M. (2005) Vasorelaxant Effects of Forsythiaside from the Fruits of Forsythia suspensa. Yakugaku Zasshi, 125 (2): 219-224.
125. Lee KJ, Woo ER, Choi CY, Shin DW, Lee DG, You HJ, Jeong HG. (2004) Protective Effect of Acteoside on Carbon Tetrachloride-Induced Hepatotoxicity. Life Sci, 74 (8): 1051-1064.

126. Xiong Q, Hase K, Tezuka Y, Tani T, Namba T, Kadota S. (1998) Hepatoprotective Activity of Phenylethanoids from Cistanche deserticola. Planta Med, 64 (2): 120-125.
127. Jung HY, Seo DW, Hong CO, Kim JY, Yang SY, Lee KW. (2015) Nephroprotection of plantamajoside in rats treated with cadmium. Environ Toxicol Pharmacol, 39 (1): 125-136.
128. Pan CW, Zhou GY, Chen WL, Zhuge L, Jin LX, Zheng Y, Lin W, Pan ZZ. (2015) Protective effect of forsythiaside A on lipopolysaccharide/d-galactosamine-induced liver injury. Int Immunopharmacol, 26 (1): 80-85.
129. Zhu M, Zhu H, Tan N, Wang H, Chu H, Zhang C. (2016) Central anti-fatigue activity of verbascoside. Neurosci Lett, 616: 75-79.
130. Huang DF, Tang YF, Nie SP, Wan Y, Xie MY, Xie XM. (2009) Effect of phenylethanoid glycosides and polysaccharides from the seed of Plantago asiatica L. on the maturation of murine bone marrow-derived dendritic cells. Eur J Pharmacol, 620 (1): 105-111.
131. Prescott TAK, Veitch NC, Simmonds MSJ. (2011) Direct inhibition of calcineurin by caffeoyl phenylethanoid glycosides from Teucrium chamaedrys and Nepeta cataria. J Ethnopharmacol, 137 (3): 1306-1310.
132. Potapovich AI, Kostyuk VA, Kostyuk TV, de Luca C, Korkina LG. (2013) Effects of pre- and post-treatment with plant polyphenols on human keratinocyte responses to solar UV. Inflamm Res, 62 (8): 773-780.
133. Akdemir Z, Kahraman Ç, Tatlı II, Küpeli Akkol E, Süntar I, Keles H. (2011) Bioassay-guided isolation of anti-inflammatory, antinociceptive and wound healer glycosides from the flowers of Verbascum mucronatum Lam. J Ethnopharmacol, 136 (3): 436-443.
134. Shin HS, Park SY, Song HG, Hwang E, Lee DG, Yi TH. (2015) The Androgenic Alopecia Protective Effects of Forsythiaside-A and the Molecular Regulation in a Mouse Model. Phytother Res, 29 (6): 870-876.
135. Cheng Y, Liang X, Feng L, Liu D, Qin M, Liu S, Liu G, Dong M. (2017) Effects of phillyrin and forsythoside A on rat cytochrome P450 activities in vivo and in vitro. Xenobiotica, 47 (4): 297-303.

136. Fleer H, Verspohl EJ. (2007) Antispasmodic activity of an extract from Plantago lanceolata L. and some isolated compounds. Phytomedicine, 14 (6): 409-415.
137. Funes L, Fernández-Arroyo S, Laporta O, Pons A, Roche E, Segura-Carretero A, Fernández-Gutiérrez A, Micol V. (2009) Correlation between plasma antioxidant capacity and verbascoside levels in rats after oral administration of lemon verbena extract. Food Chem, 117 (4): 589-598.
138. Park BG, Lee HS, Jung SH, Hong CO, Won HJ, Park HY, Ryu YS, Lee SJ, Kim KH, Park KW, Lee KW. (2007) A 90 day repeated oral toxicity study on plantamajoside concentrate from Plantago asiatica. Phytother Res, 21 (12): 1118-1123.
139. Koo YC, Jung SH, Yang JH, Ryu YS, Kim EJ, Lee KW. (2009) Cytogenetic investigation of chromosomal aberrations in cells treated with plantamajoside from Plantago asiatica. Phytother Res, 23 (10): 1479-1481.
140. Zhao L, Yan X, Shi J, Ren F, Liu L, Sun S, Shan B. (2015) Ethanol extract of Forsythia suspensa root induces apoptosis of esophageal carcinoma cells via the mitochondrial apoptotic pathway. Mol Med Rep, 11 (2): 871-880.
141. Wallander E. (2008) Systematics of Fraxinus (Oleaceae) and evolution of dioecy. Plant Sys Evol, 273 (1-2): 25-49.
142. Zhi W, Green PS. Fraxinus. From: Flora of China. Available from: http://www.efloras.org/florataxon.aspx?flora_id=2&taxon_id=113002 Access Date: 18.04.2021.
143. Boshier D, Cordero J, Harris S, Pannell J, Rendell S, Savill P, Stewart J, Cundall N, Hubert J, Samuel S, Eriksen B, Wallander E, Martinsson O, Bellido J, García-Fayos P, López R, Roldan-Medina M, Verdú M, Mateu I, Slobodník B. Ash Species in Europe: Biological Characteristics and Practical Guidelines for Sustainable Use. Oxford Forestry Institute, University of Oxford, Oxford, 2005: 8.
144. Ripka G, De Lillo E. (1997) New data to the knowledge on the eriophyoid fauna in Hungary (Acari: Eriophyoidea). Folia ent hung, 58: 147-158.
145. Raman A. (2011) Morphogenesis of insect-induced plant galls: facts and questions. Flora, 206 (6): 517-533.

146. Çaliş İ, Hosny M, Khalifa T, Nishibe S. (1993) Secoiridoids from Fraxinus angustifolia. Phytochemistry, 33 (6): 1453-1456.
147. von Kruedener S, Schneider W, Elstner EF. (1995) A combination of Populus tremula, Solidago virgaurea and Fraxinus excelsior as an anti-inflammatory and antirheumatic drug. A short review. Arzneimittelforschung, 45 (2): 169-171.
148. Kostova I, Iossifova T. (2007) Chemical components of Fraxinus species. Fitoterapia, 78 (2): 85-106.
149. Kostova I. (2001) Fraxinus ornus L. Fitoterapia, 72 (5): 471-480.
150. Hosny M. (1998) Secoiridoid glucosides from Fraxinus oxycarba. Phytochemistry, 47 (8): 1569-1576.
151. Damtoft S, Franzyk H, Jensen SR. (1992) Excelsioside, a secoiridoid glucoside from Fraxinus excelsior. Phytochemistry, 31 (12): 4197-4201.
152. Iossifova T, Vogler B, Klaiber I, Kostova I, Kraus W. (1999) Caffeic acid esters of phenylethanoid glycosides from Fraxinus ornus bark. Phytochemistry, 50 (2): 297-301.
153. Çaliş İ, Hosny M, Lahloub MF. (1996) A secoiridoid glucoside from Fraxinus angustifolia. Phytochemistry, 41 (6): 1557-1562.
154. Iossifova T, Kostova I, Evstatieva LN. (1997) Secoiridoids and hydroxycoumarins in Bulgarian Fraxinus species. Biochem Syst Ecol, 25 (3): 271-274.
155. Kuwajima H, Morita M, Takaishi K, Inoue K, Fujita T, Zheng-Dan H, Chong-Ren Y. (1992) Secoiridoid, coumarin and secoiridoid-coumarin glucosides from Fraxinus chinensis. Phytochemistry, 31 (4): 1277-1280.
156. Iossifova T, Vogler B, Kostova I. (2002) Escuside, a new coumarin-secoiridoid from Fraxinus ornus bark. Fitoterapia, 73 (5): 386-389.
157. Tissut M, Egger K. (1972) Les glycosides flavoniques foliaires de quelques arbres, au cours du cycle vegetatif. Phytochemistry, 11 (2): 631-634.
158. Tsukamoto H, Hisada S, Nishibe S. (1984) Lignans from Bark of Fraxinus mandshurica var. japonica and F. japonica. Chem Pharm Bull, 32 (11): 4482-4489.

159. Greger H, Hofer O. (1980) New unsymmetrically substituted tetrahydrofurofuran lignans from Artemisia absinthium: Assignment of the relative stereochemistry by lanthanide induced chemical shifts. Tetrahedron, 36 (24): 3551-3558.
160. Iossifova T, Mikhova B, Kostova I. (1993) A secoiridoid glucoside and a phenolic compound from Fraxinus ornus bark. Phytochemistry, 34 (5): 1373-1376.
161. Patonnier MP, Peltier JP, Marigo G. (1999) Drought-induced increase in xylem malate and mannitol concentrations and closure of Fraxinus excelsior L. stomata. J Exp Bot, 50 (336): 1223-1229.
162. Oddo E, Sajeva M, Bellini E. (2002) Seasonal pattern of mannitol and malate accumulation in leaves of two manna ash species (Fraxinus ornus L. and F. angustifolia Vahl) growing in Sicily. Plant Biosyst, 136 (1): 29-34.
163. Blake PS, Taylor JM, Finch-Savage WE. (2002) Identification of abscisic acid, indole-3-acetic acid, jasmonic acid, indole-3-acetonitrile, methyl jasmonate and gibberellins in developing, dormant and stratified seeds of ash (Fraxinus excelsior). Plant Growth Regul, 37 (2): 119-125.
164. Gonçalves S, Romano A. (2016) The medicinal potential of plants from the genus Plantago (Plantaginaceae). Ind Crop Prod, 83: 213-226.
165. Beara IN, Lesjak MM, Orčić DZ, Simin NĐ, Četojević-Simin DD, Božin BN, Mimica-Dukić NM. (2012) Comparative analysis of phenolic profile, antioxidant, anti-inflammatory and cytotoxic activity of two closely-related Plantain species: Plantago altissima L. and Plantago lanceolata L. LWT, 47 (1): 64-70.
166. Gonda S, Tóth L, Parizsa P, Nyitrai M, Vasas G. (2010) Screening of common Plantago species in Hungary for bioactive molecules and antioxidant activity. Act Biol Hung, 61: 25-34.
167. Marhold K. Plantago. From: Euro+Med PlantBase. Available from: http://ww2.bgbm.org/EuroPlusMed/PTaxonDetail.asp?NameId=27878&PTRefFk=7200000 Access Date: 18.04.2021.
168. Rahn K. (2008) A phylogenetic study of the Plantaginaceae. Bot J Linn Soc, 120 (2): 145-198.
169. Rønsted N, Chase MW, Albach DC, Bello MA. (2002) Phylogenetic relationships within Plantago (Plantaginaceae): evidence from nuclear ribosomal ITS and plastid trnL-F sequence data. Bot J Linn Soc, 139 (4): 323-338.

170. Cui H, Li Z, Wei L, Hoggard RK. Plantago. From: Flora of China. Available from: http://www.efloras.org/florataxon.aspx?flora_id=620&taxon_id=125735 Access Date: 18.04.2021.
171. Adom MB, Taher M, Mutalabisin MF, Amri MS, Abdul Kudos MB, Wan Sulaiman MWA, Sengupta P, Susanti D. (2017) Chemical constituents and medical benefits of Plantago major. Biomed Pharmacother, 96: 348-360.
172. Heimler D, Isolani L, Vignolini P, Tombelli S, Romani A. (2007) Polyphenol Content and Antioxidative Activity in Some Species of Freshly Consumed Salads. J Agric Food Chem, 55 (5): 1724-1729.
173. Pawar H, Varkhade C. (2014) Isolation, characterization and investigation of Plantago ovata husk polysaccharide as superdisintegrant. Int J Biol Macromol, 69: 52-58.
174. Chaibakhsh N, Ahmadi N, Zanjanchi MA. (2014) Use of Plantago major L. as a natural coagulant for optimized decolorization of dye-containing wastewater. Ind Crop Prod, 61: 169-175.
175. Rønsted N, Franzyk H, Mølgaard P, Jaroszewski JW, Jensen SR. (2003) Chemotaxonomy and evolution of Plantago L. Plant Sys Evol, 242 (1): 63-82.
176. Murai M, Tamayama Y, Nishibe S. (1995) Phenylethanoids in the Herb of Plantago lanceolata and Inhibitory Effect on Arachidonic Acid-Induced Mouse Ear Edema. Planta Med, 61 (5): 479-480.
177. Janković T, Zdunić G, Beara I, Balog K, Pljevljakušić D, Stešević D, Šavikin K. (2012) Comparative study of some polyphenols in Plantago species. Biochem Syst Ecol, 42: 69-74.
178. Kawashty SA, Gamal-el-din E, Abdalla MF, Saleh NAM. (1994) Flavonoids of Plantago species in Egypt. Biochem Syst Ecol, 22 (7): 729-733.
179. Pailer M, Haschke-Hofmeister E. (1969) Inhaltsstoffe aus Plantago major. Planta Med, 17 (2): 139-145.
180. Hiltibran RC, Wadkins CL, Nicholas HJ. (1953) The Distribution of Triterpenes in Rugel's Plantain. J Am Chem Soc, 75 (20): 5125-5126.
181. Tarvainen M, Suomela JP, Kallio H, Yang B. (2010) Triterpene Acids in Plantago major: Identification, Quantification and Comparison of Different Extraction Methods. Chromatographia, 71 (3): 279-284.

182. Kartini K, Piyaviriyakul S, Siripong P, Vallisuta O. (2014) HPTLC simultaneous quantification of triterpene acids for quality control of Plantago major L. and evaluation of their cytotoxic and antioxidant activities. Ind Crop Prod, 60: 239-246.
183. Schneider G. Arzneidrogen: Ein Kompendium für Pharmazeuten, Biologen und Chemiker. Spektrum Akademischer Verlag, München, 1990: 131.
184. Ahmed ZF, Hammouda FM, Rizk AM, Wassel GM. (1968) Phytochemical Studies Of Egyptian Plantago Species (Lipids). Planta Med, 16 (4): 404-410.
185. Ahmad MS, Ahmad MU, Osman SM. (1980) A new hydroxyolefinic acid from Plantago major seed oil. Phytochemistry, 19 (10): 2137-2139.
186. Smith MA, Zhang H, Purves RW. (2014) Identification and Distribution of Oxygenated Fatty Acids in Plantago Seed Lipids. J Am Oil Chem Soc, 91 (8): 1313-1322.
187. Guil JL, Rodríguez-Garcí I, Torija E. (1997) Nutritional and toxic factors in selected wild edible plants. Plant Foods Hum Nutr, 51 (2): 99-107.
188. Ahmed ZF, Rizk AM, Hammouda FM. (1965) Phytochemical Studies Of Egyptian Plantago Species (Glucides). J Pharm Sci, 54 (7): 1060-1062.
189. Samuelsen AB, Lund I, Djahromi JM, Paulsen BS, Wold JK, Knutsen SH. (1999) Structural features and anti-complementary activity of some heteroxylan polysaccharide fractions from the seeds of Plantago major L. Carbohydr Polym, 38 (2): 133-143.
190. Olennikov DN, Tankhaeva LM, Stolbikova AV, Petrov EV. (2011) Phenylpropanoids and polysaccharides from Plantago depressa and P. media growing in Buryatia. Chem Nat Compd, 47 (2): 165.
191. Samuelsen AB, Paulsen BS, Wold JK, Otsuka H, Yamada H, Espevik T. (1995) Isolation and partial characterization of biologically active polysaccharides from Plantago major L. Phytother Res, 9 (3): 211-218.
192. Zennie TM, Ogzewalla D. (1977) Ascorbic acid and Vitamin A content of edible wild plants of Ohio and Kentucky. Econ Bot, 31 (1): 76-79.
193. Forsythia. In: Pua EC, Davey MR (Eds.), Transgenic Crops VI. Springer Berlin Heidelberg, Berlin, Heidelberg, 2007: 299-318.

194. Ha YH, Kim C, Choi K, Kim JH. (2018) Molecular phylogeny and dating of Forsythieae (Oleaceae) provide insight into the Miocene history of Eurasian temperate shrubs. Front Plant Sci, 9: 99.
195. KewScience. Forsythia. From: World Checklist of Selected Plant Families (WCSP). Available from: http://wcsp.science.kew.org/ Access Date: 17.04.2021.
196. Kim KJ. (1999) Molecular phylogeny of Forsythia (Oleaceae) based on chloroplast DNA variation. Plant Sys Evol, 218 (1): 113-123.
197. Chang MC, Chiu LC, Wei Z, Green PS. Forsythia. From: Flora of China. Available from: www.efloras.org/florataxon.aspx?flora_id=2&taxon_id=112951 Access Date: 17.04.2021.
198. Zhang Q, Jia C, Xu H, Wang Y, Zhang M, Huo C, Shi Q, Yu S. (2012) Chemical Constituents of Plants from the Genus Forsythia. Mini Rev Org Chem, 9 (3): 303-318.
199. Cui Y, Wang Q, Shi X, Zhang X, Sheng X, Zhang L. (2010) Simultaneous quantification of 14 bioactive constituents in Forsythia Suspensa by liquid chromatography–electrospray ionisation–mass spectrometry. Phytochem Anal, 21 (3): 253-260.
200. Ryuk JA, Choi GY, Kim YH, Lee HW, Lee MY, Choi JE, Ko BS. (2010) Application of Genetic Marker and Real-Time Polymerase Chain Reaction for Discrimination between Forsythia viridissima and Forsythia suspensa. Biol Pharm Bull, 33 (7): 1133-1137.
201. Nishibe S, Okabe K, Tsukamoto H, Sakushima A, Hisada S. (1982) The Structure of Forsythiaside isolated from Forsythia suspensa. Chem Pharm Bull, 30 (3): 1048-1050.
202. Guo H, Liu AH, Li L, Guo DA. (2007) Simultaneous determination of 12 major constituents in Forsythia suspensa by high performance liquid chromatograph-DAD method. J Pharmaceut Biomed Anal, 43 (3): 1000-1006.
203. El-Desouky SK, Kim YK. (2008) A Phenylethanoid Glycoside and Other Constituents from the Fruits of Forsythia koreana. Z Naturforsch B, 63 (1): 90-94.
204. Matsuo K, Tokoroyama T, Kubota T. (1972) Bitter constituents of Forsythia viridissima. Phytochemistry, 11 (4): 1522-1523.

205. Nishibe S, Okabe K, Tsukamoto H, Sakushima A, Hisada S, Baba H, Akisada T. (1982) Studies on the Chinese Crude Drug Forsythiae Fructus; VI. The Structure and Antibacterial Activity of Suspensaside isolated from Forsythia suspensa. Chem Pharm Bull, 30 (12): 4548-4553.
206. Kuo PC, Chen GF, Yang ML, Lin YH, Peng CC. (2014) Chemical Constituents from the Fruits of Forsythia suspensa and Their Antimicrobial Activity. Biomed Res Int, 2014: 304830.
207. Bai Y, Li J, Liu W, Jiao XC, He J, Liu J, Ma L, Gao XM, Chang YX. (2015) Pharmacokinetic of 5 components after oral administration of Fructus Forsythiae by HPLC-MS/MS and the effects of harvest time and administration times. J Chromatogr B, 993-994: 36-46.
208. Jiao J, Fu YJ, Zu YG, Luo M, Wang W, Zhang L, Li J. (2012) Enzyme-assisted microwave hydro-distillation essential oil from Fructus forsythia, chemical constituents, and its antimicrobial and antioxidant activities. Food Chem, 134 (1): 235-243.
209. Yang J, Wei H, Teng X, Zhang H, Shi Y. (2014) Dynamic Ultrasonic Nebulisation Extraction Coupled with Headspace Ionic Liquid-based Single-drop Microextraction for the Analysis of the Essential Oil in Forsythia suspensa. Phytochem Anal, 25 (2): 178-184.
210. Jensen SR, Franzyk H, Wallander E. (2002) Chemotaxonomy of the Oleaceae: iridoids as taxonomic markers. Phytochemistry, 60 (3): 213-231.
211. Inoue H, Nishioka T. (1973) Über die Monoterpenglucoside und verwandte Naturstoffe. Über die Struktur des Forsythids, eines neuen Iridoidglucosides aus Forsythia viridissima. Chem Pharm Bull, 21 (3): 497-502.
212. Damtoft S, Franzyk H, Jensen SR. (1994) Biosynthesis of iridoids in Forsythia spp. Phytochemistry, 37 (1): 173-178.
213. Iizuka T, Sakai H, Moriyama H, Suto N, Nagai M, Bagchi D. (2009) Vasorelaxant effects of forsythide isolated from the leaves of Forsythia viridissima on NE-induced aortal contraction. Phytomedicine, 16 (4): 386-390.
214. Endo K, Seya K, Hikino H. (1987) Stereostructure of Rengyol and Isocengyol, Phenylethanoids of Forsythia suspensa. Tetrahedron, 43 (12): 2681-2688.

215. Seya K, Endo K, Hikino H. (1989) Structures of rengyosides A, B and C, three glucosides of Forsythia suspensa fruits. Phytochemistry, 28 (5): 1495-1498.
216. Dai SJ, Ren Y, Shen L, Zhang DW. (2009) New Alkaloids from Forsythia suspensa and their Anti-Inflammatory Activities. Planta Med, 75 (4): 375-377.
217. Ming DS, Yu DQ, Yu SS, Liu J, He CH. (1999) A New Furofuran Mono-Lactone from Forsythia Suspensa. J Asian Nat Prod Res, 1 (3): 221-226.
218. Endo K, Hikono H. (1984) Structures of rengyol, rengyoxide, and rengyolone, new cyclohexylethane derivatives from Forsythia suspensa fruits. Can J Chem, 62 (10): 2011-2014.
219. Chen X, Beutler JA, McCloud TG, Loehfelm A, Yang L, Dong HF, Chertov OY, Salcedo R, Oppenheim JJ, Howard OM. (2003) Tannic acid is an inhibitor of CXCL12 (SDF-1α)/CXCR4 with antiangiogenic activity. Clin Cancer Res, 9 (8): 3115-3123.
220. Sedlák É, Boldizsár I, Borsodi L, Füzfai Z, Molnár-Perl I, Preininger É, Gyurján I. (2008) Identification and Quantification of Lignans, Carboxylic Acids and Sugars in the Leaves of Forsythia Species and Cultivars. Chromatographia, 68 (1): 35-41.
221. Horváti K, Bacsa B, Mlinkó T, Szabo N, Hudecz F, Zsila F, Bősze S. (2017) Comparative analysis of internalisation, haemolytic, cytotoxic and antibacterial effect of membrane-active cationic peptides: aspects of experimental setup. J Amino Acids, 49 (6): 1053-1067.
222. Frisch MJ, Trucks GW, Schlegel HB, Scuseria GE, Robb MA, Cheeseman JR, Scalmani G, Barone V, Petersson GA, Nakatsuji H, Li X, Caricato M, Marenich AV, Bloino J, Janesko BG, Gomperts R, Mennucci B, Hratchian HP, Ortiz JV, Izmaylov AF, Sonnenberg JL, Williams-Young D, Ding F, Lipparini F, Egidi F, Goings J, Peng B, Petrone A, Henderson T, Ranasinghe D, Zakrzewski VG, Gao J, Rega N, Zheng G, Liang W, Hada M, Ehara M, Toyota K, Fukuda R, Hasegawa J, Ishida M, Nakajima T, Honda Y, Kitao O, Nakai H, Vreven T, Throssell K, Montgomery Jr. JA, Peralta JE, Ogliaro F, Bearpark MJ, Heyd JJ, Brothers EN, Kudin KN, Staroverov VN, Keith TA, Kobayashi R, Normand J, Raghavachari K, Rendell AP, Burant JC, Iyengar SS, Tomasi J, Cossi M, Millam JM, Klene M,

Adamo C, Cammi R, Ochterski JW, Martin RL, Morokuma K, Farkas O, Foresman JB, Fox DJ. Gaussian 16 Rev. B.01. Wallingford, CT, 2016.

223. Becke AD. (1993) Density-functional thermochemistry. III. The role of exact exchange. J Chem Phys, 98 (7): 5648-5652.
224. Tomasi J, Mennucci B, Cammi R. (2005) Quantum mechanical continuum solvation models. Chem Rev, 105 (8): 2999-3093.
225. Mucsi Z, Szabó A, Hermecz I, Kucsman A, Csizmadia IG. (2005) Modeling rate-controlling solvent effects. The pericyclic meisenheimer rearrangement of N-propargylmorpholine N-oxide. J Am Chem Soc, 127 (20): 7615-7631.
226. Emeny JM, Morgan MJ. (1979) Regulation of the interferon system: evidence that Vero cells have a genetic defect in interferon production. J Gen Virol, 43 (1): 247-252.
227. Mosmann T. (1983) Rapid colorimetric assay for cellular growth and survival: application to proliferation and cytotoxicity assays. J Immunol Methods, 65 (1-2): 55-63.
228. Kisiel W, Michalska K. (2002) A new coumarin glucoside ester from Cichorium intybus. Fitoterapia, 73 (6): 544-546.
229. Harborne JB. Phytochemical Methods. Springer Netherlands, Dordrecht, 1984: 46.
230. Clifford MN, Knight S, Kuhnert N. (2005) Discriminating between the six isomers of dicaffeoylquinic acid by LC-MS(n). J Agric Food Chem, 53 (10): 3821-3832.
231. Schlauer J, Budzianowski J, Kukułczanka K, Ratajczak L. (2004) Acteoside and related phenylethanoid glycosides in Byblis liniflora Salisb. plants propagated in vitro and its systematic significance. Acta Soc Bot Pol, 73 (1): 9-15.
232. Budzianowska A, Kikowska M, Małkiewicz M, Karolak I, Budzianowski J. (2019) Phenylethanoid glycosides in Plantago media L. organs obtained in in vitro cultures. Acta Biol Cracov Bot, 61 (1): 75-86.
233. Michalak B, Filipek A, Chomicki P, Pyza M, Woźniak M, Żyżyńska-Granica B, Piwowarski JP, Kicel A, Olszewska MA, Kiss AK. (2018) Lignans from Forsythia x Intermedia leaves and flowers attenuate the pro-inflammatory function of leukocytes and their interaction with endothelial cells. Front Pharmacol, 9: 401.

234. Noro Y, Hisata Y, Okuda K, Kawamura T, Tanaka T, Nishibe S. (1992) Phenylethanoid Glycoside in the Leaves of Forsythia spp. Shoyakugaku Zasshi, 46: 254-256.
235. Jia J, Zhang F, Li Z, Qin X, Zhang L. (2015) Comparison of fruits of Forsythia suspensa at two different maturation stages by NMR-based metabolomics. Molecules, 20 (6): 10065-10081.
236. Mucsi Z, Chass GA, Csizmadia IG. (2008) Amidicity change as a significant driving force and thermodynamic selection rule of transamidation reactions. A synergy between experiment and theory. J Phys Chem B, 112 (26): 7885-7893.
237. Mucsi Z, Chass GA, Viskolcz B, Csizmadia IG. (2008) Quantitative scale for the extent of conjugation of carbonyl groups: "carbonylicity" percentage as a chemical driving force. J Phys Chem A, 112 (38): 9153-9165.
238. Kovács E, Rózsa B, Csomos A, Csizmadia IG, Mucsi Z. (2018) Amide Activation in Ground and Excited States. Molecules, 23 (11): 2859.
239. Xu K, Feng ZM, Yang YN, Jiang JS, Zhang PC. (2016) Eight new eudesmane- and eremophilane-type sesquiterpenoids from Atractylodes lancea. Fitoterapia, 114: 115-121.
240. El-Bassuony AA, Abdel-Hamid N. (2006) Antibacterial coumarins isolated from Launaea resedifolia. Химия растительного сырья, 1: 65-68.
241. Kuo PC, Hung HY, Nian CW, Hwang TL, Cheng JC, Kuo DH, Lee EJ, Tai SH, Wu TS. (2017) Chemical Constituents and Anti-inflammatory Principles from the Fruits of Forsythia suspensa. J Nat Prod, 80 (4): 1055-1064.

DOI:10.14753/SE.2022.2639

11 BIBLIOGRAPHY OF CANDIDATE'S PUBLICATIONS

11.1 Publications related to the thesis

Zürn M, Tóth G, Kraszni M, Sólyomváry A, Mucsi Z, Deme R, Rózsa B, Fodor B, Molnár-Perl I, Horváti K, Bősze S, Pályi B, Kis Z, Béni S, Noszál B, Boldizsár I. (2019) Galls of European Fraxinus trees as new and abundant sources of valuable phenylethanoid and coumarin glycosides. Ind Crop Prod, 139: 111517.

Zürn M, Tóth G, Ausbüttel T, Mucsi Z, Horváti K, Bősze S, Sütöri-Diószegi M, Pályi B, Kis Z, Noszál B, Boldizsár I. (2021) Tissue-Specific Accumualtion and Isomerization of Valuable Phenylethanoid Glycosides from Plantago and Forsythia Plants. Int J Mol Sci, 22 (8): 3880.

11.2 Publications unrelated to the thesis

Könye R, Tóth G, Sólyomváry A, Mervai Zs, **Zürn M**, Baghy K, Kovalszky I, Horváth P, Molnár-Perl I, Noszál B, Béni Sz, Boldizsár I. (2018) Chemodiversity of *Cirsium* fruits: Antiproliferative lignans, neolignans and sesquineolignans as chemotaxonomic markers. Fitoterapia, 127: 413-419.

DOI:10.14753/SE.2022.2639

12 ACKNOWLEDGMENT

On the front page, there is only enough space for one author; however, the formulation of the present thesis would not have been possible without the helping hands of lots of people.

Firstly, I would like to thank my family and the Nguyen family for their constant support and reassurement. Without the help of my parents, I would have never come to Budapest in the first place.

This thesis would not have been possible without the guidance and positive attitude of my supervisor Dr. Imre Boldizsár. I am grateful to him for offering me the position as his Ph.D. student and to teach me various techniques and the handling of analytical machines. Also, I must thank Dr. Gergő Tóth and Dr. Szilvia Bősze for conducting and evaluating the NMR and *in vitro* analyses, respectively.

From my time at the department, I will always remember the great coffee breaks, Christmas parties and mischiefs with Ildi, Sanyi, Dani, Tim, Richard, Roumaissa, and everybody else from the Ph.D. room.

Next to my friends from the department, I am also thankful to Peter, Kata, and Vera with whom I could spent time talking about other things than my thesis as well. I am confident that the friendships I made during my stay here are lasting ones.

Together with my supervisor, we are thankful for the grant EFOP-1.8.0-VEKOP-17-2017-00001. This work was completed in the ELTE Thematic Excellence Programme 2020 supported by the National Research, Development and Innovation Office – TKP2020-IKA-05.